2015

Generation and Delivery of Charged Aerosols to Infant Airways

Landon T. Holbrook
Virginia Commonwealth University, holbrooklt@vcu.edu

Generation and Delivery of Charged Aerosols to Infant Airways

A dissertation submitted in partial fulfillment of the requirements for the degree of Doctor of Philosophy at Virginia Commonwealth University.

by

LANDON TUCKER HOLBROOK
Bachelor of Science, Virginia Commonwealth University, USA, 2009

Director: Dr. P. WORTH LONGEST
Professor, Department of Mechanical and Nuclear Engineering and
Department of Pharmaceutics

Virginia Commonwealth University
Richmond, Virginia
July 24, 2015

Acknowledgment

The personal and professional transitions that have occurred during my graduate degree at Virginia Commonwealth University are many and various. I am grateful for the guidance of my advisor, Dr. Worth Longest, who was patient while I learned the value of the scientific process. I am also grateful for the instruction and insight provided by Dr. Michael Hindle from the School of Pharmacy at VCU. I am thankful for the lessons that my parents, Bruce and Kathy, taught me about the value of education or training and I am happy to complete the requirements of training for the Doctorate of Engineering. Thank you to all of my co-workers and mentors, from Dr. Samir Vinchurkar to Dr. James McLeskey and the numerous friends I have had the pleasure to make within the Engineering school at VCU. I have been blessed by Eternity Church at 1900 Chamberlayne Avenue, my wife Lisa, and our son Isaac.

TABLE OF CONTENTS

List of Tables

List of Figures

Abstract

GENERATION AND DELIVERY OF CHARGED AEROSOLS TO INFANT AIRWAYS

By Landon Tucker Holbrook

A dissertation submitted in partial fulfillment of the requirements for the degree of Doctor of Philosophy at Virginia Commonwealth University.

Virginia Commonwealth University, 2015

Director: Dr. P. WORTH LONGEST
Professor, Department of Mechanical and Nuclear Engineering and
Department of Pharmaceutics

The administration of pharmaceutical aerosols to infants on mechanical ventilation needs to be improved by increasing the efficiency of delivery devices and creating better ways of evaluating potential therapies. Aerosolized medicines such as surfactants have been administered to ventilated infants with mixed results, but studies have shown improvement in respiratory function with a much lower dose than with liquid instillation through an endotracheal tube (ETT). An aerosolized medicine must be transported through the ventilation tubing and deposit in the lungs to have the desired therapeutic response.

This work has taken a systematic approach to (i) develop new devices for the efficient production of small sized charged pharmaceutical aerosols, (ii) adapt a lead device to an infant ventilation system, (iii) develop a novel breathing infant lung (BIL) *in vitro* model capable of capturing lung delivery efficiency in an infant without the need for human subjects testing, and (iv) evaluate the hypothesis that small sized charged pharmaceutical aerosols can improve drug delivery efficiency to the lungs of a ventilated infant. Three new devices were developed and screened for the efficient generation of small sized charged pharmaceutical aerosols, which were: wick electrospray, condensational vapor, and a modified vibrating mesh nebulizer in a streamlined low flow induction charger (LF-IC). Of these devices, only the LF-IC produced a small [mean(SD) = 1.6(0.1) micrometers] and charged (1/100 Rayleigh limit) aerosol at a pharmaceutically relevant production rate [mean(SD) = 183(9) micrograms per minute]. The LF-IC was selected as a lead device and adapted for use in an infant ventilation system, which produced an increase in *in vitro* lung filter deposition efficiency from 1.3% with the commercial system to 34% under cyclic ventilation conditions. The BIL model was first shown to produce a realistic pressure-volume response curve when exposed to mechanical ventilation. The optimized LF-IC was then implemented in the BIL model to demonstrate superior reduction in inspiratory resistance when surfactant was delivered as an aerosol compared to liquid instillation. For the delivery of an aerosolized medication, the lung deposition efficiency increased from a mean(SD) 0.4(0.1)% when using the conventional delivery system to 21.3(2.4)% using the LF-IC in the BIL model, a 59-fold increase. The charged aerosol produced by the LF-IC was shown to have more depositional loss in the LF-IC than an uncharged aerosol, but the

charge decreased the exhaled fraction of aerosol by 17%, which needs additional study to achieve statistical significance.

Completion of this work has produced a device that can achieve lung delivery efficiency that is 59-fold greater than aerosols from conventional vibrating mesh nebulizers in invasively ventilated infants using a combination of small particle size, synchronization with inspiration and appropriate charge. The BIL model produced in this work can be used to test clinically relevant methods of administering medications to infants and can be used to provide more accurate delivery estimates for development of new nebulizers and inhalers. The LF-IC developed in this work could be used for controlled and efficient delivery of aerosolized antibiotics, steroids, non-steroidal anti-inflammatories, surfactants, and vasodilators.

Chapter 1 Specific Aims

The goal of this project is to improve the delivery of aerosolized medications to the lungs of infants receiving mechanical ventilation. The approach taken is to use an aerosol that is sufficiently small to reduce deposition in the ventilation system and then enhance aerosol deposition within the lungs using aerosol charge. An aerosol generator is therefore needed that can produce pharmaceutically relevant concentrations of highly charged submicrometer or sufficiently small aerosols with low device losses. To develop an appropriate aerosol generation device, multiple new systems are developed and tested using a series of *in vitro* experiments. The best performing device is then selected and optimized for high efficiency lung delivery. Lung delivery of the aerosol is evaluated using a novel highly realistic *in vitro* model of a breathing infant lung connected to a clinical mechanical ventilation system. Optimization of device performance is based on the selection of an appropriate aerosol size and charge level to maximize lung delivery, minimization of loss in the ventilation system, and potentially control the site of deposition within the lungs.

Aerosol generation systems considered are wick electrospray (WES), condensational vapor (CV), and a conventional vibrating mesh nebulizer with a modified signal that is charged by a streamlined low flow induction charger (LF-IC). These systems are constructed using 3D modeling software and further developed utilizing Computational

Fluid Dynamics (CFD) to minimize particle loss before being constructed using rapid prototyping technology and evaluated experimentally. The device development process will have three different particle generation options that have each been designed and refined before comparison and selection.

Device implementation and optimization will involve realistic *in vitro* model creation from infant patient CT data and will result in a novel prototyped infant lung model with a flexible membrane that is able to reproduce *in vivo* lung characteristics such as inspiratory resistance and biophysical response to surfactant therapy. This model can then be used to quantify particle deposition during respiration and allow for the optimization of the selected delivery device. Upon completion of this work an optimized device will be available that can achieve improved lung delivery of aerosols in ventilated infants. Potential clinical applications include the controlled delivery of aerosolized antibiotics, steroids, non-steroidal anti-inflammatories, surfactants, and vasodilators.

Objective 1: Development of an effective method for generating charged pharmaceutical aerosols with low depositional loss for use with invasive mechanical ventilation.

The devices that currently produce charged aerosols typically do so with the disadvantages of high device losses, low particle charging, or the production of ozone as a byproduct. These shortcomings motivate the need for a device that is able to produce a charged aerosol with a pharmaceutically relevant concentration of inhalable medications without the production and inhalation of harmful gasses like ozone.

The WES device is composed of a streamlined airspace that connects a counter electrode and a liquid reservoir containing a shaped wick submerged in a conductive solution at a high voltage. The electric field causes a Taylor Cone to form at the tip of the wick producing a jet which breaks into highly charged droplets. Electrospray has been researched extensively, and a typical setup consists of a small capillary connected to a syringe pump. This capillary is held at a high voltage and a grounded target is held some distance away from the capillary tip. The WES proposed utilizes a self regulating wick to replace the syringe pump and capillary, thereby reducing complexity and cost. This device is intended for long delivery times, which is made possible by the low delivery rate that is common for electrospray devices. A custom prototyped streamlined shell is used to hold the liquid reservoir, wick, and counter electrode while connecting to standard ventilator tubing.

The CV device uses a heated capillary to vaporize a solution that is held at a high voltage. Forty coils of 40 gauge electrically insulated wire are wrapped around the 30 gauge metal needle to provide the necessary heat for change of phase. This device has more components than the WES, but is able to operate with a higher aerosol output rate. The solution is ejected from the capillary as a vapor which condenses to form an aerosol. Capillary aerosol generation has previously been described; however, the CV system considered here is intended to form a charged aerosol.

The LF-IC system is a commercially available AeroNeb Lab nebulizer with a modified driving signal to deliver one tenth of the normal aerosol mass. A highly charged electrode is located below the vibrating mesh and creates a charged aerosol through

induction. A streamlined shell is designed and prototyped to reduce loss in the device and maintain a consistent gap between the vibrating mesh and the counter electrode. A controlled signal is sent to the mesh plate which has more than one thousand tapered holes vibrating over 128,000 times per second to produce a particular droplet production rate and size for a given solution.

Each charged aerosol generation system is tested using a filter capture apparatus to determine the emitted dose and aerosolization rate. Next, the particle size distribution is evaluated using the mini-MOUDI impactor at 2 liters per minute (LPM). Finally, a modified Electrical Low-Pressure Impactor (ELPI) is used to simultaneously determine the particle size distribution and charge on each impactor stage at a flow rate of 30 LPM. The best performing generator is then selected to be tested in an infant ventilation circuit. Initial testing is done with steady flow into a filter. The tasks that comprise objective one are listed below.

Task 1.1: Develop and evaluate a wick electrospray (WES) device for generating charged aerosols.

Task 1.2: Develop and evaluate a condensational vapor (CV) spray device for generating charged aerosols.

Task 1.3: Develop a vibrating mesh nebulizer system (LF-IC) for generating charged aerosols.

Task 1.4: Evaluate and optimize aerosol delivery through an infant ventilation circuit at steady state flow for the best performing charged aerosol generator.

Task 1.5: Evaluate the effects of cyclic ventilation on depositional loss and emission in the infant ventilation system.

Objective 2: Use of charged aerosols for targeted deposition in infant airways.

After a device is selected to deliver the small sized (MMAD <1.8 μm) and highly charged (~ 1/100 Rayleigh limit) aerosol through the infant ventilation circuit a new breathing infant lung model will be developed to test the airway delivery efficiency. Infant CT scans will be used to reconstruct the pleural space of a 3.55 kg neonatal patient. The pleural space is scaled and filled with 6mm spheres to simulate the infant alveolar region by the air gaps that form between the spheres. This is connected to a previously designed model, Model D, of the mouth-throat down to the third airway bifurcation that has been scaled down to an appropriate tracheal diameter for an infant. This model is then constructed using a Viper Stereolithography rapid prototyper from 3D Systems. This prototyping is an additive process which cures a single layer of the computer aided design (CAD) model with a beam width of 0.01 inches and a layer thickness of 0.1 mm. This model will first be compared to infant physiology data which documents the pressure-volume (P-V) curve demonstrated by infant lungs. Surfactant will then be introduced to determine the physiological response of the model as compared to the lungs. Aerosolized drug will then be released into the ventilation circuit to determine the delivery efficiency of the selected generation device within this new model. The tasks to accomplish objective two are listed below.

Task 2.1: Develop an in vitro breathing infant lung model for a full term neonate.

Task 2.2: Evaluate targeted aerosol delivery in the breathing infant lung model.

These tasks detail significant potential for progress in the field of aerosol therapy in infants. The overarching theme of this work is to increase the understanding and quantification of the deposition of particulate matter in human lungs and to develop and compare methods of delivering therapeutic aerosols capable of improving patient treatment outcomes.

Chapter 2 Background

Objective 1: Development of an effective method for generating charged pharmaceutical aerosols with low depositional loss for use with invasive mechanical ventilation.

The lungs provide a way of distributing oxygen systemically while filtering out particles and unwanted pollutants during respiration. Inhaled pharmaceutical aerosols can be utilized to deliver medicines to the lungs (locally) or the blood (systemically) through the alveolar region. For instance, asthma medication is typically administered through inhalation to act locally on the surface of the airways. Systemic administration can occur through particle deposition in the alveolar region, which enters the blood in the capillaries through the alveolar epithelium (Finlay 2001). Particles larger than 6 micrometers tend to deposit in the mouth-throat before they can be effective. Particles smaller than 2 micrometers deposit mainly in the alveolar region and provide the best systemic administration or are exhaled, while particles larger than 2 micrometers and smaller than 6 micrometers are best suited to treat localized issues in the central and small airways (Darquenne 2012).

The aerosol size and concentration, the patient's breathing pattern and clinical disorder, the delivery device and correct usage of the device all contribute to the distribution of deposition within the lungs and the efficacy of an inhaled therapy (Cole

2000). In addition, the charge of an aerosol effects the distribution of deposition and reduces the exhaled fraction of particles (Bailey 1997; Bailey et al., 1998; Balachandran et al., 1997). Highly charged pharmaceutical aerosols with a mass median aerodynamic diameter (MMAD) of 3-7 μm have high mouth-throat deposition (Azhdarzadeh et al., 2014a; Azhdarzadeh et al., 2014b) as measured by *in vitro* methods. Using *in vivo* methods, lung deposition has been greatly increased with particle charging, suggesting that the submicron (MMAD <1 μm) particle sizes used imply the electrostatic effects on deposition are primarily within the alveolar region (Melandri et al., 1983). High drug losses and high deposition variability have likely caused potentially effective medications to not be effective and ultimately fail clinical trials, such that they never reached patients. (Armangil et al., 2011; Berggren et al., 2000; Cole et al., 1999; Fink 2004; Mazela and Polin 2011; Shah et al., 2007; Sood et al., 2004). As a result, poor delivery efficiency is a hurdle to new pharmaceutical drug development. Current aerosolized agents such as bronchodilators, antibiotics and surfactants need to be implemented with optimized delivery systems (Mazela and Polin 2011). The goal of this work is to increase the efficiency of therapeutic delivery to enable superior treatment and new pharmaceutical drug development through the use of targeted delivery.

Based on the study of Longest et al. (2014b), aerosols with MMADs ≤ 1.8 μm are expected to efficiently penetrate the infant ventilation system. Initial estimates, calculated from non-dimensional quantities set forth by Finlay (2001), indicate that aerosols with a charge in the range of the Raleigh limit / 100 will not have significantly increased deposition in the large (relative to infant airways) diameter ventilation system connectors and will have improved retention in the lungs due to the image attraction force and

reduced velocities and airway diameters within the alveolar region. Three new devices are developed and prototyped for *in vitro* aerosol characterization. Aerosol performance testing is evaluated in terms of the delivered dose (and reproducibility), aerosol droplet size distribution (DSD), and net charge per particle. Based on this analysis, the best performing device is implemented in an infant ventilation system under steady state and cyclic flow conditions. The purpose of this objective is to design and develop a new device for generating small charged particles that are suitable to maximize respiratory drug delivery in ventilated infants with realistically low tidal volumes.

Task 1.1: Develop and evaluate a wick electrospray (WES) device for generating charged aerosols.

Many devices currently exist which produce charged micrometer and submicrometer aerosols. Corona charging is used to charge aerosols that have been generated from a variety of methods (Hinds 1999); however, ozone from both positive and negative corona makes this method incompatible with respiratory drug delivery. Electrospray is a thoroughly documented method for generating particles with high charge (Chen et al., 1995; de Juan and De la Mora 1997). The output mass of electrospray is typically low compared with the needs of pharmaceutical delivery unless special techniques such as multiple nozzles or the use of liquid sheets are applied (Lee et al., 2011; Park et al., 2011). It is not known if the highly charged aerosol associated with electrospray will be detrimental to the lung. The aerosol generated by an electrospray device is typically discharged (Ijsebaert et al., 2001), but the corona needle used for charge neutralization is associated with ozone formation (Hinds 1999), which makes them

impractical for use in an inhaler. Highly charged electrosprayed particles are associated with high device losses if they are not discharged (Fu et al., 2011).

The development of electrospraying goes back more than one hundred years as John Zeleny published multiple works on the production of fine droplets from a conical meniscus resulting from the interaction of an electric stress on a fluid (Zeleny 1914; Zeleny 1915; Zeleny 1917). About fifty years later, Sir Geoffrey Taylor established the theoretical groundwork backed by precise experimentation, which allowed for photo documentation of jet formation from the tip of an oscillating conical surface near the calculated equilibrium of 49.3 degrees (1964). This structure is now called a Taylor cone. The Taylor cone spray regimes reviewed by Cloupeau and Prunet-Foch (1994) are still incompletely understood, but the most understood regime is the cone-jet mode. In this simple and useful mode, a spray of charged droplets issues out of a steady jet which is emitted from the Taylor cone apex (de la Mora 2007). This mode has also been used with a carbon dioxide sheath flow to overcome the electrical breakdown and sparking through the air and achieve electrospray with a sucrose solution in pure water (Chen et al., 1995).

Noakes et al. (1998) patented the first electrospray inhaler, however, Tang and Gomez (1994) improved upon this design by using carbon dioxide instead of air to surround the capillary tip and enable spray of high surface tension liquids without electric breakdown and sparking. Even though there are many academic efforts and patents, there are currently no commercially viable inhalation products which are electrospray based (Yurteri et al., 2010). The studies of Ijsebaert et al. (2001) and Bacon et al. (2009) both included a needle corona discharger in their electrospray setup to neutralize the charge

and allow for particle penetration in the lungs. These dischargers, unfortunately, also produce ozone which has been seen to cause irritation in the airways, especially of diseased patients (Koren et al., 1989; Stenfors et al., 2002).

Reduction of electrospray system complexity has been achieved by removing the syringe pump or micro-controller. Electrospray-based air purifiers have been built using small polymer wicks in place of the metal capillary to transfer charge from the charged spray to contaminated airstreams and act as an ozone-free precipitator (Tepper and Kessick 2008; Tepper et al., 2007). In the study of Hu et al. (2011) various samples were analyzed using wooden tips (toothpicks) in place of capillaries to obtain the mass spectra. An electrospray was also formed using a paper triangle that wicks a small volume of solution (Liu et al., 2010). These substitutions provided a less complicated electrospray system which was disposable and self regulating. Maintaining a stable electrospray with solutions containing a high water content is difficult; a 25% solution of methanol in water was not able to produce a stable Taylor cone due to the rate of flow through the porous material, which is governed by the solution properties (Chiarot et al., 2012). The use of chromatography paper with tips cut at increasing angles has demonstrated a continuous increase in ion current for increasing angle, but a significant increase in electrospray onset voltage from sixty degrees to ninety degrees (Yang et al., 2012). An expected outcome of Task 1.1 is a testable electrospray device and a determination as to whether this aerosol generation method should be used to deliver a charged aerosol to a ventilated infant.

Task 1.2: Develop and evaluate a condensational vapor (CV) spray device for generating charged aerosols.

Condensational vapor (CV) generators operate by boiling and vaporizing a pumped liquid vehicle and ejecting this hot vapor into a cooler gas, in which it condenses to form an aerosol. An example of this design was patented by Howell and Sweeney (1998). The formation of particles by homogeneous nucleation is affected by the turbulent mixing that occurs in the interface between the hot vapor jet and the cooler gas stream (Lesniewski and Friedlander 1995). Elucidating the aerosol formation within turbulent gas jets from homogeneous nucleation, the study of Lesniewski and Friedlander (1998) demonstrated the dependence of the modality of an aerosol on the vapor mole fraction and location of nucleation. CV is often referred to as CAG in the literature, and while not typically associated with charged aerosols, a capillary aerosol generation (CAG) is known to produce high fractions of submicrometer aerosols.

The historically complex and limited CAG was simplified and expanded to generate stable and monodisperse aerosols with a particle size between 0.1 and 2 micrometers and a number concentration between 10^4 and 10^6 cm^{-3} over the course of several hours (Tu 1982). The usefulness of the CAG was expanded by investigating the heating voltage, vehicle water content, and solute concentration in an optimization process which produced a mean aerodynamically sized diameter of 0.54 +/- 0.05 micrometers and established its pharmaceutical use (Hindle et al., 1998). Control of output MMAD has been demonstrated by controlling initial aerosol characteristics and increasing the spacer chamber holding time and residual volume for a CAG with direct heating of the 28-gauge stainless steel capillary (Hong et al., 2002). Further control of output size was demonstrated on the PG

vehicle by considering the optimal thermal energy required to vaporize the formulation without overheating (Shen et al., 2004). The capabilities of the CAG were further expanded to be able to operate with ethanol/water formulations instead of propylene glycol and it was also shown that the formulation could be used to control particle size (Hindle et al., 2004). A computational fluid dynamic (CFD) approach of simulating the multi-scale, multiphase numerical model allowed designers of CAG to optimize considering turbulent mixing and dispersion near the capillary tip (Longest et al., 2007).

The CV process pumps a solution containing dissolved drug through a heated capillary producing a vapor or vapor and droplet spray, which exits a nozzle at high pressure and velocity (Hindle 2004; Hindle et al., 2004; Shen et al., 2004). Condensation in the vicinity of the nozzle produces an aerosol with properties that depend on the evaporating/condensing vehicle and delivery rate. The CV approach was later considered in a series of studies to better understand the underlying physics and optimize operation in an inhaler (Hindle and Longest 2013; Longest and Hindle 2009; Longest et al., 2007). One aim of this task is to test the hypothesis that applying a high voltage to a capillary will set up a radial gradient with zero potential at the center of the capillary resulting in charging or modification of the physics of formation during vaporization. As result of the completion of Task 1.2, a testable CV device will be used to determine whether this aerosol generation device can be used to deliver a charged aerosol to a ventilated infant in the current configuration.

Task 1.3: Develop a vibrating mesh nebulizer system (LF-IC) for generating charged aerosols.

A voltage source held near a conducting object polarizes it and can induce a charge on it when polarized charges are not allowed to leave the object. As opposed to many other methods of charging, induction charging is capable of operation without being exposed to the flow. Highly tunable induction charging was developed in a vibrating orifice aerosol generator (VOAG) and allowed for control over the particle charge by the induction voltage applied (Reischl et al., 1977). Both conducting and poorly conducting solutions demonstrated linear charging to a level above the field and diffusion limit, but below the Rayleigh limit. Reischl's induction charger was implemented and the elementary charges corresponded to the applied induction voltage linearly (Vehring et al., 1997). The frequency of the VOAG was also considered at various voltages and it was shown that particle charge changes considerably for minor changes in frequency (Vehring et al., 1997). Instead of a VOAG, a collision nebulizer was used with an induction charger to carry biological and non-biological particles at elevated charges with the result that conductive non-biological particles carried charge at a much lower induction voltage (Mainelis et al., 2002).

Vibrating mesh nebulizers typically produce aerosols with MMADs in the size range of 2-6 μm (Dhand 2002), but a new mixer-heater device was developed to evaporate aerosol from a vibrating mesh nebulizer and produce high concentrations of submicrometer pharmaceutical aerosols suitable for direct inhalation(Longest et al., 2012; 2013c). Loss within the mixer-heater system was <10% and production of submicrometer aerosols required significant heating of the flow stream at the nebulizer's commercially

available output rate(Longest et al., 2012; 2013c). The low flow-induction charger (LF-IC) was based on the same commercially available vibrating mesh nebulizer, the Aeroneb Lab, and used the same principle of evaporation to reduce the droplet size and add water content to the ventilated patient. The nebulizer was positioned in the streamlined perforated T-connector (SLpT) design previously developed for high flow (Longest et al., 2013b). An initial design of the LF-IC has recently been developed at Virginia Commonwealth University to create a high flow (30 – 90 LPM) induction charger using a vibrating mesh nebulizer in a novel streamlined device (Golshahi et al., 2015), but the dimensions and operating flow rate of this device are different than the LF-IC.

The expected outcome of Task 1.3 is the production of a third device that is capable of generating an aerosol for delivery to an infant patient with low flow rates (about 5 LPM). This device will be compared with those developed in Task 1.1 - Task 1.2 and the device that is able to produce the most mass with a charge of approximately $1/100^{th}$ of the Rayleigh limit and a MMAD of approximately 1.8 μm will be chosen for further development and testing in an infant ventilation circuit.

Task 1.4: Evaluate and optimize aerosol delivery through an infant ventilation circuit at steady state flow for the best performing charged aerosol generator.

Infants receiving mechanical ventilation can frequently benefit from pharmaceutical aerosols with the goal of improving lung function while minimizing systemic exposure of the medication and associated side effects (Fink 2004; Mazela and Polin 2011; Rubin and Fink 2001). However, the delivery of aerosolized medication to infants is a significant challenge with lung delivery efficiencies reported in the range of <1-14% (Dubus et al.,

2005; Fink 2004; Fok et al., 1996; Mazela and Polin 2011; Sidler-Moix et al., 2013). Impediments to effective aerosol delivery include small diameter connective ventilator tubing, small tidal volumes, short inhalation periods (Fink 2004; Rubin and Fink 2001), and ventilation components that are designed for gas delivery and not aerosol administration (Longest et al., 2014a; Longest et al., 2014b). Low delivery efficiency wastes valuable medications and makes the administration of high dose drugs very challenging. Furthermore, low delivery efficiency is typically associated with high variability in the delivered dose, which makes the use of medications with a narrow therapeutic window difficult. Both low delivery efficiency and high variability are implicated as reasons for the clinical failure of some aerosolized medications delivered to infants (Mazela and Polin 2011; Shah et al., 2007). Improved dose delivery is needed for ventilated infants in order to maximize the clinical benefit of existing medications and to help develop new inhaled therapies (Brion et al., 2006; Cole et al., 1999; Fink 2004; Rubin and Williams 2014; Shah et al., 2007).

Several recent studies have proposed strategies for improving pharmaceutical aerosol delivery to ventilated infants. The use of vibrating mesh nebulizers and synchronization of nebulization with inhalation was reported to deliver approximately 12-14% of the aerosolized dose in a macaque animal model of ventilated infants (Dubus et al., 2005). The study of Mazela et al. (2014) introduces a newly designed Y-connector, referred to as the VC connector (also known as Afectair), that separates nebulizer and ventilation gas bias flows thereby improving the lung delivery efficiency of a jet nebulizer when used with infants. Using ventilation parameters for a premature infant, the delivery efficiency at a filter before an endotracheal tube (ETT) was approximately 1% or less with a commercial

Y-connector and increased to approximately 7% with the VC connector (Mazela et al., 2014). In the study of Longest et al. (2014b), optimal aerosol delivery conditions were evaluated for a newborn full-term infant receiving mechanical ventilation through an ETT using *in vitro*, CFD, and whole-lung modeling techniques and the predicted lung deposition fraction was found to range from 6.8-13.5%, which was similar to the *in vivo* animal model predictions of Dubus et al. (2005) with a lung deposition fraction range of 12.6-14%. Aerosol deposition in infant lungs was then optimized in the study of Longest et al. (2014b) for mesh nebulized aerosols with the use of a new streamlined (SL) Y-connector, delivery of the aerosol during only a portion of inspiration, and selection of optimal droplet sizes. The study of Longest and Tian (2015) evaluated the delivery of a submicrometer excipient enhanced growth (EEG) aerosol in a port on top of a new streamlined Y-connector. With appropriate timing of delivery, a maximum tracheobronchial deposition fraction of 56% was achieved and a method of growing an initially small dry powder aerosol was demonstrated (Longest and Tian 2015).

A new strategy to target the deposition of pharmaceutical aerosols within the lungs of ventilated infants is the use of small charged droplets generated from an initial solution or suspension liquid formulation. In this approach, the droplet size is sufficiently small to allow for effective penetration through the delivery system and upper infant airways without significant depositional drug loss, which likely requires an aerosol mass median aerodynamic diameter (MMAD) of approximately 1.8 μm or less (Longest et al., 2014b). As described in the study of Longest et al. (2014b), exhalation of the aerosol dose is a significant problem with ventilated infants. To reduce the exhalation of large dose fractions, charge on the pharmaceutical aerosol will foster deposition within the lung

airways and potentially allow for targeting the site of delivery. An optimal level of charge is required to minimize deposition in the delivery system or extrathoracic airways, where velocities are relatively high, and then maximize deposition in the tracheobronchial and/or alveolar airspace. While a number of studies in adults have considered the use of aerosol charge to target deposition in the lungs (Bailey 1997; Bailey et al., 1998; Balachandran et al., 1997; Chan et al., 1978), previous studies have not applied this approach to infants and have not attempted to use initially small particles to minimize extrathoracic or ventilation system deposition. Additionally, the run time will be varied to examine the effect of static charge accumulation on electrically insulated components under steady-state flow conditions.

The expected outcomes of Task 1.4 include the measured deposition fraction in the ventilation system through the 3 mm endotracheal tube, the impact of runtime on charged aerosol delivery, and the comparison of LF-IC device efficiency in streamlined components as compared to the commercial mesh nebulizer in commercial components.

Task 1.5: Evaluate the effects of cyclic ventilation on depositional loss and emission in the infant ventilation system.

The extent to which poor delivery efficiency of aerosolized medicines limits treatment options for ventilated infants has been highlighted in Task 1.4. Increasing the lung delivery efficiency of pharmaceutical aerosols creates opportunities for improved clinical effects of existing medications and will likely expand the number of aerosol therapies available for infants. Aerosol delivery during mechanical ventilation is considered less efficient compared with spontaneously breathing delivery as highlighted in

the study of MacIntyre et al. (1985), who clinically demonstrated 2% nominal lung deposition in intubated adult subjects on mechanical ventilation and 12% in non-intubated adult subjects using a nebulizer which generated an aerosol with a mass median aerodynamic diameter between 1 and 5 μm. In this study, seven patients over the age of 49 with various reasons for being connected to mechanical ventilation received aerosolized treatment through a 7 mm endotracheal tube (ETT), while 3 healthy volunteers received aerosolized treatment through a mouthpiece (Macintyre et al., 1985). Transport of aerosol through gas delivery tubing, connection components and patient interface device is a significant challenge during mechanical ventilation because ventilation components are typically designed for gas delivery and not aerosol administration (Longest et al., 2014a; Longest et al., 2014b). In addition to this, the nebulizer type, nebulizer location within the ventilation circuit, gas flow, and mode of nebulizer operation are important considerations for increasing aerosol delivery efficiency during mechanical ventilation (Fink and Ari 2013).

During mechanical ventilation in infants, aerosol delivery efficiencies in the range of <1-14% are common, even considering more recent vibrating mesh nebulizer devices (Dubus et al., 2005; Fink 2004; Fok et al., 1996; Mazela and Polin 2011; Sidler-Moix et al., 2013) . Using a jet nebulizer in an *in vitro* model of a ventilated premature infant, with a new connector to separate nebulizer and ventilation gas bias flow, Mazela et al. (2014) increased albuterol sulfate delivery efficiency from 1% or less through the commercial Y-connector to a maximum of approximately 7% with the improved connector, before the ETT or mask. Additional aerosol losses are known to occur in the infant ETT, which can have an internal diameter as small as 2.5 mm. A new streamlined Y-connector was

implemented with synchronized delivery and reduced droplet sizes (~ 1.8 μm) to optimize aerosol deposition in the infant lungs using *in vitro*, whole lung, and CFD modeling (Longest et al., 2014b). For a full term (3.6 kg) infant and 3 mm ETT, maximum total lung delivery efficiency of a polydisperse aerosol with a mass median aerodynamic diameter (MMAD) of 1.78 μm reached 45.2%.

In Task 1.5, depositional losses in a commercial infant ventilation circuit are determined using a commercial mesh nebulizer and the previously determined (Task 1.3) best performing charger design, the low-flow induction-charger (LF-IC). The ventilation circuit is driven by a cyclic air-flow provided by an infant ventilator and the estimated lung delivered dose is collected on a filter at the end of a curved 3 mm (ID) ETT and quantified using a validated HPLC method. The drug remaining in the nebulizer, LF-IC, Y-connector, and a 3 mm ETT are collected and compared to the lung delivered dose. The performance of the delivery system is also quantified in terms of time as the delivery rate of drug to the lung. The reduced mass output of the LF-IC compared to a commercial nebulizer is expected to have a lower drug delivery rate to the lung, but the increased efficiency is intended to minimize drug waste and reduce intersubject variability in cases where adequate delivery times are available, as with mechanical ventilation. The LF-IC is designed to target the deposition of pharmaceutical aerosols in ventilated infants by reducing the particle size to penetrate the delivery system with the addition of an induced charge on the droplets to foster lung deposition and reduce exhalation of the inhaled dose (Task 1.3). An aerosol mass median aerodynamic diameter that is smaller than typically delivered, i.e., approximately 1.8 μm or less, is necessary to reduce depositional loss in the delivery system at typical flow rates used with a neonate (Longest et al., 2014b). The LF-IC

is redesigned to minimize device volume for use with cyclic flow conditions and to allow for the inclusion of a ventilator flow meter in the ventilator circuit, a new common feature in mechanical ventilation systems that has not adequately been considered in previous studies. This redesigned LF-IC also incorporates a breath actuated nebulizer to increase delivery of aerosolized drug to the patient and reduce the exhaled dose.

The purpose of Task 1.5 is to compare the performance of the previously developed LF-IC with a commercially available nebulizer in an infant ventilation circuit under cyclic flow conditions. The LF-IC and commercial device performances are evaluated by the quantification of model drug mass using HPLC in the following system components: exhalation filter, in-line ventilator flow meter, ventilator components (commercial or streamlined Y-connector), nebulizer and connectors (Aeroneb Lab, commercial T-connector, LF-IC), endotracheal tube, and lung filter.

Objective 2: Use of charged aerosols for targeted deposition in infant airways

Efficient delivery of pharmaceutical aerosols to infants has not been achieved due to high variability and low pulmonary deposition, resulting in unclear clinical results (Longest and Tian 2014). *In vitro* models have been used to represent infant patients, but none of these models simulate realistic exhalation of aerosol (Fink 2004). Considering an *in vitro-in vivo* parallel study with two jet nebulizers, a smaller initial MMAD was more efficient *in vitro*, but that did not lead to improved delivery to the patient *in vivo* (Watterberg et al., 1991). Comparing a metered dose inhaler and an ultrasonic nebulizer, a neonatal test lung was used to obtain delivery results that were similar to the simultaneously obtained

clinical delivery results for intubated infants (Grigg et al., 1992). Both of these studies highlight the benefits and difficulty of using an *in vitro* model to predict device losses and patient delivery before conducting an *in vivo* study and perfectly motivate the creation of a superior model for testing device, drug, or delivery methods in pre-clinical studies.

Task 2.1: Develop an in vitro breathing infant lung model for a full term neonate.

In vitro experiments are important to establish parameters for the safe delivery of aerosol therapies before commencing *in vivo* studies (Byron et al., 2010; Carrigy et al., 2014; Martin and Finlay 2014). For instance, in the study of Finer et al. (2010), an *in vitro* infant model was used to determine the maximum possible delivered dose using a vibrating mesh nebulizer and a 2% synthetic surfactant solution, assuming that none of the aerosol that reached the patient was exhaled. These types of studies provide exposure limits for protecting patients during *in vivo* studies but are not representative of the actual dose delivered to the lung because they do not currently account for drug exhalation and often do not include realistic upper airway anatomies and breathing physiology. *In vitro* testing of mean, small, and large models of the mouth and upper airways has been used to produce an *in vitro-in vivo* correlation to predict *in vivo* aerosol drug deposition using an *in vitro* test method for dry powder inhalers (Delvadia et al., 2013; Delvadia et al., 2012). However, most in vitro models do not account for the drug distribution within the lungs. It is well known that drug distribution within the lungs can have a significant impact on therapeutic benefit (Usmani et al., 2003).

Healthy lungs expand evenly due to work done by the diaphragm to increase volume in the chest cage, resulting in inhalation. After inhalation, the diaphragm relaxes and the

pressure returns to its original value, causing the lungs to contract in an elastic manner thereby driving exhalation and a return to a resting volume (Drake et al., 2005). At the end of inspiration or expiration in a healthy patient there is no airflow and the intrapleural pressure does not reflect forces associated with airflow, only the elastic recoil forces (West 2012). Compliance is a metric of the lung's elastic recoil and is measured as the change in volume per unit change in pressure across the lung. If the compliance of the lungs was only due to elastic tissue forces, it would be graphed on a pressure vs. volume plot as a single straight line connecting maximum and minimum lung volume points. However, airway resistance and changes in surface tension cause the volume response to an applied pressure to deviate from a linear relationship during inhalation vs. exhalation. In this chapter, the Pressure-Volume (P-V) graph was used to determine realistic response of the BIL model to mechanical ventilation because it is known that patient inhalation will deviate from a linear compliance due to the pressure needed for gas flow through narrow resistive airways (Walsh and DiBlasi 2010). The pressure difference between the alveoli and the mouth divided by the airflow is defined as the airway resistance and the area under the linear compliance line but bounded by the P-V curve is the work required to overcome airway and tissue resistance (West 2012).

In healthy individuals, the lungs are able to control the surface tension of the alveolar region by adjusting the amount of surfactant present on the surface. Patients with insufficient surfactant have alveoli that tend to collapse during normal tidal breathing, frequently leading to respiratory failure if not treated with surfactant replacement therapy (Willson 2015). In a multicenter randomized trial, dramatic oxygenation improvement occurred within 5 minutes, mortality decreased from 51% to 31%, and the mean time

patients were on mechanical ventilation was 35% less with instilled surfactant therapy (Collaborative European Multicenter Study 1988). According to the American Academy of Pediatrics, "…the optimal method of surfactant administration in preterm infants has yet to be clearly proven" and additional data is needed to recommend a method such as aerosolized surfactant delivery (Polin et al., 2014). Considering non-invasive aerosol delivery of synthetic lung surfactant in rabbits, surfactant deficiency was effectively relieved, but large portions of the surfactant were not nebulized and more than 40% of the aerosolized surfactant was lost in the ventilation circuit (Walther et al., 2014).

The upper tracheobronchial airways of the breathing infant lung (BIL) model were scaled from a previously constructed adult mouth-throat model (Walenga et al., 2013) and digitally joined to a new model of the infant pleural space before being prototyped. Model D extends from the mouth through three generations of bifurcating geometries and was constructed from a single CT scan that was consistent with mean airway dimensions of adults (Walenga et al., 2013). An average infant height of 50 cm was used with the morphological correlation from Phalen (1985) to determine a mean (SD) infant outlet diameter of generation three as 2.59 (0.37) mm, which was used to scale model D. Ventilation parameters for a 3.55 kg infant were selected from Walsh & DiBlasi (2010), which represents 50th percentile conditions at full term delivery. The chosen functional residual capacity (the amount of air left in the lung after exhalation) was based on the youngest ICRP (1994) model, a 3 month old Caucasian infant. The pleural cavity was modeled from a CT scan of an infant, prototyped, and filled with plastic spheres having a diameter of 6 mm. The characteristic diameter of the smallest possible gap between three adjacent spheres was 1.36 mm and provided an initial approximation of the expected

alveolar airway outer diameter of 0.54 mm (Khajeh-Hosseini-Dalasm and Longest 2014). The expected surfactant pool (amount of surfactant) in healthy lungs is approximately 4 mg/kg (Rebello et al., 1996). However, it is known that a small amount of surfactant (0.5 mg lipid/kg) delivered to the lungs via aerosol can have a large impact on physiological response in surfactant deficient airways (Lewis et al., 1993).

Common methods of surfactant delivery include liquid bolus administration (referred to as instillation of single or multi-dose), continuous infusion (or continuous instilation), and aerosolization. Special consideration needs to be given to the patient to prevent transient oxygen desaturation and severe airway obstruction which have been seen more frequently in extreme low birth weight infants with more severe lung disease when surfactants are instilled (Tarawneh et al., 2012). The instillation process involves the insertion of an endotracheal tube, which carries a number of risks, pouring between 1.25 ml/kg and 5.8 ml/kg (Polin et al., 2014) of surfactant solutions down the endotracheal tube into the patient's lungs (or approximately 4 ml), and application of mechanical ventilation, which is also associated with lung injury and infection risks. Instillation of surfactant in infants has caused airway obstruction immediately following administration in multiple studies (Miedema et al., 2011; Wheeler et al., 2009). Although instillation is currently the only approved method for surfactant administration it requires an artificial airway and some positive pressure ventilation, which may be harmful to any patient, especially infants (Willson 2015).

In Task 2.1, inspiratory resistance and compliance were determined in the breathing infant lung (BIL) model across three methods of surfactant administration:

instilled, commercial, and modified-charged. A low flow-induction charger, capable of delivering a charged aerosol with a mass median aerodynamic diameter (MMAD) < 1.8 μm (Golshahi et al., 2015; Holbrook et al., 2015), was developed and characterized in Task 1.3. The LF-IC was redesigned in Task 1.5 to utilize a lower charging voltage, a smaller device volume, breath synchronized delivery, and relocation of the nebulizer proximal the patient. These changes allowed for implementation in an infant ventilation circuit under cyclic ventilation and provided an *in vitro* inhaled dose for "commercial" (CM) and "modified and charged" (M-C) delivery. The maximum efficiencies and delivery rates from Task 1.5 only measure the drug mass inhaled and do not measure the fraction exhaled, as is widely done in the literature (Dhand 2008; Fink and Ari 2013; Fink 2004; Guerin et al., 2008). Results from Tasks 1.3 – 1.5 are used to estimate the fraction delivered to the newly developed BIL model and provide standard methods and protocols to be used in Task 2.2 and future studies.

In general, aerosolized delivery of medication to infants and adults suffers from high variability and low delivery efficiency (Brion et al., 2006; Cole et al., 1999; Fink 2004; Rubin and Williams 2014; Shah et al., 2007). Considering instilled and aerosolized delivery of surfactant to rats with acute lung injury, a highly inefficient device delivered a dose at least 4-fold lower than the instilled dose (100 mg/kg) to produce an equivalent increase is oxygenation and decrease in breath rate (Sun et al., 2009). New technologies provide an opportunity to efficiently deliver aerosolized surfactant with a low total administered dose and enhanced homogeneity of distribution (Pillow and Minocchieri 2012). The improvement of lung function with minimal systemic exposure can be accomplished by

administering pharmaceutical aerosols to infants receiving mechanical ventilation (Fink 2004; Mazela and Polin 2011; Rubin and Fink 2001).

The purpose of Task 2.1 was to develop a BIL model that will respond in physiologically consistent ways and capture both deposited and exhaled dose in future studies. Conventional and modified aerosol delivery techniques with a vibrating mesh nebulizer were considered and compared against an instilled surfactant case. After creating a realistic BIL model that is capable of distinguishing between three surfactant administration methods, the BIL model is suggested for use with the developed LF-IC from Task 1.5 to deliver a model drug such as albuterol sulfate to determine the exhaled fraction and the delivery rate to the lung, which is evaluated in Task 2.2. *In vitro* testing of the BIL model is developed to enable testing of next generation medications, increase the efficiency of current inhaled therapies, and test surfactant administration techniques.

Task 2.2: Evaluate targeted aerosol delivery in the breathing infant lung model.

Inertia, gravity, diffusion, interception, and electrostatic forces cause particles to deposit in the lung airways (Hinds 1999). Each of these forces presents a potential opportunity to target deposition in the airways, but the focus of this work is on deposition enhancement by electrostatic forces. Electrostatics affect deposition by the space charge effect and an image attraction force with a conducting surface; the space charge effect is a repulsion of similarly charged particles within an aerosol that causes better dispersion and the image force is an attractive force to the lung wall (Koolpiruck et al., 2004). Since the wall of the airway is lined with electrically conductive mucus, a charged particle nearing the wall will experience an attractive force that increases by a power of two as the distance

to the wall decreases. Deposition due to electrostatic forces is therefore extremely important in the alveolar region where the distance to the wall is small (Kwok and Chan 2009).

Charged aerosols have been shown to have the potential for controlling deposition, particularly in reducing the exhaled fraction of particles (Bailey 1997; Bailey et al., 1998; Balachandran et al., 1997). Highly charged pharmaceutical aerosols have high mouth-throat deposition when the particle size is large (3-7 micrometers)(Azhdarzadeh et al., 2014a; Azhdarzadeh et al., 2014b). Melandri found that the charge on inhaled particles greatly increased deposition *in vivo* and suggested that the submicron particle sizes used in his study imply the electrostatic effects on deposition are primarily within the alveolar region(Melandri et al., 1983). The impact that particle charging has on lung deposition of particles is unclear; the polarity and magnitude of the charge still need to be considered in future human subjects testing(Wong et al., 2013).

The BIL model designed and constructed for Task 2.1 was evaluated with the modified and charged delivery system of Task 1.5 to determine the amount of drug delivered to and retained in the lungs. Development of aerosol delivery protocols often relies on *in vitro* studies to determine the mass of drug delivered to the lung. However, these *in vitro* studies are not able to account for the reduction in lung deposition caused by exhalation. *In vitro* models over estimate the dose to a patient because they use an absolute filter which cannot simulate drug loss due to exhalation (Dhand 2008; Fink and Ari 2013; Fink 2004; Guerin et al., 2008), as was applied in Task 1.5. For example, a novel connector has been developed to bypass the bias-flow and increase delivery of a jet

nebulized aerosol, but the improvement was measured before the ETT, without an inline flow meter, and not considering exhalation (Mazela et al., 2014). Large particles are often filtered out by ventilation circuitry such that the aerosol MMAD after an infant ventilation circuit and a 3 mm ETT was measured as 1.4 μm for a vibrating mesh and a jet nebulizer which generated aerosols with MMADs of 4.6 and 4.8 μm, respectively (Dubus et al., 2005). Inefficient delivery and exhalation of inhaled aerosol therapy has been addressed by reducing aerosol MMAD to < 1.8 μm, as suggested by Longest et al. (2014b), and inducing a charge on the aerosol to increase deposition in the lung (Holbrook et al., 2015).

In Task 2.2, depositional losses and delivery efficiency were determined in the BIL model using the same techniques described in Task 1.5. A modified signal was supplied to a vibrating mesh nebulizer to reduce the output rate and initial momentum of the generated aerosol (described in Task 1.3 – Task 1.5). This modified output was sprayed into a streamlined induction charger that has been previously optimized (Task 1.5) to deliver aerosol efficiently under cyclic ventilation conditions in an infant ventilation circuit. The experiments of Task 1.5 demonstrated a 26-fold increase in delivery efficiency, but a reduction in the rate of delivered mass to the inhalation filter. The systems designed and implemented in Task 1.3 – Task 1.5 will be applied to a test case of aerosolized albuterol sulfate (a model drug commonly used as a bronchodilator) to determine the impact of charging on the exhalation of an aerosol < 1.8 μm (MMAD) and test the ability of the BIL model to simulate the exhalation of inhaled aerosol. The lung deposition in this study is expected to be lower than the filter data collected in Task 1.5 (34%), but the difference between the commercial system and the modified and charged delivery system is expected to be greater than the 26-fold increase demonstrated in Task 1.5.

An *in vitro* model of an infant capable of realistically capturing the lung dose of an administered pharmaceutical aerosol under actual ventilation conditions would clearly be a beneficial tool for testing inhaled therapies with expensive drugs or significant side effects. Development of inhaled therapies for infants has been hindered by low delivery efficiency (high waste) and high variability (uncontrolled dose) (Mazela and Polin 2011; Shah et al., 2007). Surfactants are very expensive, steroids need low variability because of adverse side effects, and antibiotics need to be delivered in high and consistent doses to prevent bacteria from surviving (Lehne and Rosenthal 2014). Bronchodilators such as albuterol sulfate (AS) are typically inexpensive, have low side effects, and don't require a large dose. AS was selected as a marker to determine the depositional loss and delivery efficiency of the LF-IC in the novel BIL model. Implementation of the BIL model in Task 2.2 will quantify the depositional reduction due to aerosol exhalation using an *in vitro* experiment.

The purpose of Task 2.2 was to compare the performance of the previously implemented LF-IC with a commercially available nebulizer under realistic flow conditions in a BIL model (Task 2.1) designed to capture both deposited and exhaled dose. Conventional and modified aerosol delivery techniques with a vibrating mesh nebulizer were considered and suggestions are given for method of administration. The expected outcome of Task 2.2 is an *in vitro* method of testing lung deposition of aerosol therapy without assuming perfect capture within the lungs as compared to Task 1.5.

Chapter 3 Generating Charged Pharmaceutical Aerosols Intended to Improve Targeted Drug Delivery in Ventilated Infants

Preface: This chapter has been published as a research article in Journal of Aerosol Science, October 2015, Vol. 88, 35-47.

Abstract. The delivery of pharmaceutical aerosols to infants receiving mechanical ventilation is extremely challenging due to small diameter flow passages, low tidal volumes, and frequent exhalation of the aerosol. The use of small charged particles is proposed as a novel method to prevent deposition in ventilator components and foster deposition in the lower infant airways. The objective of this study was to compare the performance of multiple new devices for generating small charged particles that are expected to maximize respiratory drug delivery in ventilated infants. Criteria used to select a leading device included production of a charged aerosol with a mass median aerodynamic diameter (MMAD) ≤ approximately 1.8 μm; low device depositional loss of the aerosol (<20%); particle charge in the range of the Rayleigh limit/100; and high drug output with low performance variability. Proposed new devices were a wick electrospray (WES) system with accelerated cross-flow air; a condensational vapor (CV) system with a charged solution and strong field gradient; and a low flow - induction charger (LF-IC) designed to operate with a modified commercial mesh nebulizer. Based on infant ventilation conditions, flow rates through the devices were in a range of 2-5 L/min and the devices were assessed in terms of depositional drug loss and emitted drug mass; droplet size

distribution (DSD) using a Mini-MOUDI; and DSD and net charge with a modified ELPI. Considering the WES, primary limitations were (i) low and variable aerosol production rates and (ii) high device depositional losses. The CV device produced a high quality aerosol with a MMAD of 0.14 μm and a drug delivery rate of 25 μg/min. However, the device was excluded because it failed to produce a charged aerosol. In contrast, the LF-IC produced a 1.6 μm aerosol with high net charge, low device depositional loss (<15% based on recovery), and low variability. In the ELPI size fraction bin nearest the MMAD, the LF-IC produced >100 elementary charges per particle, which was an order of magnitude increase compared to the case of zero charging voltage. In conclusion, the LF-IC was selected as a leading system that is expected to improve aerosol delivery efficiency in ventilated infants through the use of small charged particles.

3.1 Introduction

Infants receiving mechanical ventilation can frequently benefit from pharmaceutical aerosols with the goal of improving lung function while minimizing systemic exposure of the medication and associated side effects (Fink 2004; Mazela and Polin 2011; Rubin and Fink 2001). However, the delivery of aerosolized medication to infants is a significant challenge with lung delivery efficiencies reported in the range of <1-14% (Dubus et al., 2005; Fink 2004; Fok et al., 1996; Mazela and Polin 2011; Sidler-Moix et al., 2013). Impediments to effective aerosol delivery include small diameter connective ventilator tubing, small tidal volumes, short inhalation periods (Fink 2004; Rubin and Fink 2001), and ventilation components that are designed for gas delivery and not aerosol administration (Longest et al., 2014a; Longest et al., 2014b). Low delivery efficiency wastes valuable

medications and makes the administration of high dose drugs very challenging. For example, surfactant delivery with a mesh nebulizer was reported in one study to require a 3 hour period for the administration of a 72 mg dose (Finer et al., 2010). Furthermore, low delivery efficiency is typically associated with high variability in the delivered dose, which makes the use of medications with a narrow therapeutic window difficult. Both low delivery efficiency and high variability are implicated as reasons for the clinical failure of some aerosolized medications delivered to infants (Mazela and Polin 2011; Shah et al., 2007). Improved dose delivery is needed for ventilated infants in order to maximize the clinical benefit of existing medications and to help develop new inhaled therapies (Brion et al., 2006; Cole et al., 1999; Fink 2004; Rubin and Williams 2014; Shah et al., 2007).

Several recent studies have proposed strategies for improving pharmaceutical aerosol delivery to ventilated infants. The use of vibrating mesh nebulizers and synchronization of nebulization with inhalation was reported to deliver approximately 12-14% of the aerosolized dose in a macaque animal model of ventilated infants (Dubus et al., 2005). Mazela et al. (2014) describes a newly designed Y-connector, referred to as the VC connector (also known as Afectair), that separates nebulizer and ventilation gas bias flows thereby improving the lung delivery efficiency of a jet nebulizer when used with infants. Based on an *in vitro* model of ventilated premature infants, Mazela et al. (2014) reported delivery efficiency at the exit of a commercial Y-connector to be approximately 1% or less vs. a maximum of approximately 7% with the VC connector. In a previous study, Longest et al. (2014b) evaluated optimal aerosol delivery conditions for a newborn full-term infant receiving mechanical ventilation through an endotracheal tube (ETT) using *in vitro*, CFD, and whole-lung modeling techniques. With a mesh nebulizer, commercial Y-connector, and

a 3 mm ETT, the predicted lung deposition fraction was found to range from 6.8-13.5%, which was similar to the *in vivo* animal model predictions of Dubus et al. (2005) with a lung deposition fraction range of 12.6-14%. Aerosol deposition in infant lungs was then optimized by Longest et al. (2014b) for mesh nebulized aerosols with the use of a new streamlined (SL) Y-connector, delivery of the aerosol during only a portion of inspiration, and selection of optimal droplet sizes. The study of Longest and Tian (2015) evaluated the delivery of a submicrometer excipient enhanced growth (EEG) aerosol in a port on top of a new streamlined Y-connector. With appropriate timing of delivery, a maximum tracheobronchial deposition fraction of 56% was achieved and a method of growing an initially small dry powder aerosol was demonstrated.

A new strategy to target the deposition of pharmaceutical aerosols within the lungs of ventilated infants is the use of small charged droplets generated from an initial solution or suspension liquid formulation. In this approach, the droplet size is sufficiently small to allow for effective penetration through the delivery system and upper infant airways without significant depositional drug loss, which likely requires an aerosol mass median aerodynamic diameter (MMAD) of approximately 1.8 μm or less (Longest et al., 2014b). As described by Longest et al. (2014b), exhalation of the aerosol dose is a significant problem with ventilated infants. To prevent the exhalation of large dose fractions, charge on the pharmaceutical aerosol will foster deposition within the lung airways and potentially allow for targeting the site of delivery. An optimal level of charge is required to minimize deposition in the delivery system or extrathoracic airways, where velocities are relatively high, and then maximize deposition in the tracheobronchial and/or alveolar airspace. The ability to tune the charge level is an important design factor of the delivery technology.

While a number of studies in adults have considered the use of aerosol charge to target deposition in the lungs (Bailey 1997; Bailey et al., 1998; Balachandran et al., 1997; Chan et al., 1978), previous studies have not applied this approach to infants and have not attempted to use initially small particles to minimize extrathoracic or ventilation system deposition.

A number of devices are available for the production of charged micrometer and submicrometer aerosols. Corona charging is frequently used to provide high charge to existing aerosols (Hinds 1999); however, ozone from both positive and negative corona makes this method incompatible with respiratory drug delivery. Electrospray is a well known method to generate particles with high charge (Chen et al., 1995; de Juan and De la Mora 1997). However, output mass is typically low compared with the needs of pharmaceutical delivery unless advanced techniques such as the use of liquid sheets or multiple nozzles are applied (Lee et al., 2011; Park et al., 2011). Furthermore, it is not known if the high charges associated with electrospray aerosols will be detrimental to efficient lung delivery. The use of corona needles for electrospray discharge (Ijsebaert et al., 2001) is associated with ozone formation (Hinds 1999), making them impractical for use in inhalers. Vibrating orifice charged particle generators are limited by very low mass output (Azhdarzadeh et al., 2014a; Azhdarzadeh et al., 2014b; Reischl et al., 1977).

While not typically associated with charged aerosols, devices known to produce high doses of submicrometer aerosols are capillary aerosol generation (CAG) and vibrating mesh nebulizers coupled with evaporation-type devices. The CAG process pumps a solution containing dissolved drug through a heated capillary producing a vapor or vapor and droplet spray, which exits a nozzle at high pressure and velocity (Hindle 2004; Hindle

et al., 2004; Shen et al., 2004). Condensation in the vicinity of the nozzle produces an aerosol with properties that depend on the evaporating/condensing vehicle and delivery rate. The CAG approach was later considered in a series of studies to better understand the underlying physics and optimize operation in an inhaler (Hindle and Longest 2013; Longest and Hindle 2009; Longest et al., 2007).

Vibrating mesh nebulizers typically produce aerosols with MMADs in the size range of 2-6 μm (Dhand 2002). Longest et al. (2012; 2013c) demonstrated the use of a new mixer-heater device to evaporate these aerosols and produce high concentrations of submicrometer pharmaceutical aerosols suitable for direct inhalation. Loss within the mixer-heater system was <10% and production of submicrometer aerosols required significant heating of the flow stream at the nebulizer's commercially available output rate.

A recent advance of electrospray aerosols is the introduction of inexpensive and disposable spray elements to feed the liquid solution and produce the Taylor cone (Tepper and Kessick 2008; Tepper and Kessick 2009; Tepper et al., 2007). Electrosprays have been produced with polymer wicks, toothpicks, and shaped paper (Hu et al., 2011; Liu et al., 2010; Tepper and Kessick 2009; Yang et al., 2012). An advantage of this approach is the replacement of the expensive spray pump control unit with a self-feeding and disposable unit. Considering condensational aerosols, Ouyang (1995) has previously demonstrated the production of charged condensational aerosols with the addition of high voltage charging.

The objective of this study is to compare the performance of multiple new devices for generating small charged particles delivered at flows that are that are suitable to

maximize respiratory drug delivery in ventilated infants. Evaluation criteria of the devices include:

1. Production of a charged aerosol with a MMAD ≤ approximately 1.8 μm;
2. Low device depositional loss of the aerosol (< 20%);
3. Net Particle charge in the range of the Rayleigh limit / 100; and
4. High drug output (>10 μg) with low performance variability (<10% coefficient of variation for emitted dose).

Based on the study of Longest et al. (2014b), aerosols with MMADs ≤ 1.8 μm are expected to efficiently penetrate the infant ventilation system. Initial estimates, calculated from non-dimensional quantities set forth by Finlay (2001), indicate that aerosols with a charge in the range of the Raleigh limit / 100 will not have significantly increased deposition in the large diameter ventilation system connectors and will have improved retention in the lungs due to the image attraction force and reduced velocities and airway diameters within the alveolar region. Furthermore, high drug output is required for the delivery of high dose medications like inhaled surfactants and antibiotics. Three new devices are developed and prototyped for *in vitro* aerosol characterization. Aerosol performance testing is evaluated in terms of the delivered dose (and reproducibility), aerosol droplet size distribution (DSD), and net charge per particle. Based on this analysis, the best performing device is selected for future study in terms of emitted dose from an infant ventilation system and infant lung delivery.

3.2 Methods

3.2.1 Overview of Devices

In this study, three new devices for the production of charged small (≤1.8 μm) pharmaceutical aerosols are developed and compared. Each device begins with an existing aerosol generation platform and includes significant modifications in order to attain the desired aerosol characteristics. Each of the devices is operated at air flow rates consistent with infant ventilation conditions (2-5 LPM) to deliver aerosol out of the device. The first device implements the paper wick electrospray platform (Figure 3.1a), which has the advantages of low cost and no moving parts. However, low aerosol emission is expected due to the high charging field. Modifications include the addition of a narrow flow channel intended to accelerate the cross-flow air and remove the aerosol from the electrical field region prior to deposition on the charged electrode. The second device employs the CAG approach and is termed the condensational vapor (CV) device (Figure 3.1b). In this method, a drug solution is pumped through a heated capillary to produce a vapor. Nearly complete vaporization of the solution is used to eliminate the need for a nozzle at the capillary tip, which may reduce the potential for device clogging. A high voltage charge is also applied to the capillary, which is electrically isolated from the heating element. The space inside the metal capillary represents a region of high field gradient with zero field strength at the center of the capillary in the evaporation zone. This high field gradient is expected to potentially charge the evaporating liquid filaments and droplets. It was not known if this potential charge would influence the evaporation or condensation processes and potentially produce a charged aerosol, as with the condensational vapor strategy of

Ouyang et al. (1995). Modifying the size of a recovered condensational aerosol or producing a charged aerosol by charging the base solution was seen as a potentially advantageous development. Finally, a commercial mesh nebulizer (Aeroneb Lab; Aerogen, Galway, Ireland) was employed as a convenient aerosol source in the low flow - induction charger (LF-IC; Figure 3.1c). Modifications included altering the vibration amplitude to reduce liquid output, thereby enabling evaporation to near submicrometer size at the low flow rates required for infant ventilation, and including a charged electrode positioned below the mesh to charge the aerosol by induction charging. Other studies have used induction charging with single orifice plates (Azhdarzadeh et al., 2014a; Azhdarzadeh et al., 2014b), but the application of induction charging to a vibrating mesh system with low airflow is a new advancement. Further details in device development and experimental testing methods for these new systems are described in the following sections.

3.2.2 Overview of test systems

A schematic of the three experimental setups that were employed to generate albuterol sulfate (Spectrum Chemicals, New Brunswick, NJ; model drug commonly used as a bronchodilator) aerosols is provided in Figure 3.2. To quantify performance, options considered for each system were assessing aerosol depositional drug loss in the device, collection of the emitted drug mass on an aerosol filter, determination of aerosol droplet size distribution (DSD) with the Mini-MOUDI (MSP Corp., Shoreview, MN) at a flow of 2 LPM, and determination of net charge on separate aerosol size fraction bins and DSD with a modified electrical low pressure impactor (ELPI; Dekati, Finland) at a flow rate of 30 LPM. Separate flow rates were required by the Mini-MOUDI and ELPI based on internal

calibrations by the respective manufacturers. Sampling at 2 LPM provides for an accurate view of the aerosol DSD emitted from the device because makeup air is not required. In contrast, sampling at 30 LPM will result in some evaporation of aerosol droplets; however, the ELPI device allows for quantification of the net aerosol charge within 12 different aerosol size fraction bins. In a bipolar aerosol, the ELPI measures the net charge of the combined positive and negative charges for a given size bin. Selection of an appropriate series of tests depended in part on operation of the individual devices.

Both the WES and LF-IC contain internal flow passages such that depositional drug loss was evaluated. In these experiments, the device was operated for a specified amount of time and then disassembled. Device components were washed in distilled deionized water. Drug mass recovered was quantified using a previously validated High Performance Liquid Chromatography (HPLC) method for albuterol sulfate (AS). Device deposition was not assessed for the CV system (only delivered dose was determined) because an enclosure housing was not constructed. This was because, as described later, this device was not selected for future study and an enclosure system was not required.

Delivered dose testing was conducted by operating the device at its specified flow rate and collecting the delivered dose on a high-efficiency respiratory filter (Pulmoguard II; Quest Medical, Brockton, MA). An airflow of 10 LPM was maintained through the filter using a vacuum pump. HPLC analysis was again used to determine the drug mass delivered to the filter. If the filter drug mass was below a typical infant drug delivery mass (10 μg for albuterol sulfate) or had a coefficient of variation greater than 10% , then the device was considered not to be a viable option and testing with additional methods was not pursued.

Impactor measurements consisted of employing either the Mini-MOUDI or modified ELPI at the manufacturer specified flow rates of 2 or 30 LPM, respectively. The aerosol generation devices operated in a flow rate range of 2-5 LPM. During sampling of the aerosol, room-condition makeup air was used to satisfy the various flow rate requirements of the generation devices and impactors. The Mini-MOUDI was implemented as received from the manufacturer and drug mass on each stage was determined by washing with deionized water before HPLC analysis quantified AS recovery. The ELPI was operated in a modified mode as described by Kotian et al. (2009) in order to determine both aerosol size and net charge. In this approach, the corona charger of the ELPI was removed. Drug mass deposition on individual stages was determined by HPLC analysis and used to determine the DSD at 30 LPM. The electrical reading of each stage was used to determine the net aerosol charge within each respective size fraction bin. Further details of these testing methods describing how they were applied to each aerosol generation system are provided in the following sections.

Table 3.1 provides a comparison of device parameters selected for the performance characterization experiments. Considering the number of possible variables with three charged aerosol generation systems, device optimization can be a daunting task. To address this issue, preliminary screening experiments were conducted to guide parameter selection and maximize device performance. As a result, the devices selected for comparison and the parameters defined in Table 3.1 represent the end product of a large amount of preliminary optimization work. For example, the minimum stable operating voltage for an electrospray was found to be 6 kV with the WES system. In contrast, the LF-IC system was found to effectively emit charged aerosols with a charging voltage of 1 kV.

The CV system was limited to 1 kV applied voltage due to the dielectric material coating the heating wire breaking down at higher voltages. Aerosolization rates in Table 3.1 report liquid volume emitted from each system determined by weighing the devices before and after use. Due to the low aerosolization rate of the WES (μL/hour), compared with the CV and LF-IC (mL/hour), the drug concentration in the WES device was increased to 5%$^{w}/_{v}$, which resulted in a highly conductive solution and enhanced electrospray performance. In contrast, producing small aerosols with CV and LF-IC require using <1% $^{w}/_{v}$ solution concentration. WES was enhanced with a surfactant (0.02% $^{w}/_{v}$ poloxamer 188 (Leutrol F68) donated from BASF Corporation, Florham Park, NJ) to reduce surface tension of the solution, whereas NaCl (Sigma Chemical Company, St. Louis, MO) was used as a charging excipient in the CV and LF-IC devices. Finally, typical inhalation waveforms used with full term neonates have a mean tracheal flow rate of approximately 2-5 LPM (Walsh and DiBlasi 2010). The lower end of this range was found to generate a sufficiently small aerosol with the WES and CV systems. In contrast, a combination of 5 LPM flow and modification of the nebulizer output signal were important to produce a near submicrometer aerosol with the LF-IC device, as described further in Section 2.5.

3.2.3 Wick electrospray (WES)

The WES device was composed of a streamlined airspace that connects a grounded electrode and a liquid reservoir containing a triangular tipped paper wick submerged in the drug solution at a high voltage, as seen in Figure 3.1a. In the device, the grounded electrode is positioned above the paper wick. The paper wick is made of Whatman Grade 3MM Cellulose Chromatography Paper cut to a width of 5 mm, a length of 15 mm and a 60

degree angle tip was formed to emit the electrospray. Air flows over the top of the wick, perpendicular to the direction of the electrical field and aerosol spray. The intent of this design was to create a highly charged aerosol via electrospray and then remove the aerosol from the electrostatic field using a crossing airflow before the droplets deposit on the grounded electrode. The distance between the paper wick tip and the grounded electrode was a constant 3 mm. Filtered air was connected to the inlet of the WES shell and regulated to flow at 2 LPM as confirmed upstream by an inline flow meter.

The formulation drug solution used was 5%$^{w}/_{v}$ AS and 0.2% $^{w}/_{v}$ Poloxamer 188 in distilled water as shown in Table 3.1. Poloxamer 188 is a surfactant that was added to reduce the surface tension of the solution and improve spraying. The solution was sonicated for at least thirty minutes to ensure complete dissolution. The solution was then pipetted into the WES reservoir to the maximum fill line of 400 microliters after the wick was inserted vertically with the sharp tip oriented toward the grounded electrode.

A high voltage power supply (CZE1000R; Spellman High Voltage Electronics Corporation, Hauppauge, NY, USA) operating in negative mode was connected to the wick reservoir, while the ground of the power supply was connected to the electrode. The high voltage power supply can be limited by either current or voltage. To operate in current limiting mode, the voltage limit was set to a value higher than the measured voltage. The current limit was set to 3 microamperes and slowly decreased to 0.6 microamperes to maintain the desired operating current with an appropriate voltage. An electrical resistor was used in series with the grounded electrode to determine the functionality of the device and the mode of electrospray achieved. Voltage across this resistor was recorded once per second for each experiment using a digital multimeter (Fluke Corporation, Everett, WA)

with data-logging software. The voltage across the resistor was observed during the run to determine the electrospray current and operating mode of the system. After the one hour run time was completed, the high voltage power supply was discharged by turning off the power supply and then connecting the high voltage lead to ground.

For assessing device drug deposition and drug delivery, a 30 cm length of 10 mm (diameter) ventilator tubing was connected to the WES device. The aerosol generated at a flow rate of 2 LPM was collected on a Pulmoguard II filter that was positioned at the outlet of the tubing. An airflow of 10 LPM airflow was maintained through the filter using a vacuum pump. The increased filter flow rate was used to ensure complete entrainment and capture of the aerosol exiting the tubing.

Performance of the electrospray system was assessed by quantifying the drug deposition in each relevant component of Figure 3.2a. To determine drug deposition in the WES system, the counter electrode, tubing and filter were all washed in deionized water and the AS concentrations of the resulting solutions determined by a validated HPLC method. Recovered drug mass was determined by multiplication of AS concentration by the dilution volume. In order to determine the percentage AS recovery, known volumes of the formulation solution were also diluted to accurately quantify the concentration of the formulation.

3.2.4 Condensational Vapor (CV)

The CV device was expected to function similar to CAG with an aqueous drug solution formulation (Longest et al., 2007) but with differences of (i) increased energy per volume of solution to achieve near full vaporization, (ii) use of a straight tip capillary, and

(iii) charging of the solution prior to vaporization and condensation. Increased energy input was intended to fully vaporize the solution and form a more consistent nano-scale condensational aerosol. Drug molecules are expected to be contained in hydrated ion clusters or un-evaporated nano-droplets. By providing sufficient energy to vaporize the solution, the capillary nozzle can be eliminated, which was a source of significant spray momentum (Longest et al., 2008) and potentially system clogging and malfunction. Charging the solution is expected to create a charged aerosol or charged evaporated droplets during the vaporization process through conduction charging (Zhao et al., 2005). In the vicinity of vaporization, high charge is expected on the walls of the capillary and fluid phase with zero charge in the vaporized core. The gradient between the charged and unchanged regions during liquid boiling-breakup was expected to create charged discrete droplet elements. The evaporation of these charged droplets could then produce charged ions. Both the presence of charge and generated ions could influence the evaporation and condensation processes altering the final aerosol size and/or producing charged condensational droplets.

Control of the capillary temperature was adjusted and monitored using electrically insulated heating wire and a thermocouple. 40 gauge (0.0031 inch) NiCr heating wire with DuPont's heavy polymide 240C enamel insulation was obtained from WireTronic Inc. (Volcano, CA). The wire was wrapped around the capillary approximately 35 times to form the heating element, as shown in Figure 3.1b. The resistance of this heating wire was measured before and after each experiment and replaced when it was not between 10 – 20 ohms. A thermocouple temperature probe was placed on the capillary approximately 1 cm away from the tip to measure the capillary wall temperature. A DC power supply

(HY3005F-3, Mastech, San Jose, CA) provided approximately 1.5 Watts to the 40 gauge heating wire to obtain heating that varied the capillary temperature (1 cm from the tip) between 100 and 160 ^{o}C. Control experiments were also performed in the absence of charging to determine the effect on both DSD and net particle charge.

The formulation drug solution used in the CV system was 0.25% $^{w}/_{v}$ AS and 0.25%$^{w}/_{v}$ NaCl in distilled water as shown in Table 3.1. The solution was sonicated for at least thirty minutes to ensure complete dissolution. 0.7 mL of solution was loaded into a 1 mL syringe and connected to the heated capillary. A syringe pump (NE – 300, New Era Pump Systems Inc. Farmingdale, NY) was used to pump the solution to the heated capillary at a constant flow rate of 0.6 mL/hour. The loaded syringe was inverted, tapped, and depressed to ensure there were no air bubbles in the syringe before each experiment.

The DSD was determined for the CV device using the Mini-MOUDI impactor for a 20 minute run. A vacuum pump provided the pressure drop needed to sample 2 LPM through the Mini-MOUDI impactor (Figure 3.2b). A flow meter was attached to the inlet of the impactor prior to aerosol generation to verify 2 LPM through the Mini-MOUDI and removed before generating an aerosol. Potential losses were minimized by spraying directly from the heated capillary to the impactor inlet to avoid deposition in connecting tubing.

The DSD and net particle charge were determined simultaneously using the ELPI at 30 LPM for a 20 minute sample time. The aerosol was sprayed directly into a streamlined connector (Figure 3.3) attached to the inlet of the ELPI. A downstream vacuum pump was used to draw 30 LPM of room-condition air containing the aerosol through the impactor.

Drug aerosol deposition was recovered by washing the inlet and each stage of the impactor and quantified using a validated HPLC technique.

With the ELPI, electrometer current data was collected for each of the 12 stages and recorded to a .CSV file using Dekati software. Using the midpoint method, this data was then numerically integrated with respect to time to give the net charge collected per stage. The HPLC-determined drug mass per stage was used with the midpoint diameter between the corresponding stages' cut sizes to determine the number of particles depositing on each stage. The net stage charge was then divided by the total number of particles per stage to determine the average number of charges per particle.

3.2.5 Low flow-induction charger (LF-IC)

The LF-IC was based on the commercially available Aeroneb Lab vibrating mesh nebulizer. The nebulizer was positioned in the streamlined perforated T-connector (SLpT) design previously developed by Longest et al. (2013b) as shown in Figure 3.1c. This connector was shown to reduce depositional loss by a factor of 4.5x compared with the commercial design of the T-connector. Two modifications of this system include adjusting the driving signal of the mesh nebulizer and the addition of a charged electrode. As described below, the driving signal of the mesh nebulizer was adjusted to reduce the mass output by a factor of 10x in order to allow for evaporation of the aerosol. The desired target was evaporation to a 1.8 μm MMAD with 5 LPM of gas flow. The charged electrode was positioned below the mesh on the opposite side of the SLpT (distance of 47.6 mm) to produce a charged aerosol by induction charging at an applied voltage of 1 kV. Induction charging with a vibrating orifice generator was previously described by Reischl et al.

(1977) and implemented by Azhdarzadeh et al. (2014a; 2014b). Our group (Golshahi et al., 2015) has recently developed an induction charger with a mesh nebulizer that operates at high flow rates (30-90 LPM). This study is the first to report the functioning of a low flow (5LPM) induction charger system with a mesh nebulizer. Use of the mesh provides a substantial increase in output compared with vibrating single orifice devices, such that pharmaceutically relevant doses of medication can be delivered.

One tenth of the aerosol output by mass with the Aeroneb Lab nebulizer was achieved by reducing the amplitude of the applied sinusoidal driving voltage while maintaining the commercial frequency of 128.2 kHz. A Rigol DG10220 function waveform generator (Beaverton, OR) produced the desired signal and was amplified using a TS200 modulated power supply from Accel Instruments (Irvine, CA). This signal was continuously monitored using a Tektronix TDS 210 oscilloscope (Beaverton, OR). This reduced output should enable adequate drying at 5 LPM as opposed to the study of Golshahi et al. (2015), where a flow rate of 90 LPM was required to dry the aerosol. 5 LPM of filtered air was directed through the LF-IC, drying and entraining the charged aerosol before it was exposed to atmospheric pressure and directed to a collection filter or an impactor. Control experiments were also performed in the absence of charging using 0 kV to determine the effect on both DSD and net particle charge.

Dose variability and device deposition were determined directly from the impactor studies. In all cases, the device was operated for 5 minutes. To determine device deposition, the system was disassembled after the aerosol generation time period and components were washed with deionized water. As with the previous systems, drug mass was determined with a validated HPLC method.

The nominal dose of each run was calculated by determining the mass of formulation nebulized. After each run, the inner wall of the nebulizer was wiped before being weighed and subtracted from the initial mass of the nebulizer. A solution density of 1 g/cm^3 was assumed and the difference between the measured masses was multiplied by the formulation AS concentration to calculate the nominal mass of AS that was aerosolized.

To determine the DSD from the LF-IC, 2 LPM of the 5 LPM airstream from the LF-IC was sampled into the Mini-MOUDI. A streamlined connector used for sampling the 5 LPM flow stream and providing 2 LPM to the impactor is displayed in Figure 3.3 a. This connector interfaces with the SLpT, the Mini-MOUDI, and a Pulmoguard II filter that was used to capture excess flow. Mass of drug on the connector, inlet, and each stage of the impactor was determined using washings and HPLC analysis.

To calculate charge per particle, the ELPI was again employed as with the CV device. The 5 LPM airstream from the LF-IC was directed into the streamlined connector added to the ELPI (Figure 3.3 b), which also pulled in 25 LPM of makeup room-condition air based on operation of a downstream vacuum pump. Current measurement data was recorded using the ELPI's electrometers and software for 30 seconds prior to aerosol generation. The nebulizer and the induction charger were turned on simultaneously. After the run the current data was recorded for 30 seconds beyond when the generator was turned off. For each experiment, the generator and charger were both operated for 5 minutes. The collected current data was processed as with the CV device. Only the current that was collected during the generation/charging time was included in the calculation of charge per particle.

Droplet particle sizing with the ELPI was expected to report smaller droplet size compared with the Mini-MOUDI due to particle evaporation at a higher airflow rate. However, evaporation is not expected to alter the charging profile. It is assumed that droplets do not evaporate beyond a critical Rayleigh limit, which would cause breakup due to electrostatic effects. Measured net charge on the droplets can then be used to approximate charge on the aerosol exiting the LF-IC device at 5 LPM.

3.3 Results

3.3.1 Wick electrospray

The WES emitted mass results captured on the filter showed high variability and high device losses within a group of four replicate experiments. As shown in Table 3.2, the WES device aerosolized a mean of about 27 μg of drug in the 1 hour period, of which about 12 μg was deposited on the device and this was associated with high variability (coefficient of variation = 106%). Device deposition ranged from approximately 1 to 25 μg of drug. Similar variability was observed for the emitted dose (109%) with the mean emitted dose of 15 ug in 1 hr. This variability was too great considering that the system needs to provide safe, reproducible, and reliable drug delivery. Also, the mean delivery rate of 15 μg per hour to the filter was a hindrance to further development because it is lower than typical electrospray systems with micropump controllers and the system was observed to not be stable over the long delivery times that would be necessary for pharmaceutical use. The measured current provided by the electrospray was observed to decrease over time, which indicated a change in spray mode. The paper wick was also observed to be physically damaged after approximately 20 minutes of spraying. This was likely because of high

temperatures associated with corona effects at the sharp wick tip as well as spraying fragments of paper. As a result of these observations, the WES approach was determined to not be effective for respiratory drug delivery to ventilated infants and was not considered further.

3.3.2 Charged vapor

Unlike the WES device, in which the delivered dose was determined by the wick characteristics, the delivered dose from the pump controlled CV device was determined and controlled by the pump flow rate. Given these fixed delivery conditions, the emitted dose of the CV device was determined using the impactor testing rather than the filter capture apparatus. With the Mini-MOUDI system, the mean (standard deviation; SD) drug mass emitted from the device and deposited in the impactor (including the inlet) was 257.6 (24.6) μg over a period of 20 minutes. The expected dose based on the pumping rate and solution concentration was 500 μg, which indicates that some drug mass remained in the capillary or escaped from the impactor inlet. Variability was lower than observed with the WES device, with a coefficient of variation of 9.5%, which was expected with this pump based system. The mean (error bars are SD) DSD of the CV aerosol measured with the Mini-MOUDI is illustrated in Figure 3.4 with a mean (SD) MMAD of 0.14 (0.015) μm. Based on measurements in the ELPI, the aerosol had a negligible amount of net charge. For example, experiments were performed with and without the high voltage charge being applied, there was only a small difference observed in the charged and uncharged elementary charge units on Stage 3 (cut size midpoint = 0.13 μm), with values of 0.21 e and 0.5 e, respectively. Furthermore, both the aerosols generated with and without the application of high voltage

had an MMAD of approximately 0.14 μm. As a result, it was observed that charging the solution had no effect on formation of the condensation aerosol. Due to the generation of relatively unchanged particles that would easily be exhaled due to their small size, the CV device was not selected for further evaluation.

3.3.3 Low flow-induction charger

For the LF-IC operated with 1 kV for 5 minutes, aerosol characterization with the Mini-MOUDI resulted in a mean (SD) emitted dose of 913.8 (45.1) μg. Considering the run time of 5 minutes, the LF-IC could potentially deliver 182.8 μg/min of charged AS particles to a patient with low emitted dose variability with a coefficient of variation of 4.9%. Based on a nominal dose of 1065.8 (38.4) μg, the mean (SD) depositional loss in the nebulizer and device was 14.3 (1.7)%. The overall recovery of drug was 96.9 (2.7)% of the nominal dose indicating good mass balance in this study. The mean DSD for the LF-IC is displayed in Figure 3.5 based on the Mini-MOUDI measurements and results in a mean (SD) MMAD of 1.57 (0.1) μm. This result demonstrates that an appropriate amount of evaporation was achieved at the airflow rate of 5 LPM with the modified nebulizer signal. Using the ELPI, the measured mean DSD is displayed in Figure 3.6. The measured MMAD was 0.88 (0.08) μm, indicating that the aerosol was composed of droplets at a flow rate of 5 LPM and that further size reduction of the aerosol was possible when the aerosol was exposed to the higher flow rate employed with the EPLI.

For particles with a mean size of 0.79 μm (midpoint size of Stage 7 which is nearest to the MMAD of the aerosol when sampled at 30 LPM), the uncharged LF-IC (0 kV) was shown to provide an average of 13.17 elementary charges for every particle collected based on

ELPI measurements. This small amount of charging is expected within a mesh nebulizer due to the difference between positive and negative ion mobility within the solution. Distilled water is expected to have a net negative charge of a similar magnitude for this reason (Finlay 2001). Increasing the induction voltage to 1 kV increased the charge by a factor of 12.9x, resulting in 169.94 elementary charges per particle. The charge per particle vs. charging voltage results are summarized in Table 3.3 along with results from other stages in the ELPI. It is observed on stages with a majority of aerosol drug mass deposition (Stages 5-10), charging at 1 kV produces conditions similar to the Rayleigh limit / 100, which can be considered a high level of charge that will have an effect on lung deposition. Net charges on other stages in Table 3.3 were excluded because of deposition on these stages was below the limit of detection for the HPLC assay, it is estimated that this mass represents < 3% of the drug deposited in the impactor.

3.4 Discussion

This study has developed and compared three new systems intended to produce charged small aerosols with the ultimate goal of integrating a lead device into an infant ventilation system and significantly improving lung delivery efficiency. The developed devices were compared in terms of emitted dose, aerosolization characteristics, and net aerosol charge. Selection criteria for the best performing device were described in the introduction. Based on these evaluations, strengths and weaknesses of each device have emerged leading to the selection of a system for further testing.

Considering the WES device, primary limitations were (i) low and variable aerosol delivery rates and (ii) high device depositional losses. This study considered the new

approach of inexpensive spray elements to replace the micropump controller. It was anticipated that known low aerosol production rates with electrospray could be counteracted by longer spray times or continuous delivery. Furthermore, controlled slow delivery of the inhaled medication may be advantageous for immature infant lungs. Unfortunately, the paper spray elements quickly broke down and had highly variable aerosol production. More robust elements like polymer wicks (Tepper and Kessick 2008; Tepper and Kessick 2009; Tepper et al., 2007) may spray for a longer time, but high variability is still expected. Electrospray delivery could be improved through the use of a traditional micropump controlled system. However, the second major limitation of this approach is the very strong electrical field compared with the available air flow rate to remove the particles at 2-5 LPM. Spraying required an initializing voltage of 6 kV for a stable ion current. It is known that the typical charge on electrospray droplets is very near the Rayleigh limit (Ganan-Calvo et al., 1997). Insufficient airflow is available to reduce deposition of this aerosol on the charged electrode without deionization. As described, use of a corona needle is not acceptable for inhalation systems. Fu et al. (2011) described the use of radioactive spot ionizers in an electrospray system. However, insufficient space is available in the system to include these units. Increasing the device volume is not practical due to the limited tidal volume used in infant ventilation. Based on these observations, it now appears that the WES system or electrospray in general may not be effective at improving lung delivery efficiency in a ventilated infant system.

Considering the CV device, a high quality submicrometer and almost nanometer scale aerosol was formed with low variability. Heating of the capillary effectively produced a condensation aerosol with some residue of drug remaining on the capillary walls. By

increasing the energy input per solution volume compared with previous CAG systems, the need for a capillary nozzle was removed and a submicrometer aerosol was formed with an aqueous solution. The thermocouple near the tip of the capillary was used to ensure temperature in the range of 100-160 ^{o}C, which may be damaging to some therapeutic molecules. However, previous analysis has indicated that a number of common respiratory medications have low thermal degradation when aerosolized using the CAG device (Hindle et al., 2004). The primary disadvantage of CV was the absence of charge on the condensed aerosol. Previous studies have demonstrated conduction charging with sprays (Zhao et al., 2005) and effects of ions on condensational aerosol formation (Ouyang et al., 1995). However, the charging approach that was selected in the CV study failed to produce a charged aerosol or alter the final aerosol size. This is likely because the system failed to provide an effective field gradient in the region of phase change or the direction of droplet separation. Furthermore, 100 nm particles lack sufficient Brownian motion (Xi and Longest 2008) to foster deposition over the short infant inhalation times. Primarily due to the failure to produce a charged aerosol, the CV device was not selected for further consideration.

The previous study of Golshahi et al. (2015) demonstrated that induction charging coupled with a mesh nebulizer was effective at high flow rates. In this study it was determined that (i) the mesh nebulizer output rate could be reduced to allow for evaporation and formation of a 1.6 μm aerosol and (ii) high delivery efficiency could be achieved at a flow rate of 5 LPM through the device with a charging voltage of 1 kV. Device depositional losses were <15% based on recovered dose, which includes losses on the nebulizer body, SLpT, and charger counter electrode. Perhaps as important, the variability

associated with the delivered aerosol dose was low, with a coefficient of variation of only 4.9%. The previous study of Longest et al. indicated that a 1.8 μm aerosol had only minor losses in a 3 mm endotracheal tube at a flow rate of 5 LPM; however, particle charge effects were not considered in that study. Considering the analysis of Finlay (2001) on electrostatic effects in the lungs, 100 elementary charge units on a 1 μm particle is expected to have a significant impact on deposition. The LF-IC produced >100e with a charging voltage of 1 kV, whereas in the absence of the charging voltage, spray charging from the nebulizer produced only ~10e.

While the LF-IC produces the targeted aerosol size and charge, integration into an infant ventilation system will require addressing several additional challenges. Infant ventilation requires very small tidal volumes. As a result, dead volume in the system may need to be reduced together with connection of the SLpT very near the Y-connector. Inspiration only occurs over approximately 0.5 s with a 1 or 2 s exhalation. Therefore, synchronization of aerosol generation with inspiration will also be necessary. Safety of the system can be ensured by covering the charged counter electrode with a plastic film. Common dielectric materials block electrical conduction but permit the passage of electrical fields.

In conclusion, the LF-IC system was found to produce a targeted aerosol size of approximately 1.6 μm with low device loss, low variability in emitted dose and what is expected to be the correct net particle charge to enhance lung deposition and reduce exhalation of the dose. In contrast, the WES system had both poor emitted dose and high variability. The CV device provided a high quality submicrometer aerosol but negligible net

particle charge. Future studies are needed to integrate the LF-IC device into the infant ventilation system, evaluate aerosol transmission through the endotracheal tube and assess lung deposition and delivery. Selection and development of the LF-IC is a first step toward using small charged aerosols to enhance the delivery of inhaled pharmaceuticals to infants in future studies.

Table 3.1 Experimental parameters of the three aerosol generation systems. A voltage of 6kV was required to generate an aerosol with the WES system, but could be reduced to 1kV with the CV and LF-IC systems. Concentration of albuterol sulfate (AS) was maximized in WES to address the expected low aerosolization rate. Excipients were selected to maximize aerosolization and charging performance of each system. The range of supply air flowing through the devices and to the infant for effective ventilation was 2-5 LPM.

Parameters	**WES**	**CV**	**LF-IC**
Charging Voltage	6 kV	1 kV	1 kV
Aerosolization Rate	0.54 μL/hour*	0.6 mL/hour	2 mL/hour
Formulation	5% $^{w}/_{v}$ AS	0.25% $^{w}/_{v}$ AS	0.25% $^{w}/_{v}$ AS
Excipients	0.02% $^{w}/_{v}$ Poloxamer 188	0.25% $^{w}/_{v}$ NaCl	0.25% $^{w}/_{v}$ NaCl
Supply Air	2 LPM	2 LPM	5 LPM

*For the specific wick and solution combination

Table 3.2 Summary of the AS aerosol delivery characteristics for the WES device (n = 4) with 1 hour of operation. *WES Device* and *Emitted Dose* represent the mass of drug in micrograms remaining in the device flow pathway and emitted from the device, respectively. For the WES, AS device loss was greater than the emitted dose. Moreover, high coefficients of variation in both WES device deposition and emitted dose indicate highly variable performance.

	Mean AS mass (μg)	Coefficient of Variation (%)	Range (μg)
WES Device	11.80	106.0	0.90 – 25.2
Emitted Dose	15.05	109.1	0.71 - 29.9
Total Recovered Dose	26.85	107.4	1.87 – 55.1

Table 3.3 Elementary charges (e) per particle produced by the LF-IC device and measured in the ELPI. Drug deposition on other stages (not shown) were below the HPLC assay limit of detection. 1 kV charging was observed to increase the net charges per particle for all stages (sizes) beyond Stage 4. At the aerosol MMAD (~0.79 μm in the ELPI), 1kV charging increases e by a factor of 12.9x. Furthermore, 1kV charging produces values consistent with Rayleigh limit charging / 100, which is viewed as advantageous for enhanced lung deposition.

ELPI	**Midpoint Diameter (μm)**	$e_{\_Rayleigh/100}$	**1 kV**(e)	**0 kV**(e)
Stage 4	0.21	43.55	2.13	14.82
Stage 5	0.33	83.43	25.91	0.94
Stage 6	0.50	159.88	79.88	12.93
Stage 7	0.79	313.59	169.94	13.17
Stage 8	1.29	653.72	513.83	34.61
Stage 9	2.02	1280.96	1590.35	126.82
Stage 10	3.23	2590.08	9646.40	1822.96

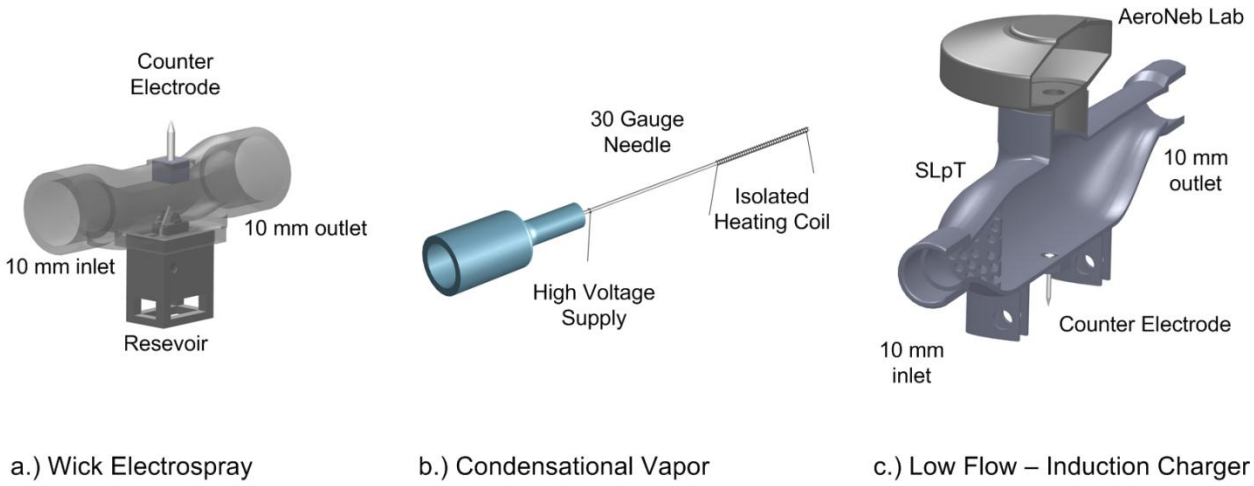

a.) Wick Electrospray b.) Condensational Vapor c.) Low Flow – Induction Charger

Figure 3.1 Pharmaceutical Aerosol Generators

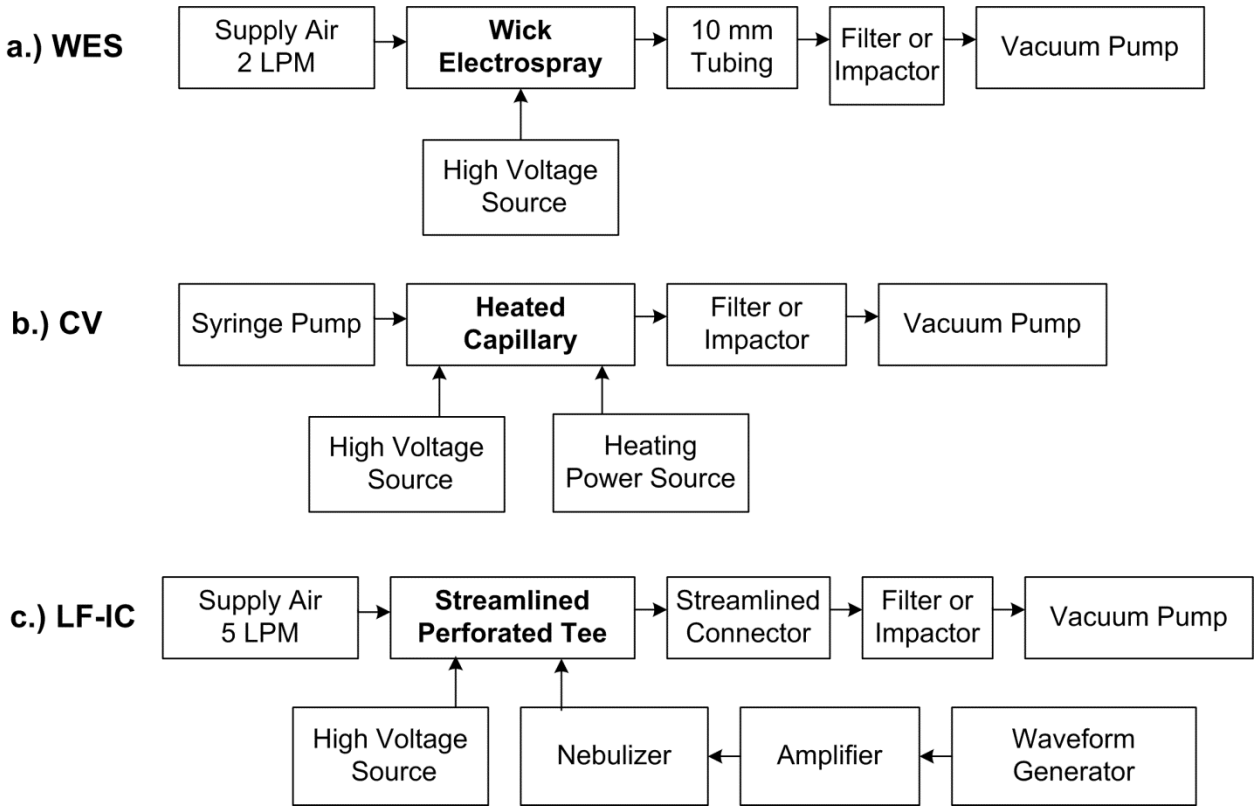

Figure 3.2 Summary of Critical System Components

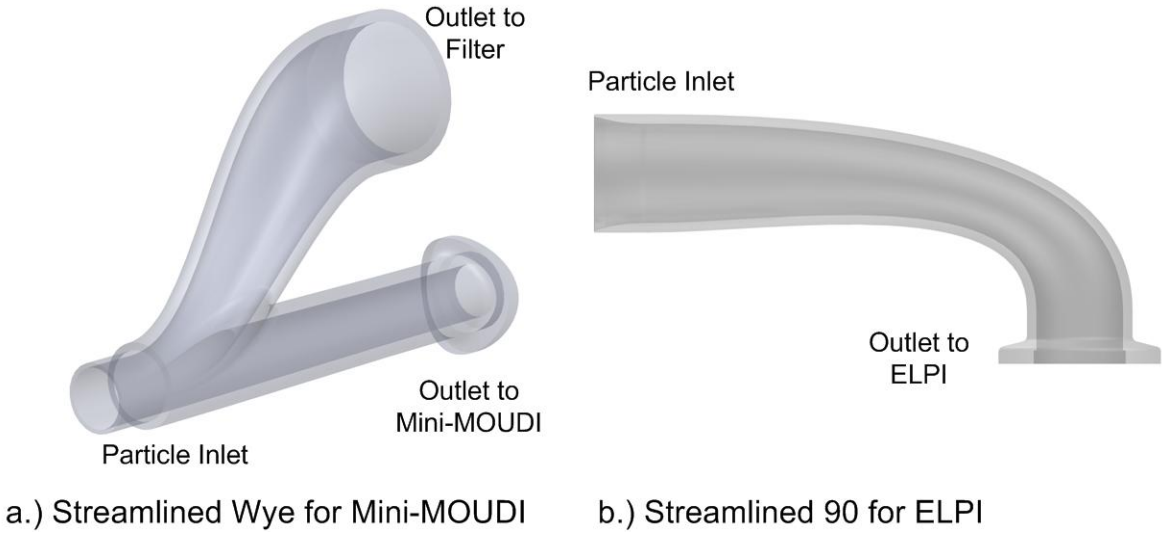

Figure 3.3 Streamlined Impactor Connectors

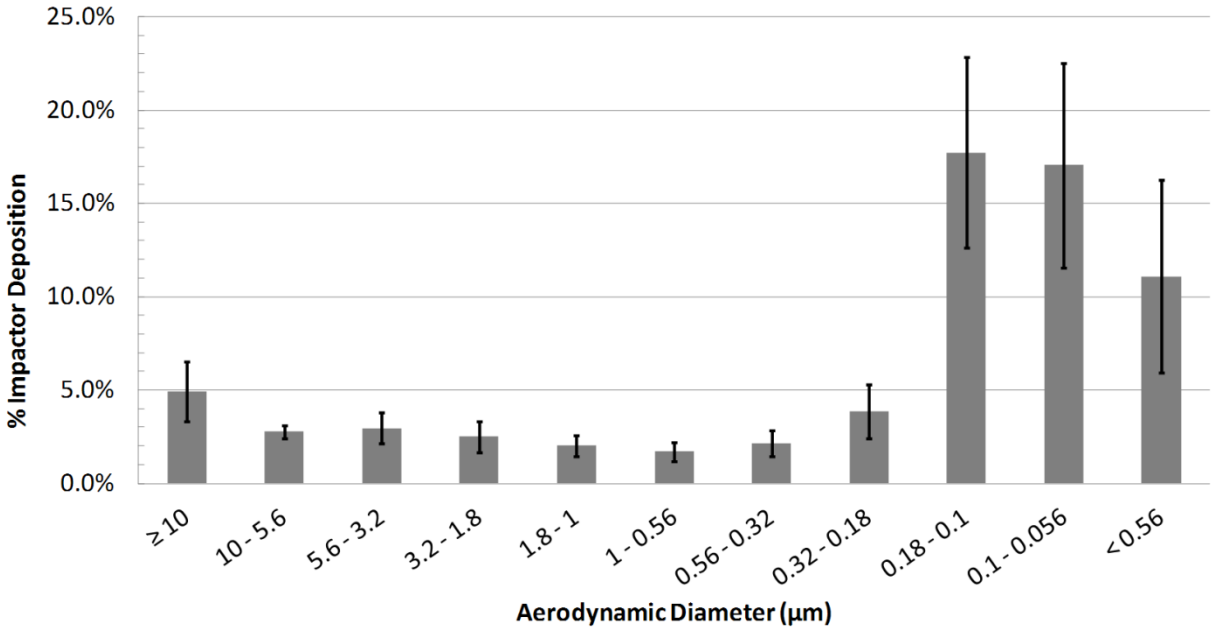

Figure 3.4 Mini-MOUDI Sizing of CV at 2 LPM and 1 kV (MMAD = 0.14 +/- 0.015 µm; n = 3)

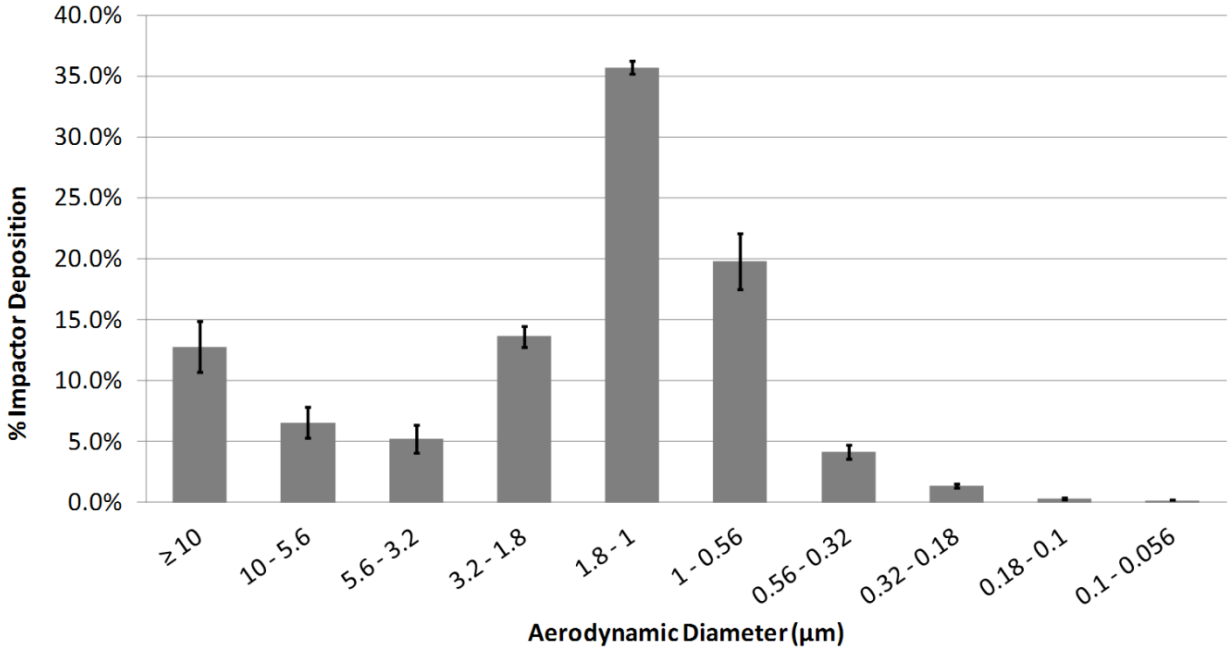

Figure 3.5 Mini-MOUDI Sizing of LF-IC at 2 LPM and 1 kV (MMAD = 1.57 +/- 0.10 µm; n = 3)

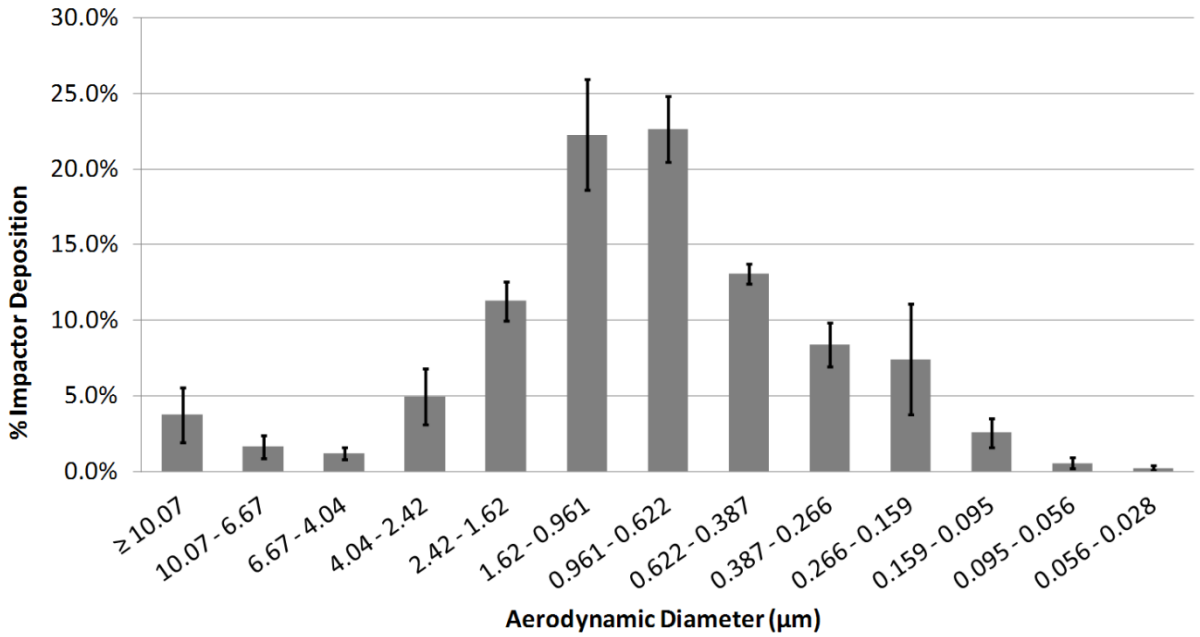

Figure 3.6 ELPI Sizing of LF-IC at 30 LPM and 1 kV (MMAD = 0.882 +/- 0.078 µm; n = 3)

Chapter 4 Charged Pharmaceutical Aerosols in Invasive Mechanical Ventilation

4.1 Introduction

The extent to which poor delivery efficiency of aerosolized medicines limits treatment options for ventilated infants has been highlighted in previous chapters. Increasing the lung delivery efficiency of pharmaceutical aerosols creates opportunities for improved clinical effects of existing medications and will likely expand the number of aerosol therapies available for infants. Aerosol delivery during mechanical ventilation is considered less efficient compared with spontaneously breathing delivery as highlighted in the study of MacIntyre et al. (1985), who clinically demonstrated 2% nominal lung deposition in intubated adult subjects on mechanical ventilation and 12% in non-intubated adult subjects using a nebulizer which generated an aerosol with a mass median aerodynamic diameter between 1 and 5 μm. In this study, seven patients over the age of 49 with various reasons for being connected to mechanical ventilation received aerosolized treatment through a 7 mm endotracheal tube (ETT), while 3 healthy volunteers received aerosolized treatment through a mouthpiece (Macintyre et al., 1985). A significant challenge to aerosol delivery during mechanical ventilation is passing the aerosol through the gas delivery tubing, connection components and patient interface device. Ventilation

components are typically designed for gas delivery, not aerosol administration (Longest et al., 2014a; Longest et al., 2014b). In addition to this, the nebulizer type, location within the ventilation circuit, gas flow, and mode of nebulizer operation are important considerations for increasing aerosol delivery efficiency during mechanical ventilation (Fink and Ari 2013).

During mechanical ventilation in infants, aerosol delivery efficiencies in the range of <1-14% are common, even considering more recent vibrating mesh nebulizer devices (Dubus et al., 2005; Fink 2004; Fok et al., 1996; Mazela and Polin 2011; Sidler-Moix et al., 2013) . In addition to very low aerosol delivery efficiencies, high variability is also a likely reason for clinical failure when infants receive aerosolized medicines (Mazela and Polin 2011; Shah et al., 2007). Small diameter connective ventilator tubing, short inhalation periods, and small tidal volumes all contribute to ineffective aerosol delivery to ventilated infants (Fink 2004; Rubin and Fink 2001). Much work is still needed to improve aerosol delivery efficiency and reduce variability in mechanically ventilated infants, such that the clinical benefit of existing medications can be maximized and new inhaled therapies can be developed (Brion et al., 2006; Cole et al., 1999; Fink 2004; Rubin and Williams 2014; Shah et al., 2007).

Through the use of mesh nebulizers and new ventilation connection components, aerosol delivery efficiency has recently been improved for ventilated infants. A macaque animal model of a ventilated infant was used to demonstrate 12 – 14% of the aerosolized dose through a 3 mm infant ETT using a vibrating mesh nebulizer synchronized with inspiration and without bias flow (Dubus et al., 2005). Using a jet nebulizer in an *in vitro* model of a ventilated premature infant, with a new connector to separate nebulizer and

ventilation gas bias flow, Mazela et al. (2014) increased albuterol sulfate delivery efficiency from 1% or less through the commercial Y-connector to a maximum of approximately 7% with the improved connector, before the ETT or mask. Additional aerosol losses are known to occur in the infant ETT, which can have an internal diameter as small as 2.5 mm. Similar to the 12.6-14% *in vivo* model deposition fraction range predictions of Dubus et al. (2005), Longest et al. (2014b) used *in vitro,* whole lung, and CFD modeling techniques to predict the lung deposition fraction for a newborn full-term infant under mechanical ventilation through an ETT using commercial connection components (6.8 – 13.5%). A new streamlined Y-connector was then implemented with synchronized delivery and reduced droplet sizes (~ 1.8 μm) to optimize aerosol deposition in the infant lungs (Longest et al., 2014b). For a full term (3.6 kg) infant and 3 mm ETT, maximum total lung delivery efficiency of a polydisperse aerosol with a mass median aerodynamic diameter (MMAD) of 1.78 μm reached 45.2%.

In this chapter, depositional losses in a commercial infant ventilation circuit are determined using a commercial mesh nebulizer and the previously determined (Chapter 3) best performing charger design, the low-flow induction-charger (LF-IC). The ventilation circuit is driven by a steady-state air-flow of 5 LPM and the estimated lung delivered dose is collected on a filter at the end of a curved 3 mm (ID) ETT and quantified using a validated HPLC method. The drug remaining in the nebulizer, LF-IC, streamlined Y-connector, and a 3 mm ETT are collected and compared to the lung delivered dose. The performance of the delivery system is also quantified in terms of time as the delivery rate of drug to the lung. The reduced mass output of the LF-IC is expected to have a smaller drug delivery rate to the lung, but the increased efficiency is intended to minimize drug waste and reduced

intersubject variability in cases where adequate delivery times are available, as with mechanical ventilation. Additionally, the run time will be varied to examine the effect of charge accumulation on electrically insulated components under steady-state flow conditions. The LF-IC is designed to target the deposition of pharmaceutical aerosols in ventilated infants by reducing the particle size to penetrate the delivery system with the addition of an induced charge on the droplets to foster lung deposition and reduce exhalation of the inhaled dose (Chapter 3). An aerosol mass median aerodynamic diameter that is smaller than typically delivered, i.e., approximately 1.8 μm or less, is necessary to bypass the delivery system with acceptable losses at typical flow rates used with a neonate (Longest et al., 2014b).

The objective of this study is to compare the performance of the previously developed LF-IC with a commercially available nebulizer in an infant ventilation circuit under steady-state and cyclic flow conditions. The LF-IC and commercial device performances are evaluated by the quantification of albuterol sulfate (AS; model drug) mass recovered using HPLC in the following system components (Figure 4.1):

1. Exhalation filter;
2. Ventilator components (commercial or streamlined Y-connector);
3. Nebulization device and connectors (Aeroneb Lab, commercial T-connector, LF-IC);
4. Endotracheal tube; and
5. Lung filter.

After implementing the previously developed LF-IC in an infant ventilation circuit experiencing steady-state air-flow, the LF-IC is redesigned to minimize device volume for

use with cyclic flow conditions and to allow for the inclusion of a ventilator flow meter, a new common feature in mechanical ventilation systems that has not adequately been considered in previous studies. This redesigned LF-IC also incorporates a breath actuated nebulizer to increase delivery of aerosolized drug to the patient and reduce the exhaled dose.

4.2 Systems & Methods

4.2.1 Overview of Systems

In this study, commercial and modified aerosol delivery systems were compared for full term neonates receiving invasive mechanical ventilation. Both systems utilized a vibrating mesh nebulizer to produce an aerosol. The commercial system included a commercial T-connector, commercial Y-connector, and a continuous nebulization signal (Figure 4.1a). Modifications to the systems included: a reduced nebulizer signal, synchronized nebulizer timing, introduction of a low flow-induction charger, and a streamlined Y-connector (Figure 4.1b). Two flow conditions were evaluated with each system, steady state and cyclic ventilation. Steady state flow conditions allow for simplified experiments to be conducted at the same flow rates of previous characterization studies (Chapter 3). The cyclic flow condition provided a better comparison with clinical use and *in vivo* studies. To avoid running a full matrix of experiments, selected cases were defined and presented in Table 4.1. An additional case was considered to evaluate the effects of extended run times and the potential for static charge buildup on insulated ventilation circuitry. Elements of the delivery systems and flow conditions are described in the following paragraphs.

As described in Chapter 3, the driving signal of the vibrating mesh nebulizer (Aeroneb Lab; Aerogen Limited, Galway, Ireland) was altered to reduce the momentum of the aerosol stream and to reduce the water mass in the system. The reduced momentum was expected to reduce depositional loss in the LF-IC. The reduced water mass allowed for evaporation of the nebulized droplets to achieve a small size (MMAD) and this was expected to reduce losses in the ventilator components and 3 mm ETT (Teleflex Medical; Research Triangle Park, NC). Drug mass deposition in system components and on the lung filter (Pulmoguard II filter; Quest Medical; Brockton, MA) were quantified for the commercial and modified systems using high performance liquid chromatography (HPLC) to determine albuterol sulfate concentrations (Spectrum Chemicals, New Brunswick, NJ; model drug commonly used as a bronchodilator). Nominal dose was determined by weighing the nebulizer after loading the nebulization solution and after nebulization. The difference was multiplied by the concentration of AS in the solution (0.25%) and the nominal sprayed mass of AS was determined. The methods for fabrication and use of the original LF-IC with an albuterol sulfate and sodium chloride nebulization solution can be found in Chapter 3. LF-IC methods presented in this chapter refer to changes in the redesigned LF-IC for cyclic ventilation.

To expand upon previous evaluations with steady state flow conditions, the current study also included analysis during cyclic ventilation. The cyclic ventilation flow condition was generated by a Galileo ventilator (Hamilton Medical Inc; Reno, NV) and a Model 1601 Adult/Infant Training/Test Lung (Michigan Instruments; Grand Rapids, MI) to simulate the breathing cycle (inhalation, exhalation, and breath pause). Expansion to cyclic ventilation required two new components in the flow circuit, which are ventilator flow meter and the

exhalation filter. Both of these necessary components provide additional sources of aerosol loss that must be analyzed and minimized in this study.

The working principles of the inline flow meters that are common to many current generation ventilators are: hot wire anemometry, variable orifice, screen pneumotacograph, and ultrasonic (Schena et al., 2015). The impact of these flow meters, which are required for most modern ventilators to properly function, on aerosol delivery to ventilated patients has not been adequately assessed. Many ventilators, such as the one used in the current study, utilize an embedded inline flow meter containing a screen with small holes which cannot be removed from the ventilator circuit due to feedback controls and patient alarms. These flow meters are needed due to the importance of monitoring the ventilated volume to reduce the incidence of ventilator induced lung injury (Slutsky 2015). (Kacmarek 2011).

During cyclic ventilation, the redesigned LF-IC (Figure 4.2) utilizes a reduced device volume and a breath synchronized nebulization phase to increase delivery efficiency. This synchronization is controlled by two electrical relays that are triggered by the breathing pattern of the infant ventilator. Further details of LF-IC redesign and experimental testing methods for these systems are described in the following sections and summarized in Table 4.1.

4.2.2 Steady State Flow Condition

Aerosol delivery during 5 LPM steady state flow is quantified in an infant ventilation circuit, System 1.1, by washing individual components in deionized water and determining

the concentration of drug mass by HPLC using validated techniques as described in Chapter 3. Depositional accumulation of droplets on the walls of the nebulizer in the commercial system caused dripping from the nebulizer into the T-connector, necessitating the grouping of nebulizer and T-connector in the wash. To retain consistency across the systems, this procedure was also followed for the LF-IC, even though the aerosol did not accumulate in the nebulizer and drip into the LF-IC. The aerosol first enters the commercial neonatal T-connector (Aerogen Limited) where it is entrained in the 5 LPM supply air (relative humidity < 10%). It then passes into a commercial Y-connector (included in a neonatal conventional ventilation circuit, (Teleflex Medical; Research Triangle Park, NC)) that has the exhalation port sealed. The base of the Y-connector connects directly to an uncuffed ETT curved through a 90 degree bend with a 3 cm radius of curvature, representing passage through the infant oropharyngeal region (Longest et al., 2014b). The sterile ETT has an inner diameter of 3 mm and an outer diameter of 4 mm, consistent with use in a full-term neonate. The outlet of the ETT is positioned inside the Pulmonguard II filter and is less than one centimeter from the filter surface inside the filter plastic housing. The connection between ETT and filter is open to atmosphere to allow different airflow through the ventilation components and the filter. 5 LPM was pushed through the system using a compressed gas source, as with invasive mechanical ventilation, while 20 LPM was pulled through the filter using a downstream vacuum pump intended to capture the aerosol exiting the ETT during the 0.5 minute experiment. A summary of the critical components in System 1.1 is shown in Figure 4.3a.

To improve aerosol delivery, streamlining, induction charging, and reduced nebulization output (modified system) were evaluated under steady state flow conditions

in System 1.2. The experimental setup for System 1.2 was the same as Figure 4.3 a, but with streamlining to reduce depositional loss and the replacement of the commercial T-connector with the LF-IC. The modified Aeroneb nebulizer operates on a sinusoidal signal with an amplitude of 32.4 volts peak-to-peak (VPP) and a frequency of 128.2 kHz to reduce the emitted mass and the initial momentum of the nebulized aerosol. Since the modified system has a mass output that is $1/10^{th}$ the commercial system, the runtime for System 1.2 was increased from 0.5 minutes to 1 minute to keep the minimum mass concentration values within the same range for the HPLC calibration curve. In addition to comparing commercial nebulization with the LF-IC under steady state conditions, the 1 minute operation of System 1.2 was increased to 30 minutes to consider the buildup of charged droplets depositing on the insulated components over time (System 1.3). HPLC washing and drug mass calculation methods are unchanged from Chapter 3.

4.2.3 Commercial Delivery System during Cyclic Ventilation

The Galileo ventilator provides pressure controlled constant mandatory ventilation (P-CMV). Positive end-expiratory pressure (PEEP) is set to 5 cm H_20 and $P_{control}$ is set to 15 cm H_20 resulting in a peak inspiratory pressure (PIP) of 20 cm H_20. The rise time for pressure in a pressure controlled setting, P_{ramp}, is set to 100 ms. The number of breaths per minute is set to 30. Each 2 second breath is composed of 0.6 seconds of inspiration and 1.4 seconds of expiration, giving an I:E ratio of 1:2.3. These choices are consistent with target infant parameters for a 3.55 kg infant from Walsh & DiBlasi (2010) and are summarized in Table 4.2.

The Galileo ventilator has a bias-flow to remove the exhaled gas and reduce patient rebreathing of CO_2. The ETT is inserted and sealed into a Pulmoguard II filter with the filter housing outlet attached to the training test lung (TTL) operating in infant mode. The resistance and compliance of the TTL are selected to have values of 20 cm H_20/L/sec (Rp20) and 0.002, respectively. Resistance and compliance value selection is based on the study of Abbasi et al. (2012). The cyclic flow conditions have an additional filter at the exhalation outlet of the Y-connector to capture the exhaled dose as shown in Figure 4.3b. The commercial cyclic ventilation setup, System 2.1, is run for one minute with continuous nebulization (Table 4.1).

4.2.4 Modified Delivery System During Cyclic Ventilation

To reduce the loss of drug due to bias flow, the commercial system was modified by changing the location of the nebulizer (Figure 4.3c). The nebulizer was moved from the inspiratory line to after the Y-connector. The LF-IC is redesigned for use in System 2.2 due to the relocation proximal to the patient. The redesigned LF-IC has a reduced internal volume to overcome the low tidal volume of air available which passes through the ETT and into a ventilated infant. The original LF-IC with the 45 mL air space was acceptable in the inspiratory line because the bias-flow prevented re-breathing of exhaled gasses. The new LF-IC shown in Figure 4.2 is streamlined to seamlessly connect the ventilator flow meter, Aeroneb Lab nebulizer, and the 3 mm ETT. The internal volume of the LF-IC has been reduced from an acceptable 45 mL (Chapter 3) positioned upstream of the Y-connector, to 6.7 mL. This reduced downstream volume is necessary to minimize re-breathing, a 45 mL device placed after the Y-connector would prevent effective ventilation

of a 3.55 kg infant having a tidal volume of approximately 28 mL. The distance between the induction electrode and the nebulizer's mesh surface is decreased from 47.6 to 46.0 mm. The induction charging voltage is also decreased from 1 kV to 0.5 kV because the depositional losses in the LF-IC were too great in preliminary experiments (data not shown). The increased losses were due to the reduced air flow during the periods of synchronized nebulization in the cyclic breathing condition. This reduction in charging voltage is expected to lessen the impact the charged aerosol has on the exhaled fraction when the system is implemented in a breathing lung. This and other system parameters are tabulated and grouped in Table 4.1.

In addition to this reduced volume, breath synchronized nebulization is utilized to reduce the amount of aerosol that is being lost before inhalation. The Galileo ventilator has an internal relay that can be used to trigger an external nebulizer for delivery of aerosol during inspiratory flow or expiratory flow. A standard external Multifunction Timer Relay (Finder Relays, INC.; Suwanee, GA) was operated in On-Delay mode and connected in series with the internal relay to allow for a delayed trigger from the beginning of inspiration or expiration (Figure 4.4). The time delay was adjusted to trigger the nebulizer 1.29 seconds after the beginning of expiration, and that is 0.11 seconds before inspiration (Figure 4.5). The duration of nebulization was 0.11 seconds. These values were based on a preliminary optimization study (data not reported) that considered both the length of nebulization and the best nebulization start time evaluated at multiple time points in the inhalation and exhalation breathing periods. A 20 volt DC signal is supplied by a laboratory DC power supply (Tenma Test Equipment; Springboro, OH) to the internal Galileo relay such that

during expiration, the 20 volt signal is supplied to the on-delay relay, and during inspiration no signal is present at the on-delay relay.

Another important difference between the commercial and modified system is the relocation of the nebulizer from before the flow-meter to after. The flow-meter embedded in the Hamilton Galileo ventilator is a variable orifice meter which has a plate that will open like a flap to create a variable resistance with respect to flow rate and a lower pressure drop across the device. Modern ventilation systems cannot be properly operated without their embedded flow-meters due to the required volume-control feedback circuit. These flow-meters have undocumented effects on aerosol delivery.

4.3 Results

4.3.1 LF-IC Performance during Steady State flow

The LF-IC (System 1.2) is compared with the commercial setup (System 1.1) under steady-state conditions to determine aerosol mass balance, locations of aerosol deposition, and delivery rate of drug to the filter. To establish mass balance, the recovered drug mass was divided by the nominal dose for Systems 1.1 and 1.2, resulting in 97.3 (2.6)% and 95.2 (2.7)% recovery during steady-state flow, respectively. The commercial nebulizer and T-connector contained 59.9 (1.5)% of the deposited AS, while the modified system had 22.2 (5.3)% of the deposited aerosol in the LF-IC (nebulizer and streamlined T-connector). Aerosol deposition in the commercial Y-connector was 12.7 (3.0)% of the albuterol sulfate mass recovered. The streamlined Y-connector connected to the LF-IC contained 4.9 (0.7)% of the deposited aerosol. In both systems, about 17% of the drug mass was recovered in

the ETT. The commercial setup, System 1.1, achieved 10.0 (2.6)% delivery of the albuterol sulfate solution to the lung filter, while the LF-IC in System 1.2 achieved 48.9 (6.4)% deposition of the charged aerosol on the lung filter (Table 4.1). These findings are shown graphically in Figure 4.6, where error bars represent +/- 1 SD.

Having determined the deposition locations of the aerosolized albuterol sulfate, the total mass recovered and rate of delivery to the filter are reported for Systems 1.1 and 1.2. The mean (SD) total masses of albuterol sulfate recovered (n = 3) in the commercial and modified setups were 976.4 (56.9) μg and 128.7 (14.4) μg, respectively. The commercial system demonstrated a drug delivery rate of 156.0 (52.0) μg/min to the lung filter with a coefficient of variation (CV) of 33.3%. The LF-IC's drug delivery rate in the modified system was 67.7 (10.5) μg/min to the lung filter at 5 LPM steady state flow, resulting in a CV of 15.5%. Therefore, the LF-IC had approximately 50% of the commercial setup drug delivery rate to the lung filter, but improved delivery efficiency to the lung filter by a factor of 5 and reduced variability in terms of the delivery rate CV 2-fold.

4.3.2 Delivery Time Comparison in Electrically Insulated Connectors

The LF-IC was run for 30 minutes at the same steady state air flow rate of 5 LPM using the same drug solution as considered in Section 4.3.1 to examine the effect of static charge buildup associated with increased runtime (i.e., System 1.3). With the 30 minute run, the mean (SD) drug mass as a percentage of total recovery in the nebulizer and T-connector was 24.2 (12.3)%. Under the 30 minute run conditions, the streamlined Y-connector had 5.9 (1.6)% of the recovered drug mass. The ETT captured 21.7 (17.0)% of the recovered drug mass. The efficiency of the LF-IC in delivering drug to the filter was

48.2 (17.2)% over the 30 minute run compared to 48.9 (6.4)% for the same conditions and a 1 min run. The drug delivery rate to the filter was 67.5 (25.8) μg/min over 30 minutes with a total recovered mass of 4182.6 (175.9) μg in the system. The overall recovery of drug was 99.0 (0.9)% of the nominal dose indicating excellent mass balance as reported in Table 4.3. The results examining the impact of runtime on deposition in the steady state circuit are summarized graphically in Figure 4.7. Based on these findings, there does not appear to be a build-up of static charge over a 30 minute run that can influence depositional loss in the system.

4.3.3 LF-IC Performance during Cyclic Ventilation

As with Systems 1.1 – 1.3, System 2.1 and System 2.2 are evaluated to determine mass balance, aerosol deposition location, and rate of drug delivery to the inhalation filter. Recovered drug normalized by nominal dose, mean (SD), for the commercial system was 94.1 (3.3)% and for the modified and charged system was 101.2 (2.4)% of the nominal dose under cyclic ventilation conditions. Evaluation under realistic cyclic flow conditions allows for measurement of the albuterol sulfate that is exhaled before it enters the patient, in the commercial [16.2 (3.7)%] and the modified [18.6 (1.7)%] systems. The mean (SD) commercial loss of drug in the Y-connector is 7.9 (3.5)% of the recovered dose. This is in contrast to the loss in the Y-connector using the LF-IC, which was only 1.2 (0.5)%. The infant ventilator's flow meter captured 4.8 (3.9)% of the drug in the commercial system and 4.0 (0.4)% of the drug in the modified system. The nebulizer and T-connector contained 67.6 (4.4)% of the recovered albuterol sulfate in the commercial system, while 25.2 (2.8)% was in the nebulizer and T-connector in the modified system. Drug mass

recoveries in the ETT for the commercial and modified systems were 1.7 (1.7) and 17.1 (1.0)%, respectively. The lung filter captured 1.3 (0.6)% of the recovered albuterol sulfate in the commercial system and 34.0 (1.7)% of the recovered albuterol sulfate in the charged and modified system. These results are displayed in Figure 4.8. The delivery efficiencies of Systems 1.1 through 2.2 are summarized in Table 4.4 and used to compared efficiencies across all the systems in the discussion.

During a runtime of 1 minute, the commercial system delivered 25.6 (10.6) μg of albuterol sulfate to the lung filter under cyclic ventilation conditions (System 2.1). The coefficient of variation (CV) of drug mass delivered for System 2.1 was 41.4%. The modifications applied to the LF-IC caused the modified setup (System 2.2) to deliver 70.4 (2.6) μg total or 3.52 (0.13) μg/min of albuterol sulfate to the lung filter during the 20 minute run. The CV of the drug mass delivered for the modified system was 3.7%. 2043.5 (253.0) μg of albuterol sulfate was recovered in the commercial system under cyclic ventilation. 207.4 (9.1) μg albuterol sulfate was recovered in the modified system under cyclic ventilation. As a result, for realistic cyclic ventilation condition, the modified system reduced drug delivery rate by a factor of 7-fold, but improved drug delivery efficiency to the lung filter by a factor of 26-fold.

4.4 Discussion

In Chapter 3, a novel aerosol generation system was designed and selected to produce a charged aerosol with a mass median aerodynamic diameter (MMAD) in the range of 1-2 μm. This approximate size was chosen to minimize deposition in the ventilation circuitry and ETT, while the charge was added to reduce the exhalation of the small aerosol inhaled

by the patient, which will be evaluated in later chapters. *In vitro* testing of the novel LF-IC system in mechanical ventilation circuits was determined to be necessary to verify the reduction in losses due to reduced MMAD and ensure the induced charge on the aerosol did not counteract the benefits associated with smaller particle size and streamlined designs.

The total losses in System 1.2 were about one half (Table 4.4) of the losses in the commercial system under steady state flow (System 1.1). As expected, the reduced momentum of the aerosol stream in System 1.2 caused the constant 5 LPM airflow to clear the aerosol more effectively than in System 1.1. In the commercial system, 40% of the aerosol exits the device, while nearly double the amount (78%) of charged aerosol exits the device in the modified system with the induction charger located in the T (LF-IC) under steady state conditions (Table 4.4). Because the droplet size of the commercial device is so large and the commercial connector has abrupt 90° changes of flow direction, 12.7% of the generated aerosol is lost in the Y-connector in System 1.1. This is in contrast to the 1.6 μm aerosol navigating the streamlined-Y and losing 4.9% in System 1.2. In Table 4.4, the fractions lost in the ETT appear to be equal, but this is deceiving because System 1.2 has a larger fraction entering the ETT than System 1.1 (72.9% vs. 27.4%). If the recovered fraction in the ETT is normalized by the amount entering, then System 1.1 will have 64% of the remaining dose deposit in the ETT, while System 1.2 will only lose 24% of the remaining dose in the ETT. The reduction of MMAD and introduction of charge on the aerosol reduces the depositional losses on the ventilation circuit as proposed in Chapter 3 and leads to a 5X improved dose to the lung filter (48.9% vs. 10.0%) under steady-state flow conditions.

Having characterized the LF-IC and evaluated it against a commercial device under steady-state flow conditions, a realistic cyclic ventilation setup was necessary to compare the LF-IC to clinical studies and examine the impact of new components and parameters. For the commercial system under cyclic flow (System 2.1), the periods of no flow with continuous nebulization increased the amount of drug lost on the nebulizer and T-connector from 59.9% to 67.6% (Table 4.4). The fraction remaining after exiting the T-connector is 32.4% of the nebulized fraction. Half of this (16.2%) is lost to the exhalation filter because of the continuous nebulization and bias flow. Three quarters of the remaining fraction is then lost in the Y-connector and flow meter. This leaves about 3% of the aerosol to either be lost in the ETT or inhaled by the patient. More than half of the aerosol that reaches the ETT is lost there. This leaves only 1.3% of the nebulized aerosol available to the patient to be inhaled (with an additional high fraction likely exhaled).

This result of 1.3% deposition in the inhalation filter with a high quality mesh nebulizer using a commercial setup is much lower than the 12.6% deposition reported in the study of Dubus et al. (2005), which considered deposition of an aerosol produced by a synchronized vibrating mesh nebulizer in four intubated macaques. One major difference is in the study of Dubus et al. (2005) the ventilator used did not have an embedded in-line flow meter or a bias flow to overcome. All of the 25 ventilators (from 10 different manufacturers) reviewed by Schena (2015) contain embedded inline flow-meters. Future mechanical ventilators will likely continue the current trend of increasing patient monitoring and feedback controlled based on various meters allowing for improved ventilation synchrony (Kacmarek 2011). The Galileo ventilator used in this study is more consistent with current and likely future mechanical ventilation practice than previous studies which often do not

include flow meters or bias-flow, and is therefore an accurate assessment of mesh nebulizer performance in current clinical scenarios.

This study maximized delivery during cyclic flow using a new LF-IC positioned downstream of the Y-connector with a modified signal and synchronized with breathing. For the modified system under cyclic flow, System 2.2, a charged aerosol is generated in a region with an electric field and zero airflow, 0.11 seconds prior to inhalation producing 25.2% deposition of the nebulized aerosol in the charging region. The remaining 74.8% is then transported by the inhalation flow through the ETT, where a fraction of the aerosol deposits, reducing the potential inhaled fraction to about 58% (based on how much is lost in the ETT during inhalation in System 2.2). 34% of the aerosol is deposited in the lung filter, leaving the remaining 24% that does not reach the filter to be exhaled through the ETT and deposited on the exhalation filter (Table 4.4). In the results of Longest et al. (2014b), approximately 60% delivery efficiency to the lung was possible using numerical modeling; but nebulizer and T-connector deposition was neglected. If nebulizer and T-connector deposition is added to the lung filter deposition for system 2.2, 59.2% deposition is estimated. This excellent agreement highlights the need for future studies to further reduce T losses. The nebulizer relocation, signal modification, and synchronization with delivery contributed to a 26 fold increase in inhaled dose in the modified system (34% vs. 1.3%).

Initial experiments (not reported here) showed very low inhaled dose when the LF-IC was upstream of the Y-connector under cyclic ventilation. Redesigning and moving the LF-IC downstream of the Y-connector and the flow-meter reduced the number of potential

deposition sites during inspiration and decreased the dead volume to increase efficiency and demonstrate the large influence of nebulizer positioning within the circuit. The charged aerosol in this study likely decreases the amount delivered to the inhalation filter, but in future studies that consider exhalation, a charged aerosol is expected to enhance deposition. Initial experiments (not reported here) also showed large influence of nebulization delivery timing as various durations and starting times of nebulization were explored before selecting 0.11 seconds prior to inhalation. The exhaled fraction can be viewed as the fraction of drug that could be gained by reducing dead volume or improving synchronization of nebulization. Additional optimization of synchronization timing may increase the delivery rate, perhaps without decreasing the delivery efficiency. Future work will need to consider timing aerosol generation to begin during exhalation, but continue into the beginning of inspiration. This will require better ventilator control of the attached nebulizer or additional hardware such as a "true-off/on delay" to implement. This additional hardware would allow for control of the activation and duration of nebulization as opposed to only controlling the onset or activation of the nebulizer and using the change of breath phase to turn off the device. Potential optimization is still available to deliver more aerosol in a shorter amount of time. The maximum delivery rate under cyclic conditions derived from the modified system under steady state conditions is 20.31 μg/min.

The device volume has been reduced through redesign, but the filter still provides a large dead volume of air that is expected to artificially reduce the capabilities of both the commercial and LF-IC systems. The dead volume of the filter and the ventilator components mean that generated aerosol will still be in the line after inhalation and

remaining mass will be exhaled. Clinically, dead volume is a critical quantity that must be minimized to reduce the amount of re-breathing of exhaled gas a patient incurs.

Commercial delivery rate decreased from 156 μg/min to 25.6 μg/min due to the cyclic breathing profile, ventilator flow meter deposition, and bias flow (System 1.1 vs. 2.1). The delivery rate of the LF-IC decreased from 67.7 μg/min to 3.52 μg/min, primarily due to the reduced spraying time of the synchronized nebulizer, 0.11 seconds spray for every 2 second breath. Based on the maximum delivery rate from System 1.2, 67.7 μg/min, and the ratio of inspiration to total breathing cycle, 0.3 (T_{insp}/ T_{Breath}), the maximum delivery rate expected is 20.3 μg/min using the current setup. The commercial system delivers 7.27-fold more drug to the inhalation filter in one minute than the modified system does; however, if the modified system is run for long enough to deliver the equivalent mean mass as the commercial system, approximately 7.3 minutes, the standard deviation is 0.95 μg as compared to the commercial standard deviation of 10.6 μg. This 10 X decrease is equally demonstrated in the 11.2 fold reduction of CV from 41.4% to 3.7% for commercial and modified delivery rate of inhaled dose, respectively. As described above, the main advantage of the modified system is a 26-fold improvement in delivery efficiency of the nebulized aerosol to the lungs. This improvement is critical for providing efficient and reproducible lung delivery of therapeutic aerosols.

In designing this system for delivering aerosolized drugs, drugs that have high cost and significant side effects are being primarily considered. Surfactants are very expensive, steroids need low variability due to adverse side effects, and antibiotics need to be delivered in high and consistent doses to prevent survival. Albuterol Sulfate is inexpensive,

has low side effects, doesn't require a large dose, and is therefore acceptable using the inefficient and highly variable devices that are currently available. The LF-IC is then ideally positioned to deliver drugs such as surfactants, antibiotics, and steroids (as well as others) because the emphasis of design is on efficiency rather than speed. Even with the reduced drug mass delivery rate of the LF-IC, the reduction in variability allows for equivalent dosing with reduced variability when the patient is treated for a longer time. Some medications, like surfactants, are very expensive. Clinical trials of surfactants have had inconclusive or mixed outcomes likely due to high variability and poor lung delivery efficiency (Berggren et al., 2000; Finer et al., 2010).

The steady state system uses room temperature air to flow through the system at 5 LPM, while the cyclic system utilizes a heater to maintain an approximately 35° Celsius inspiratory line. A humidifier was not connected in the cyclic ventilation system; rather the patient is reliant on the liquid content of the evaporating aerosolized droplets in the heated line to prevent the cooling and drying of the airways by dry and cold ventilation gas. Dubus et al. (2005), who provides the current benchmark of *in vivo* delivery in macaques with 3 mm ETTs, did not use a system with added heated or humidity. Additionally, the ventilator that was used did not have bias flow or an in-line flow meter (Dubus et al., 2005). Among others, bias flow, humidity, and position of aerosol device in the circuit, have been shown to be important factors for improving mechanically ventilated aerosol delivery efficiency (Ari and Fink 2015). The system considered in this study delivers humidity through the nebulization of an aqueous solution because removal of humidity from the inspiratory line is not recommended for the patient's well being and safety (Ari and Fink 2015). Using a heated and humidified line, Mazela et al. (2014) delivered 6.6% of a nominal albuterol

sulfate dose to the end of the Y-connector in a mechanical ventilation system; however, an ETT was not considered. This system used a novel VC connector to bypass bias flow and improve delivery of a jet nebulizer to a delivery rate of 2.9 μg/min (Mazela et al., 2014).

In conclusion, the LF-IC system was found to increase the lung delivery efficiency during steady state ventilation from 10.0% to 48.9% and during cyclic ventilation from 1.3% to 34.0%. This 26-fold improvement in the lung dose efficiency of the LF-IC over the conventional nebulizer is expected to be even higher in clinical trials due to reduced efficiency of the conventional system resulting from the increased model accuracy of predicting exhalation of inhaled pharmaceutical aerosols. The induced charge on the aerosol from the LF-IC is expected to enhance deposition in the small diameters of the infant airways, while the commercial aerosol which reaches the lungs will likely be exhaled at a higher fraction. The CV of the lung dose using commercial delivery under steady state flow (System 1.1) was 26% and decreased to 13% in the modified system under steady-state flow (System 1.2). In the cyclically ventilated systems, the CV decreased from 46.2% in the commercial system (System 2.1) to 5% in the modified system (System 2.2).

This study has implemented, with progressively more realistic flow conditions, the previously developed and characterized LF-IC. The LF-IC produces a charged aerosol with a mass median aerodynamic diameter (MMAD) of 1.6 μm and was designed to decrease losses in the device and breathing circuit while increasing efficiency of delivery to the lung. Successful integration of the LF-IC into an invasive mechanical ventilation circuit was achieved through volume reduction, streamlining, synchronization and nebulizer placement within the breathing circuit. The tested systems were compared in terms of

mass efficiency of delivery and time of therapy efficiency. Based on the superior efficiency performance (26 fold improvement of inhaled dose) and the reduced variability (11-fold reduced CV of delivery rate) of the LF-IC system over the commercial system under cyclic flow conditions, further testing and implementation of the new LF-IC in clinical or highly realistic *in vitro* models is suggested.

Table 4.1 Systems examined to evaluate aerosol transmission (steady airflow) and the effects of cyclic ventilation.

System	Charging Voltage (kV)	Runtime (min)	Air-flow Conditions	Nebulization Signal	Nebulization Timing
1.1	0	0.5	Steady	Commercial	Continuous
1.2	1	1	Steady	32.4 VPP*	Continuous
1.3	1	30	Steady	32.4 VPP*	Continuous
2.1	0	1	Cyclic	Commercial	Continuous
2.2	0.5	20	Cyclic	32.4 VPP*	0.11 (s) before inhale

***VPP – Peak-to-Peak Voltage**

Table 4.2 Ventilation parameters to represent invasive mechanical ventilation of a full term neonate (3.55 kg) based on Walsh & DiBlasi (2010).

Ventilation Parameters	
Pcontrol	15 cm H20
Peep	5 cm H20
Pramp	100 ms
Ventilation Mode	P-CMV
Breath/Min	30
Tinsp	0.6 s

Table 4.3 Total drug mass recovered (standard deviation) as a percentage of estimated nebulized drug [n = 3]. Values near 100% indicate that the washing process was thorough and aerosol was not lost from the system.

System	Recovery (% Nominal)
1.1	97.3 (2.6)
1.2	95.2 (2.7)
1.3	99.0 (0.9)
2.1	94.1 (3.3)
2.2	101.2 (2.4)

Table 4.4 Drug mass deposited in each system component as a percentage of nebulized dose. Exhaled drug mass and deposition in the Y, flow meter, Neb + T, and ETT all represent sources of drug loss. Lung filter deposition represents an approximation of the drug delivery efficiency to the lungs. This assumption neglects loss from aerosol that enters the lung and is then exhaled.

System	1.1	1.2	1.3	2.1	2.2
Exhaled	N/A	N/A	N/A	16.2 (3.7)%	18.6 (1.7)%
Y	12.7 (3.0)%	4.9 (0.7)%	5.9 (1.6)%	7.9 (3.5)%	1.2 (0.5)%
Flow Meter	N/A	N/A	N/A	4.8 (3.9)%	4.0 (0.4)%
Neb + T	59.9 (1.5)%	22.2 (5.3)%	24.2 (12.3)%	67.6 (4.4)%	25.2 (2.8)%
ETT	17.5 (4.1)%	17.4 (2.2)%	21.7 (17.0)%	1.7 (1.7)%	17.1 (1.0)%
Lung Filter	10.0 (2.6)%	48.9 (6.4)%	48.2 (17.2)%	1.3 (0.6)%	34.0 (1.7)%
Total Loss*	90.0 (5.3)%	44.4 (5.8)%	51.8 (21.0)%	98.2 (7.9)%	66.0 (3.5)%

***Defined as the aerosol depositing on components other than the lung filter.**

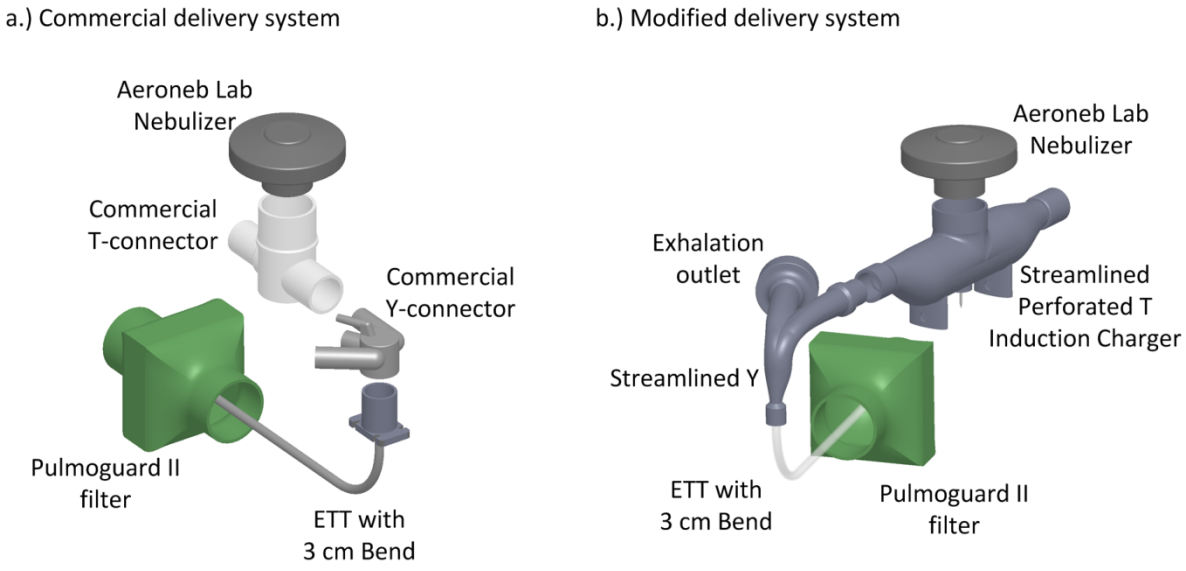

Figure 4.1 Aerosol delivery through a.) Commercial delivery system and b.) Modified delivery system. Both the T-connector and the Y-connector are streamlined in the modified delivery system before delivery through an infant endotracheal tube under steady state flow conditions (exhalation and monitoring outlets closed).

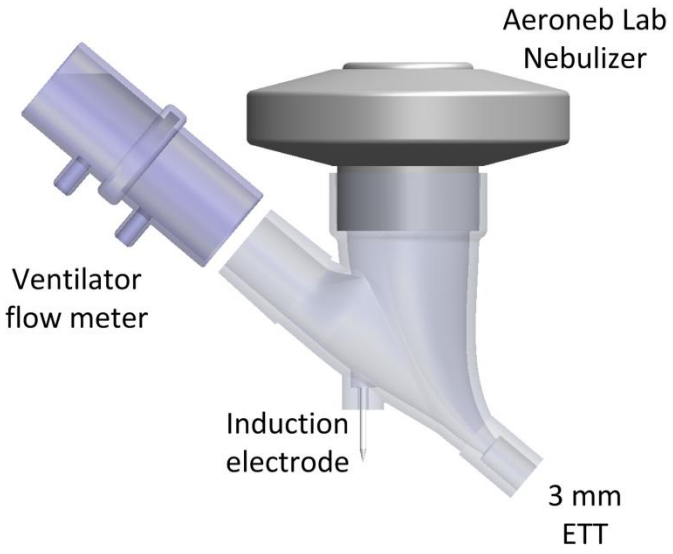

Figure 4.2 Streamlined low flow induction charger with reduced dead volume located after flow meter.

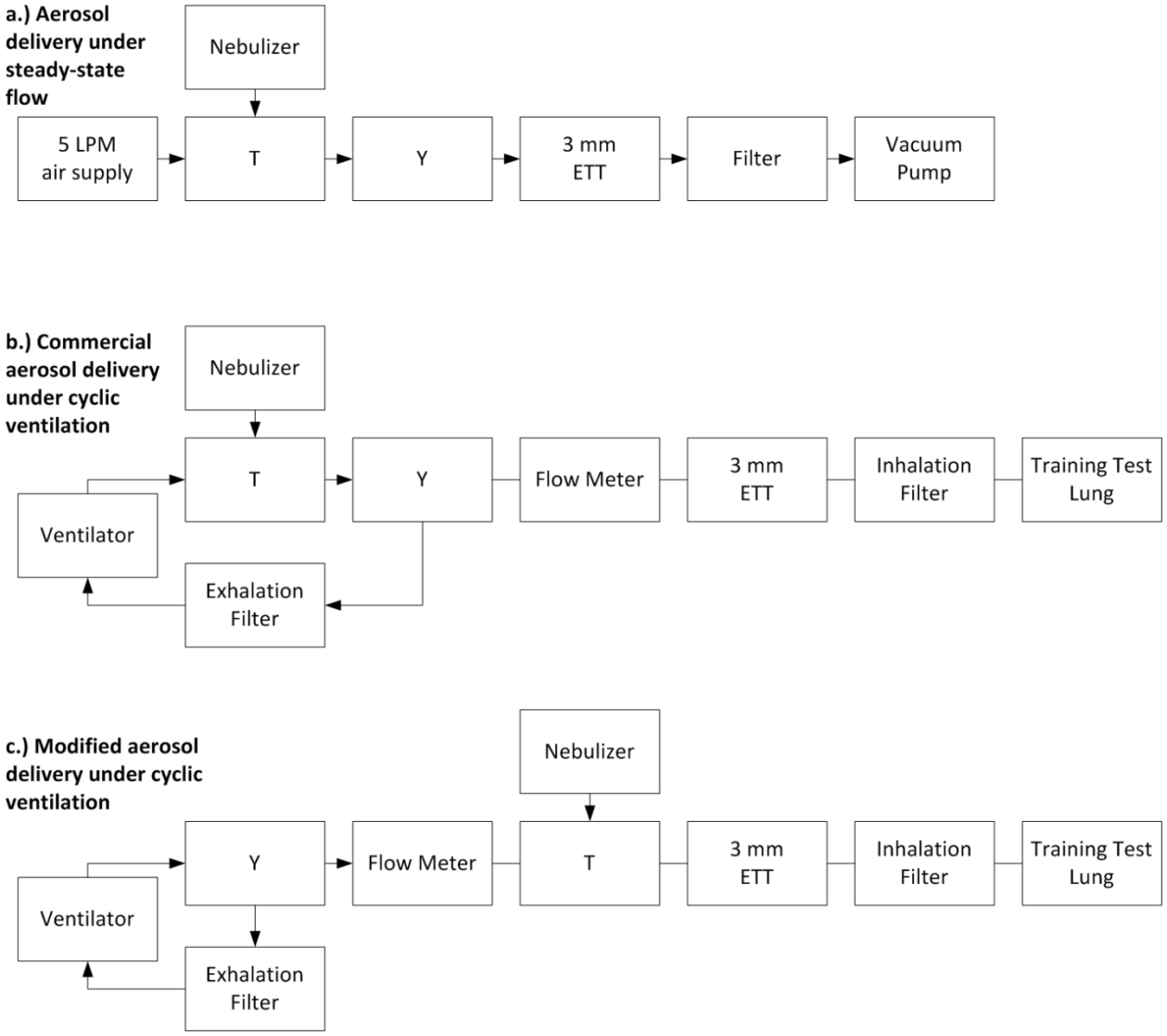

Figure 4.3 Connection configuration for the (a) aerosol delivery under steady-state flow, (b) commercial aerosol delivery under cyclic ventilation, and (c) modified aerosol delivery under cyclic ventilation

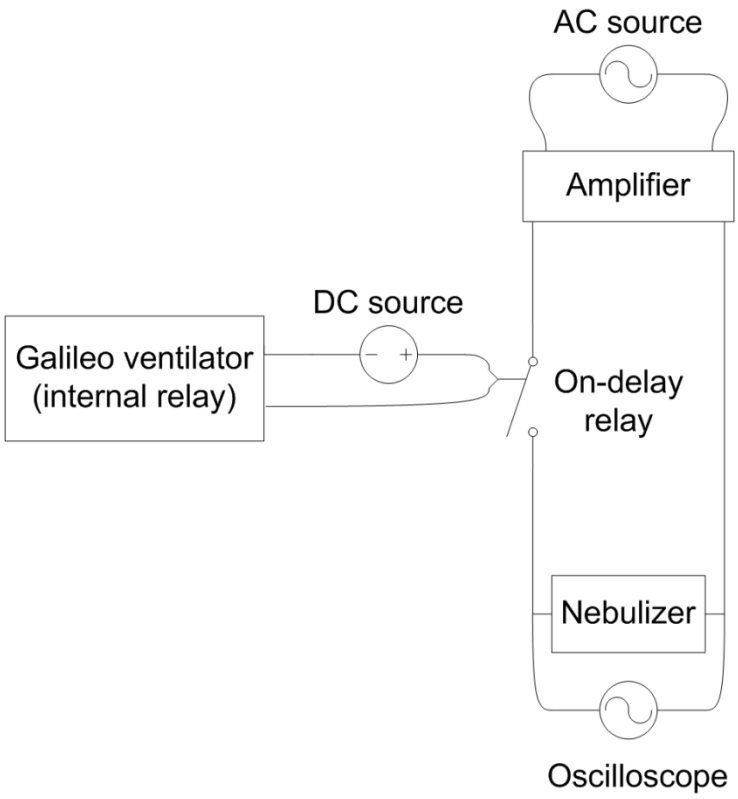

Figure 4.4 Electrical wiring diagram for the modified LF-IC system under cyclic ventilation conditions (System 2.2).

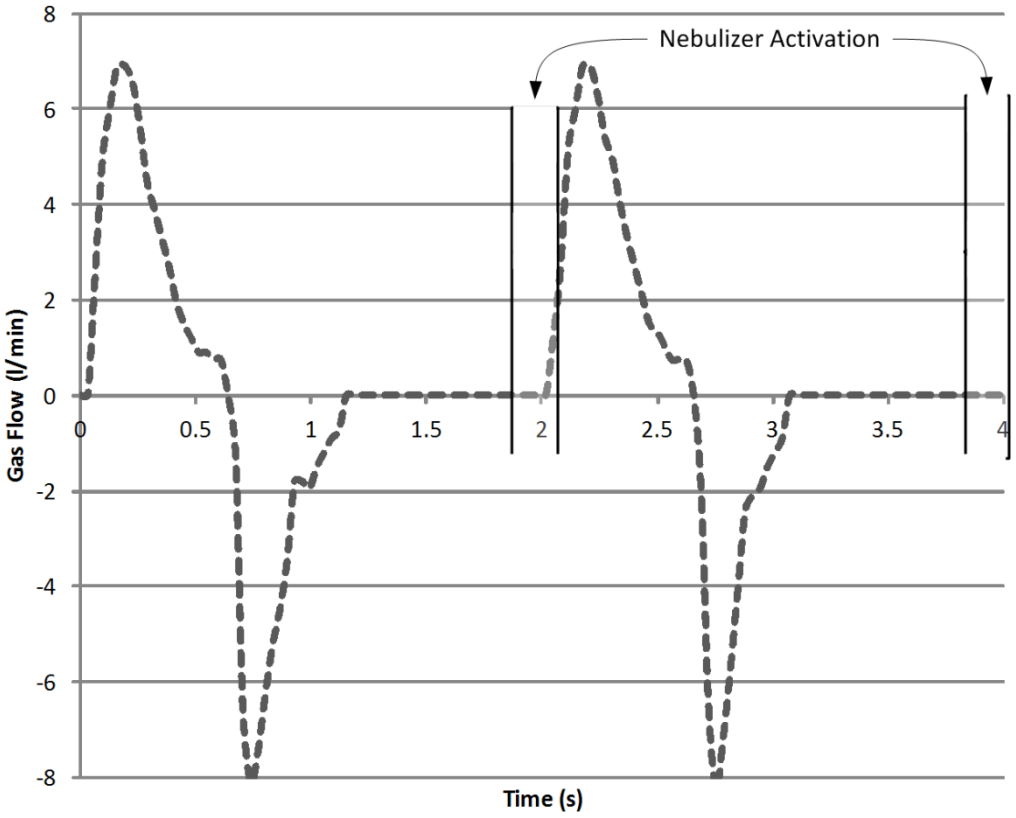

Figure 4.5 Flow profile resulting from specified control pressure (Pcontrol = 15, Peep = 5, Pramp = 100 ms) with timing of aerosol generation (synchronized nebulization) 0.11 seconds prior to inhalation.

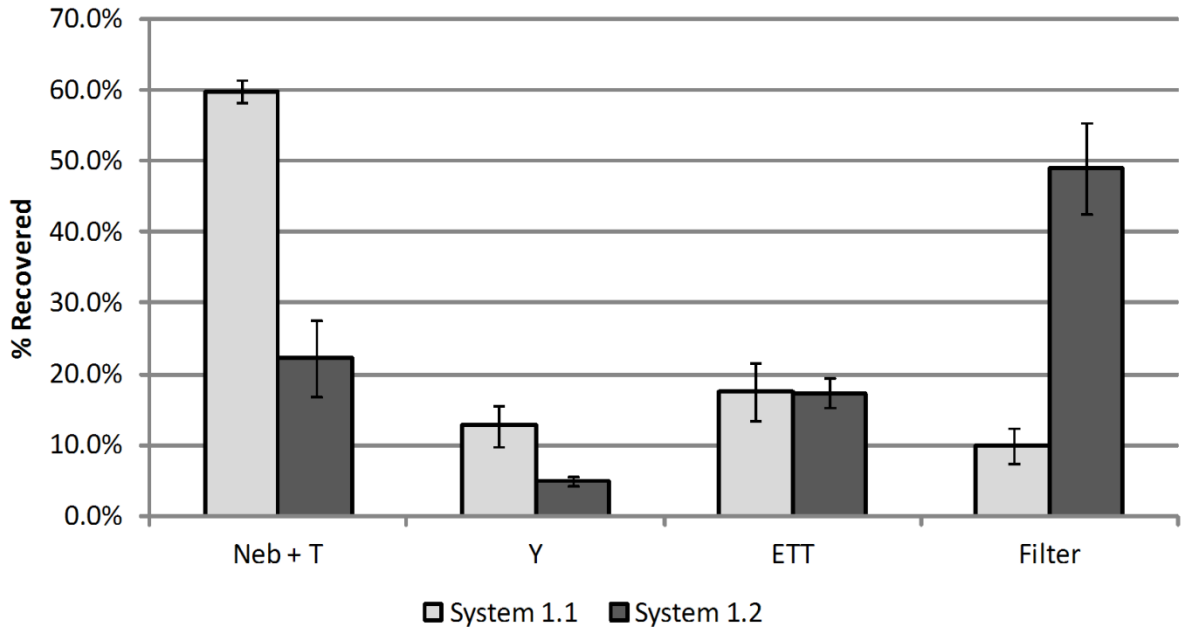

Figure 4.6 Drug mass deposition (i.e. % recovered) in ventilator circuit under steady-state flow during operation of System 1.1, commercial, and System 1.2, streamlined & 1 kV charged (n = 3 for each system; error bars represent standard deviation).

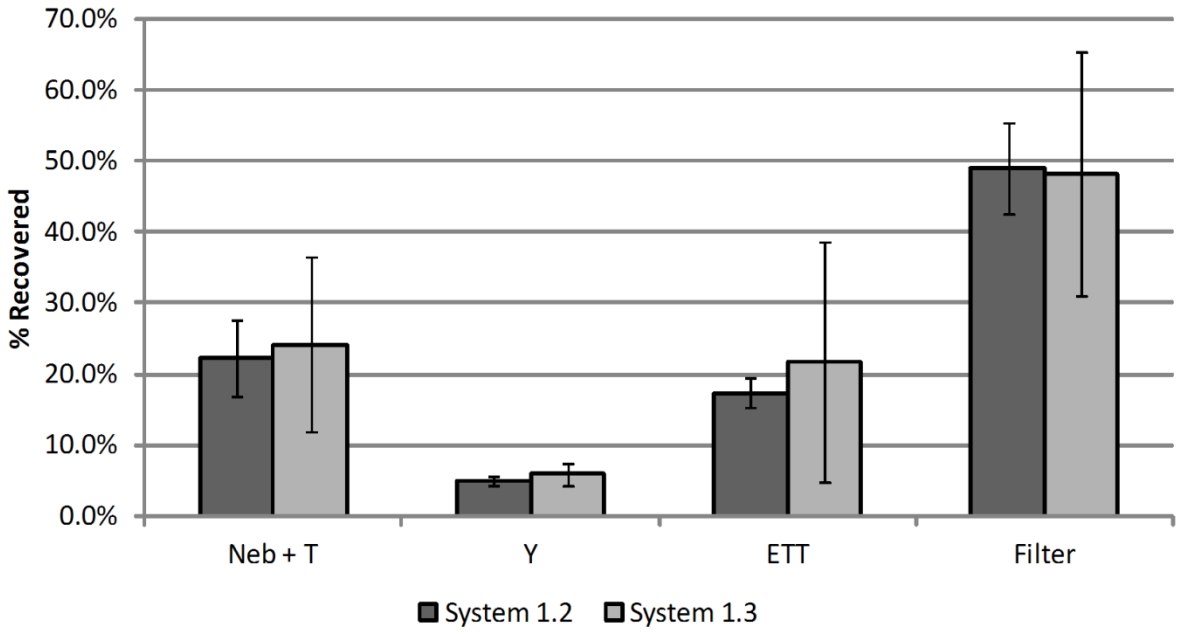

Figure 4.7 Effect of operating time on drug mass deposition (i.e. % recovered) in ventilator circuit under steady-state flow during operation of streamlined & 1 kV charged LF-IC systems 1.2 and 1.3 (n = 3 for each system; error bars represent standard deviation).

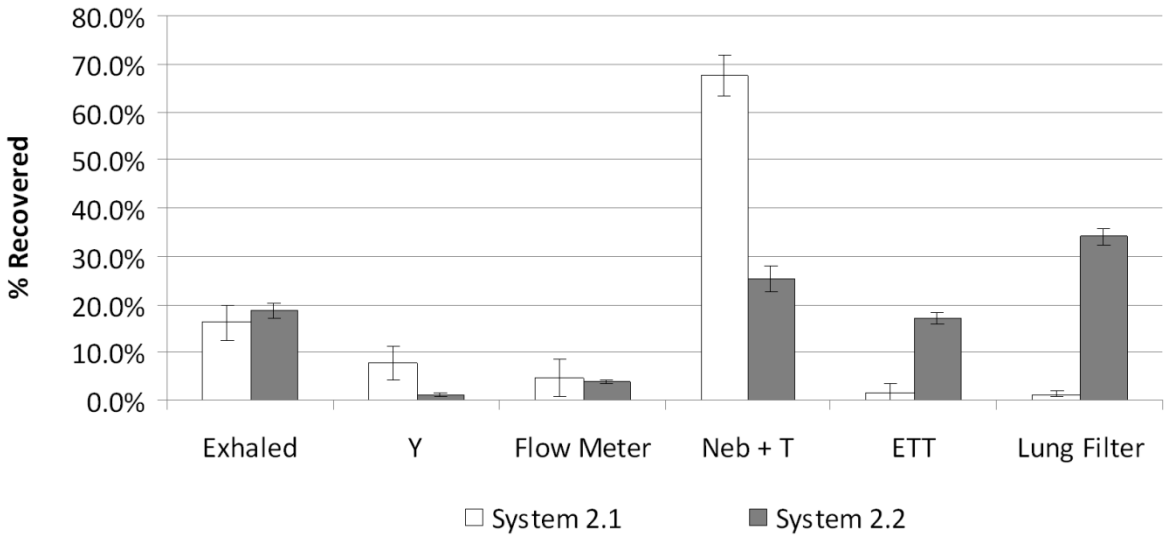

Figure 4.8 Drug mass deposition (% recovered) for System 2.1 and 2.2 under cyclic flow conditions. Run time is reduced for the commercial system to 0.5 minutes, increased for the modified system to 20 minutes and charging is reduced to 0.5 kV for the modified System 2.2 (error bars represent standard deviation).

Chapter 5 Development of a Breathing Infant Lung (BIL) Model for a Full Term Neonate to Enable In Vitro Testing of Surfactant Administration and Physiological Lung Response

5.1 Introduction

Healthy lungs expand evenly due to work done by the diaphragm to increase volume in the chest cage, resulting in inhalation. After inhalation, the diaphragm relaxes and the pressure returns to its original value, causing the lungs to contract in an elastic manner thereby driving exhalation and a return to a resting volume (Drake et al., 2005). At the end of inspiration or expiration in a healthy patient there is no airflow and the intrapleural pressure does not reflect forces associated with airflow, only the elastic recoil forces (West 2012). Compliance is a metric of the lung's elastic recoil and is measured as the change in volume per unit change in pressure across the lung. If the compliance of the lungs was only due to elastic tissue forces, it would be graphed on a pressure vs. volume plot as a single straight line connecting maximum and minimum lung volume points. However, airway resistance and changes in surface tension cause the volume response to an applied pressure to deviate from a linear relationship during inhalation vs. exhalation. In this study, the Pressure-Volume (P-V) graph was used to determine realistic response of the BIL model to mechanical ventilation because it is known that patient inhalation will deviate from a linear compliance due to the pressure needed for gas flow through narrow resistive

airways (Walsh and DiBlasi 2010). The pressure difference between the alveoli and the mouth divided by the airflow is defined as the airway resistance (West 2012). The area under the linear compliance line and bounded by the P-V curve is the work required to overcome airway and tissue resistance.

In healthy individuals, the lungs are able to control the surface tension of the alveolar region by adjusting the amount of surfactant present on the surface. Patients with insufficient surfactant have alveoli that tend to collapse during normal tidal breathing, frequently leading to respiratory failure if not treated with surfactant replacement therapy (Willson 2015). In a multicenter randomized trial, dramatic oxygenation improvement occurred within 5 minutes, mortality decreased from 51% to 31%, and the mean time patients were on mechanical ventilation was 35% less with instilled surfactant therapy (Collaborative European Multicenter Study 1988). According to the American Academy of Pediatrics, "…the optimal method of surfactant administration in preterm infants has yet to be clearly proven" and additional data is needed to recommend a method such as aerosolized surfactant delivery (Polin et al., 2014). Considering non-invasive aerosol delivery of synthetic lung surfactant in rabbits, surfactant deficiency was effectively relieved, but large portions of the surfactant were not nebulized and more than 40% of the aerosolized surfactant was lost in the ventilation circuit (Walther et al., 2014).

Common methods of surfactant delivery include liquid bolus administration (referred to as instillation of single or multi-dose), continuous infusion (or continuous instilation), and aerosolization. Special consideration needs to be given to the patient to prevent transient oxygen desaturation and severe airway obstruction which have been

seen more frequently in extreme low birth weight infants with more severe lung disease when surfactants are instilled (Tarawneh et al., 2012). The instillation process involves the insertion of an endotracheal tube, which carries a number of risks, pouring between 1.25 ml/kg and 5.8 ml/kg (Polin et al., 2014) of surfactant solutions down the endotracheal tube into the patient's lungs (or approximately 4 ml), and application of mechanical ventilation, which is also associated with lung injury and infection risks. Instillation of surfactant in infants has caused airway obstruction immediately following administration in multiple studies (Miedema et al., 2011; Wheeler et al., 2009). Although instillation is currently the only approved method for surfactant administration it requires an artificial airway and some positive pressure ventilation, which may be harmful to any patient, especially infants (Willson 2015).

In general, aerosolized delivery of medication to infants and adults suffers from high variability and low delivery efficiency (Brion et al., 2006; Cole et al., 1999; Fink 2004; Rubin and Williams 2014; Shah et al., 2007). Considering instilled and aerosolized delivery of surfactant to rats with acute lung injury, a highly inefficient device delivered a dose at least 4-fold lower than the instilled dose (100 mg/kg) to produce an equivalent increase is oxygenation and decrease in breath rate (Sun et al., 2009). New technologies provide an opportunity to efficiently deliver aerosolized surfactant with a low total administered dose and enhanced homogeneity of distribution (Pillow and Minocchieri 2012). The improvement of lung function with minimal systemic exposure can be accomplished by administering pharmaceutical aerosols to infants receiving mechanical ventilation (Fink 2004; Mazela and Polin 2011; Rubin and Fink 2001).

In this chapter, inspiratory resistance and compliance were determined in the breathing infant lung (BIL) model across three methods of surfactant administration: instilled liquid, commercial (CM) aerosol generation, and modified-charged (MC) aerosol generation. A low flow-induction charger, capable of delivering a charged aerosol with a mass median aerodynamic diameter (MMAD) < 1.8 μm (Golshahi et al., 2015; Holbrook et al., 2015), was developed and characterized in Chapter 3. The LF-IC was redesigned in Chapter 4 to utilize a lower charging voltage, a smaller device volume, breath synchronized delivery, and relocation of the nebulizer proximal the patient. These changes allowed for highly efficient implementation in an infant ventilation circuit under cyclic ventilation and provided an *in vitro* inhaled dose for "commercial" (CM) and "modified and charged" (M-C) aerosol delivery. From the nebulizer development testing of Chapter 4, The M-C aerosol system had a lung filter delivery efficiency of 34% and a delivery rate of 3.5 μg/min. The CM system demonstrated a lung delivery efficiency of 1.3% and a delivery rate of 25.6 μg/min (Chapter 4). These are maximum efficiencies and delivery rates, as they only measure the drug mass inhaled and do not measure the fraction exhaled. The measurement of maximum efficiencies and delivery rates use a filter to capture the lung dose, as is widely done in the literature (Dhand 2008; Fink and Ari 2013; Fink 2004; Guerin et al., 2008). These previous chapters are used to estimate the fraction delivered to the newly developed BIL model and provide standard methods and protocols to be used in the current and the following chapter.

The object of this study was to develop a BIL model that will respond in physiologically consistent ways and capture both deposited and exhaled dose in future studies. Conventional and modified aerosol delivery techniques with a vibrating mesh

nebulizer were considered and compared against an instilled surfactant case. After creating a realistic BIL model that is capable of distinguishing between three surfactant administration methods, the BIL model is suggested for use with the developed LF-IC from Chapter 4 to deliver a model drug such as albuterol sulfate to determine the exhaled fraction and the delivery rate to the lung, which is evaluated in Chapter 6. *In vitro* testing of the BIL model is developed to enable testing of next generation medications, increase the efficiency of current inhaled therapies, and test surfactant administration techniques.

5.2 Methods

The ventilation parameters selected for use in the BIL model were representative of a 3.55 kg infant (Walsh and DiBlasi 2010), which represents 50th percentile conditions at full term delivery. These are the same conditions used in the filter deposition study of Chapter 4. The inspiratory line of the ventilation circuit used a heater to maintain an inlet temperature of approximately 35 °C. A pressure controlled peak inspiratory pressure (PIP) of 20 cm water and a breathing rate of 30 breaths per minute were used for all experiments. An inspiratory time of 0.6 seconds was used which resulted in an approximate expiratory time of 0.5 seconds and a pause of 0.9 seconds. The only adjustable parameter for the mode of ventilation used (infant mode) was inspiratory time, the other timing parameters were not separately adjustable. The positive end-expiratory pressure (PEEP) was set to 5 cm of water and the pressure and tidal volume were measured after loading the spheres for a verification case of no liquid in the lungs and a case with 12 mL water in the pleural space to more closely approximate real lung

conditions. The resistance measured in the BIL should increase when the water is added to the lung.

The Galileo ventilator (Hamilton Medical Inc; Reno, NV) enables the measurement of inspiratory resistance and quasi-static compliance (Arnal et al., 2015). These measurements were repeated with administration of a commonly used syntheticsurfactant (instilled and aerosolized). Sodium Dodecyl Sulfate (SDS; Amresco Inc., Solon, OH) was selected for use as the surface acting agent to reduce the surface tension of the liquid in the BIL model due to low cost and availability in these preliminary experiments. The inspiratory resistance and compliance were measured before and after surfactant administration using the built-in monitoring capacity of the Galileo ventilator during invasive mechanical ventilation. The conductivity of the 0.05%($^{w}/_{v}$) Sodium Chloride (NaCl; Sigma Chemical Company, St. Louis, MO) solution, representing the airway surface liquid, was measured using an EC400 conductivity meter (Extech Instruments, Nashua, NH) and found to have a conductivity of 5000 μs/m. The ventilation circuit and connectors used were the same as described in Chapter 4.

5.2.1 Model Design and Construction

5.2.1.1 Upper Airways

The upper tracheobronchial airways of the breathing infant lung model were scaled from a previously constructed adult mouth-throat model (Walenga et al., 2013). Model D (Figure 5.1) extends from the mouth through three generations of bifurcating geometries and was constructed from a single CT scan that was consistent with mean airway

dimensions of adults (Walenga et al., 2013). To properly scale the model to infant dimensions, the areas of the eight outlets at generation three were averaged and assumed to be circular to obtain an average (SD) diameter of 6.1 (1.2) mm for Model D. An average infant height of 50 cm was used with the morphological correlation from Phalen (1985) to determine a mean (SD) infant diameter of generation three as 2.59 (0.37) mm. The approximate lower end of this acceptable range was selected, 2.3 mm, to provide a length scaling ratio of 0.377 (2.3 mm/6.1 mm). As such, Model D was scaled down to 37.7% of the starting adult size to match the average segmental bronchiole diameter of a newborn of average length and connected to the pleural space as described in the next section. The shape of the scaled glottis was modified to ensure a 4.2 mm (outer diameter) endotracheal tube would pass through the rigid model without constriction.

5.2.1.2 Lower Airways

The pleural space was digitally constructed from an infant CT scan using Mimics 14.0 (Materialise; Belgium) and 3-Matic (Materialise; Belgium) software resulting in a volume of 0.2 liters in the pleural region. The FRC was based on the youngest ICRP (1994) model, a 3 month old Caucasian infant. The chosen FRC from ICRP, 150 mL, was greater than another possible choice, 110 ml (Lumb 2012), because the fluid added to the model replaces the airspace and reduces the FRC. For this reason, the pleural space was scaled up from 0.2 to 0.42 liters to achieve an FRC of 150 mL when packed with two thousand two hundred fifty spheres at an approximate close random volume packing density of 0.641, without any added fluid.

The BIL (Figure 5.2a and 2b) was prototyped using a Viper SLA Rapid Prototyper with Accura 60 resin (3D Systems; Valencia, CA). The minimum resolution of the prototyper was 0.1 mm, which was sufficient to resolve the geometry. The appropriate number of spheres was then loaded to fill the pleural cavities while leaving room for expansion between the spheres during inhalation. A balance was used to determine the number of spheres loaded into each cavity before every experiment. To prevent bulk motion of the spheres an outlet cover (Figure 5.2c) was designed and attached after the spheres were loaded into the pleural cavity. After attaching the outlet cover to the BIL model a flexible membrane was used to close the system. The flexible membrane was a 102 μm thick sheet of nitrile (Protégé, Aurelia; Aurora, IL) that was stretched over the outlet cover and fixed with hot glue. The seal on the flexible membrane was checked by inflating the BIL model with approximately 40 mL of air while holding the model under water to identify potential leaks in the system. As described in Chapter 4, the ventilator circuit was connected to the 3 mm ETT using either a commercial Y-connector or a streamlined connector (LF-IC). The ETT bypassed the modified glottis and its outlet was placed near the bottom of the trachea of the prototyped model.

Two thousand two hundred fifty spheres with a 6 mm diameter reduced the air volume in the pleural cavities by 254 mL, making necessary a scaling of the pleural space. The spheres used were 6 mm and plastic (Crosman Corporation; Bloomfield, NY) with a mass of 0.12 grams per sphere. An effective alveolar diameter was calculated by determining the area of a triangle between three tangential circles of equal diameter (Figure 5.3). This triangle is an equilateral triangle with side length 6 mm. The area of intersection between the triangle and a single circle is calculated by the equilateral angle,

60° of a 360° circle of radius 3 mm. This area is the same in all three circles, and can thus be multiplied by 3. The area of intersection is subtracted from the area of the triangle to calculate the area between three tangential circles. This area is then assumed to be circular to calculate an effective diameter, resulting in a characteristic diameter of 1.36 mm (Figure 5.3). This diameter of 1.36 mm provides an approximation of the expected alveolar airway outer diameter of 0.54 mm (Khajeh-Hosseini-Dalasm and Longest 2014). Preliminary experiments (not shown here) determined the maximum volume of fluid to be instilled without visible pooling of the injected liquid to be 12 mL, which is consistent with the expected airway surface liquid in pediatric airways of 6-20 mL. The system was disassembled and the spheres were discarded after each experiment to remove the possibility of surfactant contamination on the spheres between runs.

5.2.2 Surfactant Administration

The BIL model developed in the previous sections was used to test surfactant therapy when administered during invasive ventilation as an instilled liquid bolus, an aerosol generated with a commercial nebulizer, or using the modified aerosol generation system developed in Chapter 4. For the instilled liquid bolus, the BIL model was disconnected from ventilation and four milliliters of water with 0.05%($^{w}/_{v}$) NaCl were injected in each pleural cavity by rotating and positioning the model, and the system was shaken to distribute the solution. The BIL was reconnected to the ventilator for measurement of inspiratory resistance and compliance. This surfactant free system is representative of an extreme case of lung surfactant dysfunction or deficiency. During instilled surfactant treatment, the BIL model was disconnected from ventilation and 2 mL

of a 1.73%($^{w}/_{v}$) SDS solution was delivered as a liquid bolus injection down the 3 mm ETT with the BIL model turned toward the right lung. The model was then rotated toward the left lung and another 2 mL of 1.73%($^{w}/_{v}$) SDS was instilled. After injection, this solution mixed with the 8 mL of 0.05%($^{w}/_{v}$) NaCl solution to create a 20 mM SDS solution with a surface tension of 37 mN/m as measured by a bubble pressure tensiometer (BP2; Krüss, Hamburg, Germany). The instillation administration technique was designed to deliver enough SDS to reduce the surface tension of the water in the BIL model to approximately half that of water (72 to 37 mN/m). After liquid bolus administration of surfactant, the BIL model was reconnected to the ventilator circuit for measurement of resistance and compliance during active ventilation after 20 minutes.

The instilled surfactant experiment was followed by nebulized delivery of surfactant using a commercial (CM) and a modified and charged (M-C) aerosol delivery system with an Aeroneb Lab nebulizer (Aerogen, Galway, Ireland). Preliminary results of the BIL model from Chapter 6 demonstrated delivery efficiency of the CM and M-C systems of 0.4 and 20%, respectively. For the CM system a concentration of 0.31%($^{w}/_{v}$) SDS was chosen for delivery over 1 minute because the spraying of the surfactant solution was hindered by the generation of bubbles on the reservoir side of the nebulizer's mesh for higher concentrations. Commercial nebulization parameters were consistent with those tested in Chapter 4. The charged and modified system was then implemented to deliver the nebulized surfactant to the BIL model using the same solution concentration used for the CM system and 20 minutes of synchronized delivery (best case conditions as described in Chapter 4).

5.2.3 Data Capture and Processing

Quasi-static compliance and resistance of the BIL model were measured using a Galileo ventilator connected through the serial port to a computer running the Galileo data collection software. This software records the breathing profiles, parameters, and lung properties every 2.5 seconds and records them to a .txt file. A second file was saved containing the pressure and volume information that was used to create the characteristic loops and visualize the lung mechanics recorded every 0.032 seconds to a .txt file. The pre-administration inspiratory resistance ($Resistance_{Pre}$) and compliance ($Compliance_{Pre}$) values immediately preceeding administration are read from the recorded file during processing. Similarly, the post-administration values ($Resistance_{Post}$ and $Compliance_{Post}$) are recorded at the end of treatment.

To make the data more comparable, the impact of the surfactant administration on resistance is assessed as the change in resistance divided by the initial resistance, %Resistance. These values are calculated using the pre and post administration resistances. Similarly, the impact of the surfactant administration on compliance is the change in compliance divided by the initial compliance, %Compliance. These processing equations are displayed below.

$$\%Resistance = \frac{Resistance_{Post} - Resistance_{Pre}}{Resistance_{Pre}}$$

$$\%Compliance = \frac{Compliance_{Post} - Compliance_{Pre}}{Compliance_{Pre}}$$

It is important to note that the pre-administration values in the instillation technique correspond to a liquid lung volume of 8 mL, while the nebulization technique has a liquid lung volume of 12 mL. When used, the coefficient of variation (CV) was calculated as the standard deviation (SD) divided by mean. An increased compliance and a decreased inspiratory resistance are both clinically desirable changes that will likely reflect improved oxygenation. The P-V curve generated by the BIL should resemble a typical infant breathing curve with normal distention as seen in the study of Fisher et al. (1988).

5.3 Results

5.3.1 Demonstration of a Characteristic P-V Curve

The generation of a realistic pressure-volume curve was the first test of the model and the foundation of a useful *in vitro* model of lung mechanics. The inspiratory resistance of the model was examined with a liquid volume of 0 mL and the largest volume of liquid that could be added without visible pooling, i.e., 12 mL. Three replicate experiments were conducted to determine the response and standard deviation of each volume of liquid to the pleural space. The mean (CV) resistance increased from 25 (0%) cm H_20/L/s at 0 mL liquid to 31 (5.9%) cm H_20/L/s for 12 mL of liquid, an increase of 24%. Two sets of three replicate experiments show the mean (CV) compliance increasing from 1.75 (3.3%) to 1.85 (3.1%) mL/cm H_20 for 12 mL of airway liquid. The increased compliance is clearly visible as the increased slope of the straight line connecting max inhalation to max exhalation in the case of 0 mL airway liquid, Figure 5.4a, and the case of 12 mL airway liquid, Figure 5.4b. The P-V curve shown in Figure 5.5 is compared with clinical results for infants and does not

exhibit the characteristic “beak” shape of over-distention, but rather the properly ventilated shape.

5.3.2 Surfactant Administration Response

To further establish the BIL model’s capabilities, the response to instilled and aerosolized surfactant administration was assessed. After ventilation on the 35°C line for 20 minutes prior to administration, the model was removed from the circuit and the instillation of 4 mL of surfactant solution increased the mean (SD) inspiratory resistance by 16.2 (8.0)% from the pre-administration values, (time = 0 minutes). The compliance changed -1.4 (2.5)%, meaning the compliance decreased as the inspiratory resistance increased (time = 0 minutes). The mass of SDS delivered to the lung during instillation was 69.12 mg, to produce 12 mL of a 20 mM SDS. These values were recorded 1 breath after being reconnected to the ventilation circuit after administration. As noted earlier, increasing the volume of liquid in the lung is expected to increase resistance and compliance. This increase is also magnified due to the presence of the bolus in the upper airways as it distributes to the lungs. Resistance and compliance of the BIL were also recorded after 20 minutes of ventilation with heated air, resulting in a reduction in mean (SD) inspiratory resistance [-1.0(1.8)%] as compared to pre-administration values and a relative reduction of -14.5 (7.2)% compared to conditions measured just after 1 breath. Similarly, the mean(SD) compliance improved, increasing from the pre-administration values by 3.1(2.7)% and increasing from conditions at breath 1 by 4.6 (0.1)%.

The other conventional method of administration evaluated was the delivery of SDS using a commercial (CM) vibrating mesh nebulizer. The CM aerosol system produced an

increase in inspiratory resistance of 7.6 (1.3)% immediately after 1 minute of nebulization during ventilation. CM administration of surfactant did not change the compliance [0.0 (8.7)%] in three replicate experiments. After 20 minutes of ventilation therapy, the mean inspiratory resistance decreased, -7.4(6.8)% and the mean compliance increased by 1.7(7.5)% compared with pre-administration conditions. The mean (SD) mass of SDS aerosolized during 1 minute was 2.96 (0.09) mg. Preliminary results from Chapter 6 indicated that only 0.36% of the nebulized dose would be deposited in the lung, or 10.67 μg SDS. This value seems very low compared with the expected surfactant pool (DPPC) in healthy lungs 4 mg/kg (Rebello et al., 1996); however, it is plausible that these improvements are related to the small amount of surfactant (synthetic) delivered considering the large effect that small amounts of surfactant can have on physiological response (Lewis et al., 1993).

The M-C aerosol system was utilized to produce a charged aerosol with a reduced mass median aerodynamic diameter to reduce losses in the ventilator circuitry and enhance deposition within the lung by allowing for improved deep lung penetration and reducing the exhaled fraction. This modified system aerosolized 0.23 (0.03) mg of surfactant during the 20 minute duration of the therapy. Preliminary results from Chapter 6 indicated that 21.3% of the nebulized dose would be deposited in the lung, or 49.5 μg SDS. The M-C system had visibly fewer bubbles in the nebulizer's reservoir after 20 minutes of administration than the commercial signal displayed after 1 minute. The M-C administration of SDS to the BIL model resulted in a 7.4 (1.7)% decrease in inspiratory resistance after the 20 minute therapy duration. This decreased resistance was accompanied by an increased compliance, 1.9 (3.2)%. The inspiratory resistance and

compliance response results are summarized in Table 5.2 and the responses of the BIL model to the administration techniques across equal ventilation times are summarized in Table 5.3.

5.4 Discussion

The novel BIL model was conceptualized, prototyped, and implemented in the ventilation circuit tested in Chapter 4 to produce realistic infant pressure-volume curves and increase the scope and usefulness of *in vitro* testing methods. The P-V curves shown in Figure 5.4 are a basic measure of model realism and demonstrate a typical *in vivo* functionality generated by an *in vitro* system. The inhalation and exhalation response occurred in the BIL model as expected with forced ventilation, are noted by the arrows of inhalation and exhalation in Figure 5.4. The comparison against clinical data in Figure 5.5 shows that the BIL model can be used to evaluate breathing conditions that result in normal distention. Furthermore, the response of the BIL model to instilled and aerosolized surfactant administration was evaluated and compared to pre-treatment values of compliance and inspiratory resistance. The inspiratory resistance increased after administration for both conventional systems, but decreased after 20 minutes of ventilation (Figure 5.6), presumably distributing the surfactant in the BIL model. Finally, the low flow-induction charger developed in Chapter 3 and improved in Chapter 4 was compared with conventional surfactant administration techniques in the newly developed BIL model and a difference was demonstrated between inhaled and instilled surfactant administration techniques.

5.4.1 BIL Model Accuracy

The primary source (80%) of inspiratory resistance is the upper conducting airways (trachea to generation 7), so if a change is observed in this model of the pleural cavities, the model must do an adequate job of capturing the effect of surface tension on the expansion of the spheres, simulating the alveolar space expansion's dependence on surface tension (West 2012). The administration of surfactant through instillation was not shown to improve the inspiratory resistance as compared in Figure 5.7 after 20 minutes of ventilation because of the airway obstruction presented by the bolus in the upper airways before and while it is distributed to the lungs. The sigmoidal shape (or the breathing curve of multiple inflection points) described by Brochard (2006) is demonstrated by the BIL model in Figure 5.4. An initial period of high stiffness (low compliance) changes at the first inflection point, approximately 10 mL, to a nearly linear section of increased compliance until max inhalation. The hysteresis of the P-V curve shown in Figure 5.4 also demonstrates higher lung volumes during exhalation for any given pressure as is typically found in the lung. Not clearly demonstrated is the increased lung stiffness at high expanding pressures due to the lung protective values selected in this study; therefore, it is recommended that the peak inspiratory pressure of the model be increased to explore this trait. As the human lung expands, geometrical arrangement of elastin and collagen changes, allowing the size of the airways to increase without changing the dimension of the individual fibers (West 2012). The BIL model is not expected to replicate this complex geometrical arrangement, rather the surface tension of the liquid layer between the airway fluid resists the expansion of the air gaps between them by acting as an elastic membrane holding the spheres together. As a result, we expect the model to accurately capture aerosol deposition (based

on airway dimensions and correct ventilation rate) and mechanical properties related to P-V curves and the application of surfactants in cases of surfactant deficient airways.

5.4.2 Similarity of Model Predictions to *In Vivo* studies

As mentioned in the Introduction, measurement of compliance and resistance was made of the BIL model during instilled and aerosolized administration of surfactant. The improvement in lung properties due to surfactant deposition and dispersion was expected for all considered cases, but was only consistently observed with the M-C system. In spite of the small amount of surfactant delivered (49.5 μg), the modified system outperformed the instilled and CM system likely due to the obstruction of the artificial airway with depositing or instilled liquid. This obstruction is documented in multiple clinical surfactant instillation studies (Tarawneh et al., 2012; Wheeler et al., 2009), but not in aerosol delivery. The amount of liquid administered in the M-C case was reduced to 74 μL from 944 μL in the CM case and 4 mL in the instilled case. The increased inspiratory resistance of the instilled case is likely a result of the large volume of instilled liquid. The increased resistance of the CM aerosol case is likely a result of the aerosolized liquid collecting in the ETT. The lack of increase in the M-C case indicates that the 74 μL is not obstructing the ETT, but is mostly humidifying the air through evaporation as the surfactant is being delivered. It is known that small amounts of aerosolized surfactant can have effects equivalent to 1000-fold doses of instilled surfactant, likely due to improved distribution of the nebulized surfactant (Willson 2015). The change in compliance was highly variable (SD > mean) in all cases, but the trend of the mean values indicate more compliant lung response in the M-C aerosol system. Factors other than an increased compliance, such as better capillary stability and

decreased leakage of fluid into alveoli, have been suggested to explain the immediate improvement in oxygenation resulting from surfactant administration in clinical studies (Bhat et al., 1990).

Pre-surfactant administration compliance was measured in a clinical study and ranged from 0.2 to 0.7 mL/cm H_2O/kg in newborn infants before surfactant replacement therapy (Kelly et al., 1993). This is compared with the pre-administration specific compliance of the BIL of 0.52 mL/cm H_2O/kg, which results from dividing the quasi-static compliance of the model with 12 mL of liquid (1.85 mL/cm H_2O) by the mass of the infant (3.55 kg). The post-administration compliance values for infants with pre-adminstration compliance of approximately 0.52 mL/cm H_2O/kg ranged from 0.45 mL/cm H_2O/kg to 0.95 mL/cm H_2O/kg (Kelly et al., 1993), which is equivalent to a percentage change of between -10% and 90% using the $\%Initial_C$ equation previously defined. In another study of instilled surfactant on 6 preterm neonates, the mean (SE) inspiratory resistance of the patient was 96.5 (23.9) cm H_2O / L · sec before treatment, and decreased to 54.2 (7.7) cm H_2O / L · sec after instillation (3.3 mL/kg) of surfactant (Bhat et al., 1990).

5.4.3 Conclusions and Model Refinement

Using smaller spheres to more closely approximate the alveolar region may increase the realism of the model by reducing the amount that the pleural space needs to be scaled and allowing for greater fluid/surface interactions between the injected water and the spheres. Using the method previously established requires a 2.38 mm sphere to produce a 0.54 mm characteristic gap. 16 spheres of diameter 2.38 mm have the same volume as one 6 mm sphere. The surface area of the 16 smaller spheres is 2.52 fold higher than the single

sphere. This leads to a larger contribution of surface forces, such as surface tension, overcoming issues of differentiating the flexible membrane compliance from the compliance of the expanding spheres. Experimentally, 2.0 and 2.5 mm spheres are more likely to be used due to manufacturing constraints. The 2.0 and 2.5 mm spheres result in characteristic diameters of 0.45 mm and 0.57 mm respectively. All of these calculations are not considering the reduction in area due to the lung volume of liquid. In future studies, It is recommended that the area be recalculated assuming a radius of curvature between the spheres to represent the dispersed liquid between the spherical contact points. This will increase the difficulty in finding an analytical solution to the question of sphere size in the BIL, but provide a more realistic characteristic area for studies utilizing *in vitro* and *in silico* methods.

The critical micelle concentration (CMC) of SDS in a water solution with 0.25%($^{w}/_{v}$) NaCl was calculated to be 0.071%($^{w}/_{v}$) (Dutkiewicz and Jakubowska 2002). This is the concentration of SDS above which the SDS will form micelles (aggregates) due to the hydrophobic and hydrophilic nature of surfactants. Micelle formation needs to be minimized in the aerosol administration of surfactant to prevent clogging of the vibrating mesh nebulizer. The amount of SDS present during instilled administration is not critical because the SDS will spread into the fluid in the BIL model after administration. The SDS concentration, 1.73%($^{w}/_{v}$) is above the CMC, as is the aerosolized concentration, 0.31%($^{w}/_{v}$). However, the LF-IC and the commercial nebulizer were still able to spray the SDS solution in spite of having a concentration higher than the CMC. A decreased amount of NaCl in the formulation is suggested for future experiments (0.05% $^{w}/_{v}$) to increase the

SDS CMC to 0.147%($^{w}/_{v}$) and maintain a conductive solution (approximately 5 mS/m) for effective induction charging with reduced micelle formation.

The novel LF-IC developed in Chapter 4 was used with the newly developed BIL model to simulate the response to surfactant administration in an *in vitro* model for the first time. Optimization of administration techniques in the BIL model could increase understanding of surfactant therapies by determining the lung response for various nebulizer – surfactant combinations without endangering infants already suffering from RDS. There are so many administration techniques to choose from and so many new drug formulations that improved *in vitro* testing moves from being an asset to a necessity to ensure patient safety and to reduce the number of failed clinical trials. For instance, the BIL model had a lower inspiratory resistance after CM aerosol administration of SDS than M-C aerosol administration, and both were lower than after instilled administration, Figure 5.8. These initial results exhibit realistic characteristics of an infant lung, but future modifications to the BIL can include:

1. Reduced sphere diameter (6 mm to 2.5 mm) to more closely model the alveolar diameter;
2. Reduced scaling of the BIL model for FRCs of healthy and distressed newborn lungs; and
3. Extension of the upper airways geometry of model D from generation three to generation five to capture more of the upper airway resistance in the model and distribute the therapy in the middle of the spheres instead of near the pleural cavity wall.

In conclusion, an infant model capable of capturing the lung's response to an administered surfactant under realistic *in vitro* ventilation conditions was developed and tested with instilled and aerosolized surfactant therapy. The physiological properties measured, inspiratory resistance and quasi-static compliance, showed a realistic response to surfactant therapy and general agreement with published values from the literature. The aerosol therapy was shown to deliver approximately $1/1000^{th}$ of the mass to the model, and yet the response of the model to the aerosol therapy was superior to the instilled therapy as is also the case in some clinical studies. Further experimentation with the BIL model will determine the exhaled losses in a breathing model and test the ability of the previously developed LF-IC (Chapter 4) to increase the lung dose in a more realistic model.

Table 5.1 Lung physiological characteristics measured in the breathing infant lung (BIL) in a completely dry system and a wet system without surfactant.

BIL Liquid Volume	Inspiratory Resistance ($cm\ H_20\ /\ L \cdot sec$)	Quasi-Static Compliance ($mL\ /\ cm\ H_20$)
0 mL 0.05% NaCl	25 (0%)	1.75 (3.3%)
12 mL 0.05% NaCl	31 (5.9%)	1.85 (3.1%)

N = 4 replicates of each measurement
Value is reported as average (CV)
BIL, Breathing Infant Lung; CV, Coefficient of Variation

Table 5.2 The effect of instilled, commercial (CM) aerosol, and modified and charged (M-C) aerosol administration of SDS on inspiratory resistance and quasi-static compliance. %Resistance and %Compliance are the change in resistance or compliance normalized by the pre-administration resistance or compliance. Decreasing resistance (-) is beneficial and increasing compliance (+) is beneficial.

SDS Administration Technique	%Resistance	%Compliance
Instilled	16.2 (8.0)%	-1.4 (2.5)%
CM Aerosol (1 min)	7.6 (1.3)%	0.0 (8.7)%
M-C Aerosol (1 min)	-1.0 (1.7)%	1.9 (3.2)%
CM Aerosol (20 min)	-7.4 (6.8)%	1.7 (7.5)%
M-C Aerosol (20 min)	-7.4 (1.7)%	1.9 (3.2)%

N = 3 replicates of Instilled, Modified & Charged (M-C) and Commercial (CM) measurements
Charged refers to the use of a 0.5 kV induction charger
Value is reported as mean (SD)
SDS, Sodium Dodecyl Sulphate

Table 5.3 The effect of instilled, CM aerosol, and M-C aerosol administration of SDS on inspiratory resistance and quasi-static compliance after 20 minutes of ventilation for each method. The instilled system had 20 minutes of ventilation after administration, the CM system had 19 minutes of ventilation after 1 minute of administration, and the M-C system had 0 minutes of ventilation after 20 minutes of administration. Decreasing resistance (-) is beneficial and increasing compliance (+) is beneficial.

SDS Administration Technique	%Resistance	%Compliance
Instilled	-1.0 (1.8)%	3.1 (2.7)%
CM Aerosol	-7.4 (6.8)%	1.7 (7.5)%
M-C Aerosol	-7.4 (1.7)%	1.9 (3.2)%

N = 3 replicates of Instilled, Modified & Charged (M-C) and Commercial (CM) measurements
Value is reported as mean (SD)
SDS, Sodium Dodecyl Sulphate

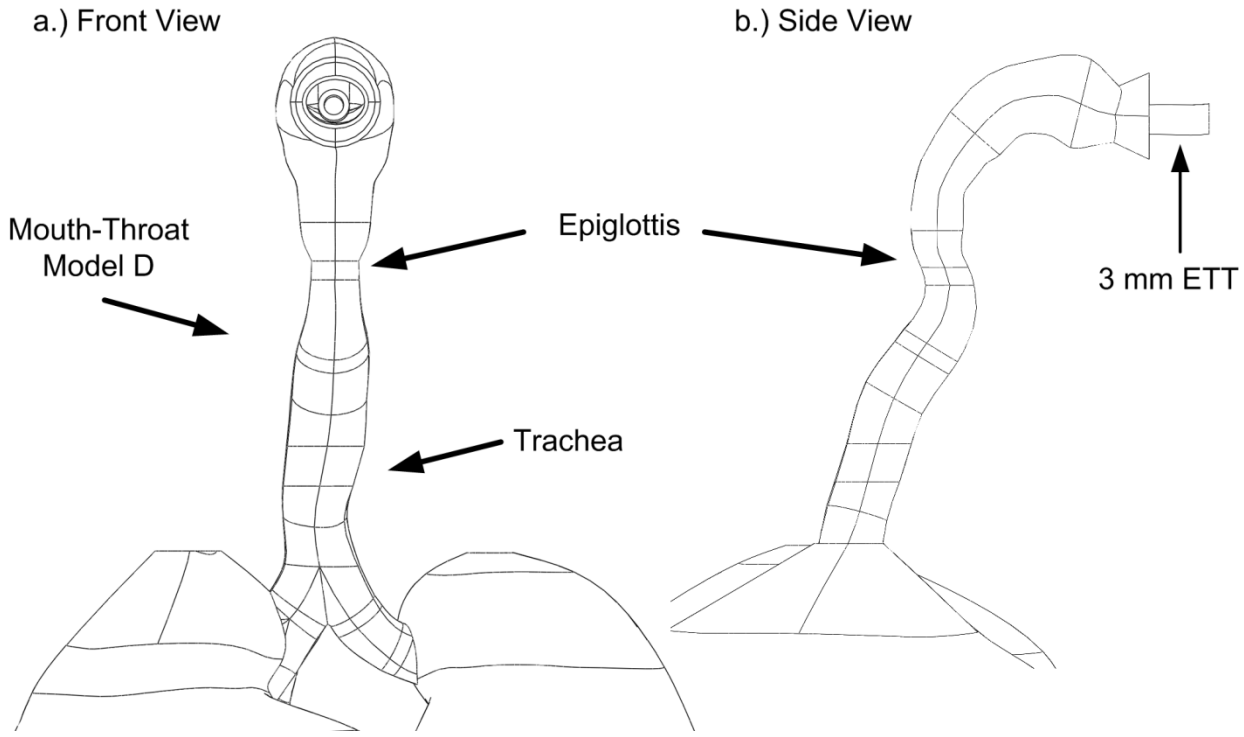

Figure 5.1 Drawing view of a.) Front and b.) Side of the mouth-throat model used to construct the upper airways of the BIL model.

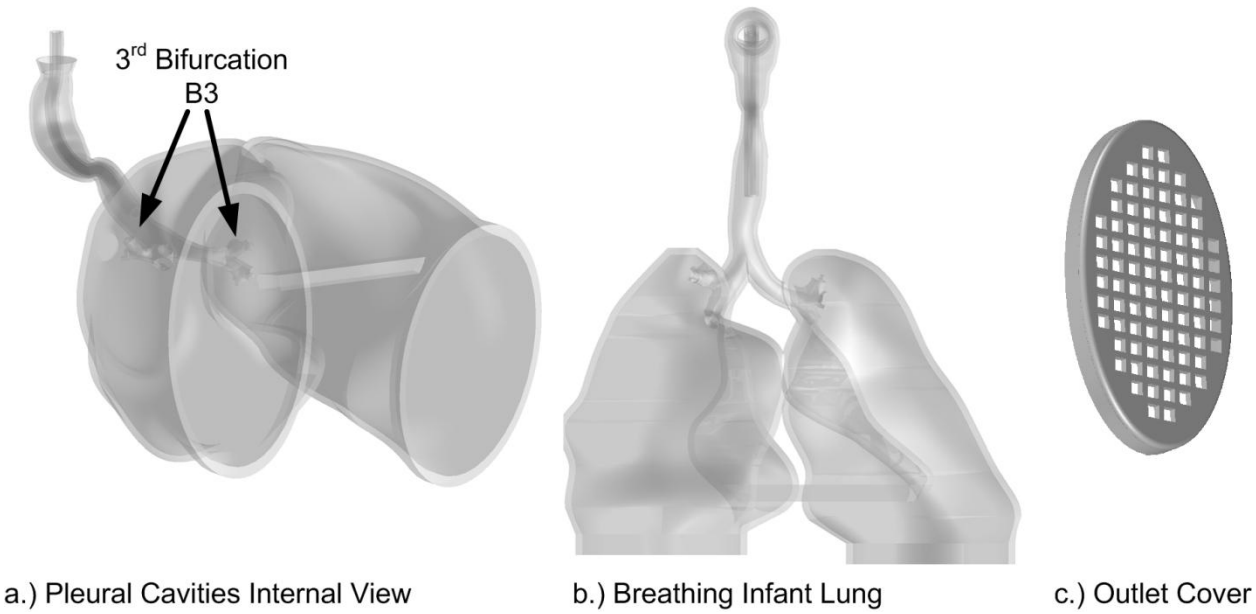

Figure 5.2 Features of the BIL model highlighting a.) the interior of the pleural cavity, b.) the front view of the BIL, and c.) one of the two outlet covers prototyped to prevent bulk motion of the spheres in the pleural cavity.

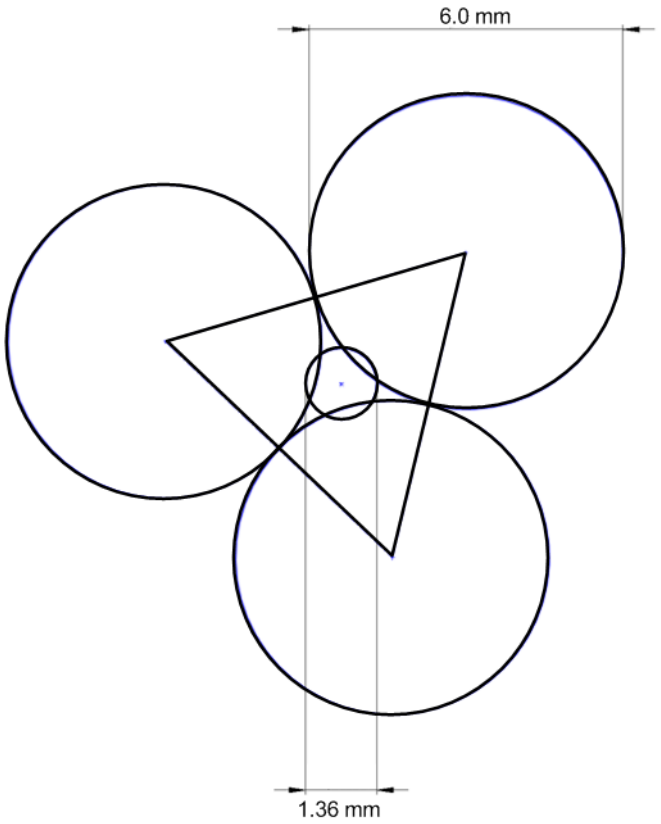

Figure 5.3 Determination of characteristic diameter between 6 mm spheres. An effective alveolar diameter is calculated by determining the area of a triangle between three tangential circles of equal diameter. This triangle is an equilateral triangle with side length 6 mm. The area of intersection between the triangle and a single circle is calculated by the equilateral angle, 60° of a 360° circle of radius 3 mm. This area is the same in all three circles, and can thus be multiplied by 3. The area of intersection is subtracted from the area of the triangle to calculate the area between three tangential circles. This area is then assumed to be circular to calculate an effective diameter, resulting in a characteristic diameter of 1.36 mm.

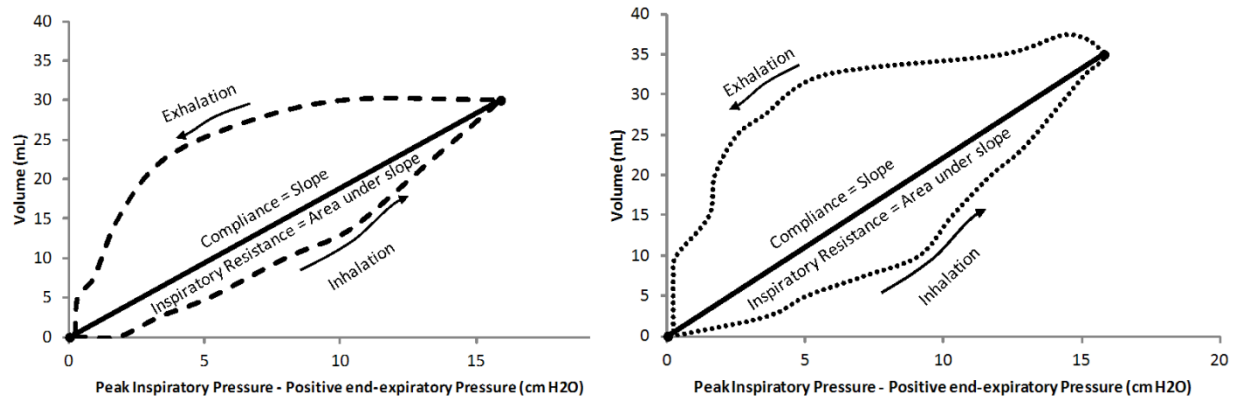

Figure 5.4 Pressure vs. Volume curves for a.) the BIL model without airway liquid and b.) the BIL model with 12 mL of airway liquid instilled without surfactant.

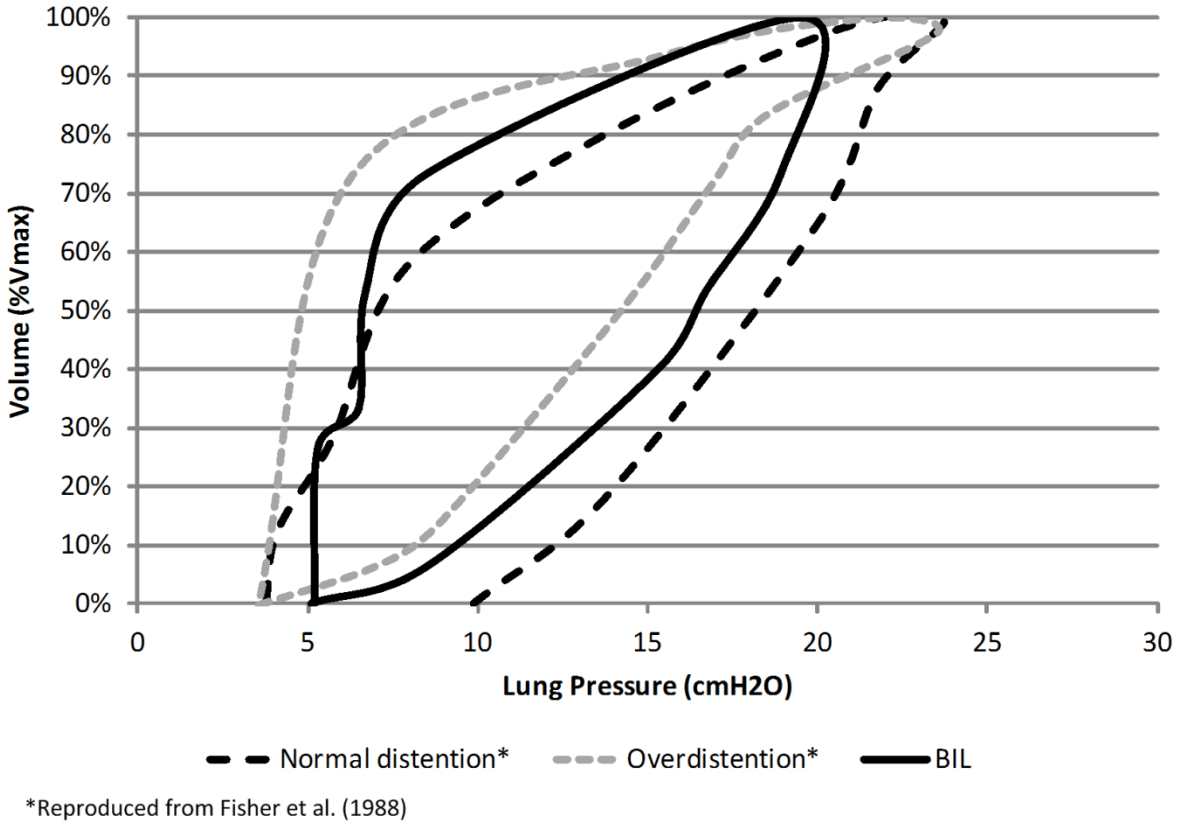

*Reproduced from Fisher et al. (1988)

Figure 5.5 P-V curve determined from BIL model and compared with data for infants between 1 and 31 days old from Fisher et al. (1988).

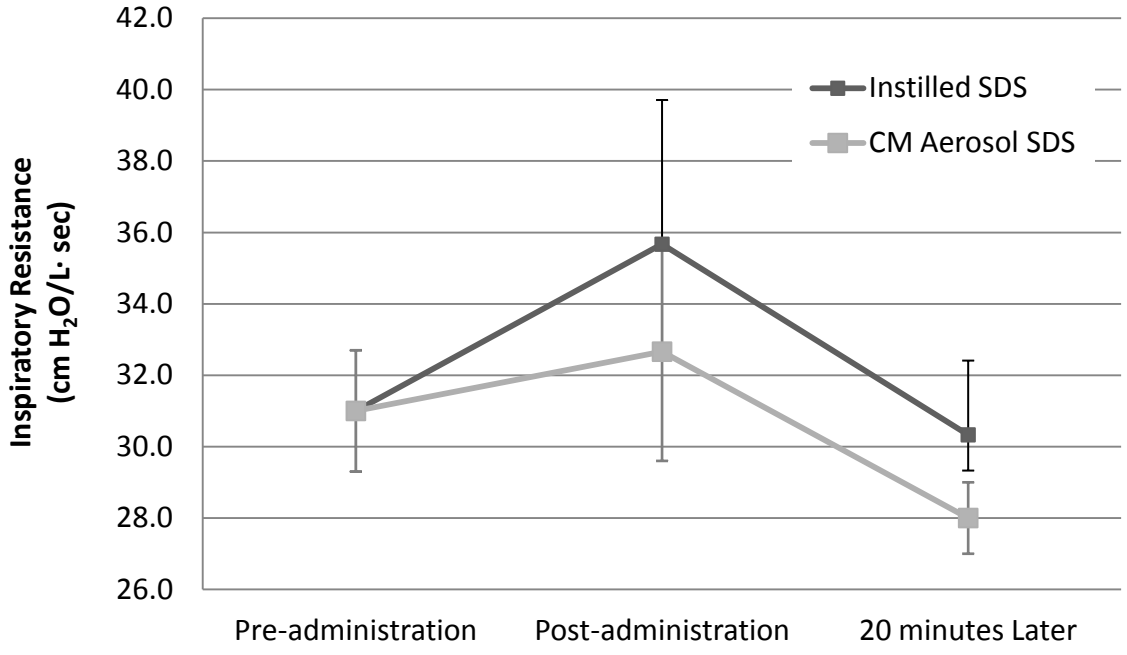

Figure 5.6 Change in inspiratory resistance during the course of treatment.

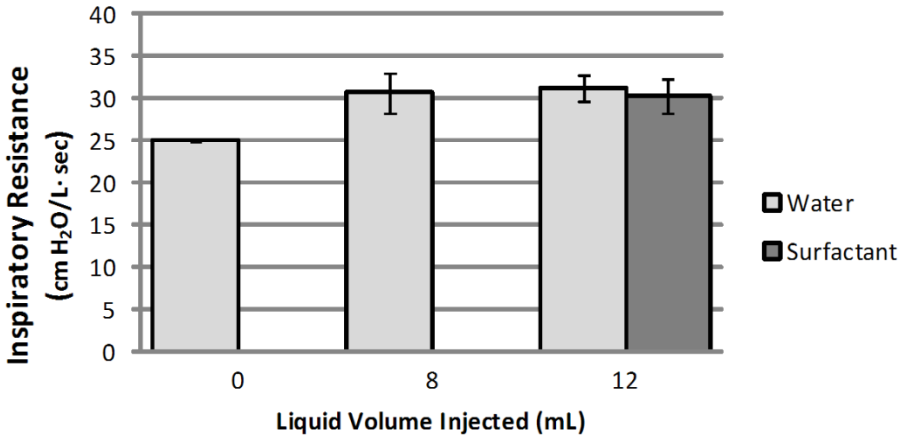

Figure 5.7 The effect of increasing liquid volume in the BIL model on mean inspiratory resistance and comparison with instilled surfactant model after 20 minutes of ventilation (error bars are ± 1 standard deviation).

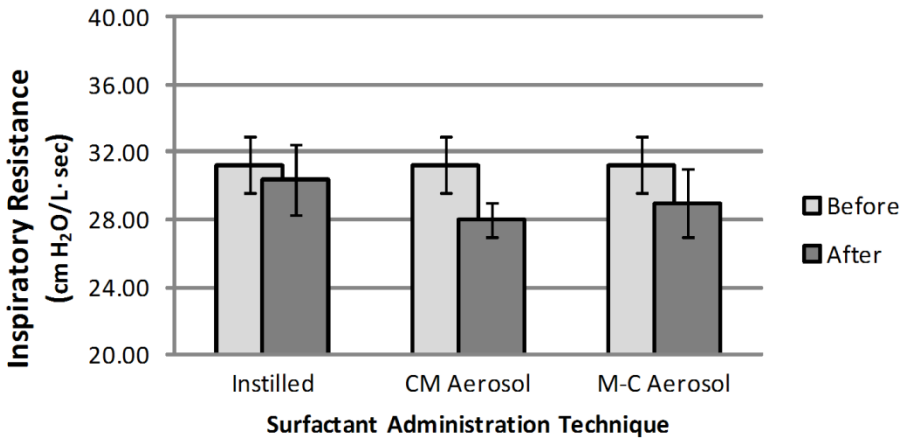

Figure 5.8 Comparison of surfactant administration techniques considered (t = 20 minutes; error bars represent ± 1 standard deviation).

Chapter 6 Evaluation of Aerosol Delivery to a Novel Breathing Infant Lung (BIL) Model

6.1 Introduction

In vitro experiments are important to establish parameters for the safe delivery of aerosol therapies before commencing *in vivo* studies (Byron et al., 2010; Carrigy et al., 2014; Martin and Finlay 2014). For instance, in the study of Finer et al. (2010), an *in vitro* infant model was used to determine the maximum possible delivered dose using an vibrating mesh nebulizer and a 2% synthetic surfactant solution, assuming that none of the aerosol that reaches the patient was exhaled. These types of studies provide exposure limits for protecting patients during *in vivo* studies but are not representative of the actual dose delivered to the lung because they do not currently account for drug exhalation and often do not include realistic upper airway anatomies and breathing physiology. *In vitro* testing of mean, small, and large models of the mouth and upper airways has been used to produce an *in vitro-in vivo* correlation to predict *in vivo* aerosol drug deposition using an *in vitro* test method for dry powder inhalers (Delvadia et al., 2013; Delvadia et al., 2012). However, most in vitro models do not account for the drug distribution within the lungs. It is well known that drug distribution within the lungs can have a significant impact on therapeutic benefit (Usmani et al., 2003).

An in vitro model of an infant capable of realistically capturing the lung dose of an administered pharmaceutical aerosol under actual ventilation conditions would clearly be a beneficial tool. In designing this breathing infant lung (BIL) model for testing inhaled therapies, drugs with high cost and significant side effects were primarily considered. Development of inhaled therapies for infants has been hindered by low delivery efficiency (high waste) and high variability (uncontrolled dose) (Mazela and Polin 2011; Shah et al., 2007). Surfactants are very expensive, steroids need low variability because of adverse side effects, and antibiotics need to be delivered in high and consistent doses to prevent resistant strains of bacteria from surviving (Lehne and Rosenthal 2014). Bronchodilators such as Albuterol Sulfate (AS) are typically inexpensive, have low side effects, and don't require a large dose. AS was used as a marker to determine the depositional loss and delivery efficiency of the LF-IC in the novel BIL model. Implementation of the BIL model will quantify the depositional reduction due to aerosol exhalation using an *in vitro* experiment.

A realistic breathing model of the infant lung was designed and constructed in Chapter 5. It was then evaluated using ventilator measurements of compliance and inspiratory resistance during instilled surfactant therapy. A model of a full term neonate respiratory system was developed using an infant patient CT scan of the pleural space and digitally assembled with a previously constructed trachea model, Model D (Walenga et al., 2013). This assembled model was rapid prototyped and filled with solid spheres to simulate the packed expansion of the alveolar region. The expected alveolar outer diameter of 0.54 mm (Khajeh-Hosseini-Dalasm and Longest 2014) was approximated by the gaps formed between the spheres. Instillation of a liquid produced a surface tension

between the spheres and created a compliance and resistance in the model that was more than just the elasticity of the flexible membrane.

Development of aerosol delivery protocols often rely on *in vitro* studies to determine the mass of drug delivered to the lung. However, these *in vitro* studies are not able to account for the reduction in lung deposition caused by exhalation. *In vitro* models over estimate the dose to a patient because they use an absolute filter which cannot simulate drug loss due to exhalation (Dhand 2008; Fink and Ari 2013; Fink 2004; Guerin et al., 2008), as was applied in Chapter 4. For example, in the recent study of Mazela et al. (2014), a novel connector was used to bypass the bias-flow and increase delivery of a jet nebulized aerosol. The lung delivery efficiency of approximately 2–7% was a significant improvement over the less than 1% efficiency achieved with standard care, but this was measured before the endotracheal tube (ETT), without an inline flow meter, and not considering exhalation (Mazela et al., 2014). Large particles are often filtered out by ventilation circuitry such that the aerosol mass median aerodynamic diameter (MMAD) after an infant ventilation circuit and a 3 mm ETT was measured as 1.4 μm for a vibrating mesh and a jet nebulizer which generated aerosols with MMADs of 4.6 and 4.8 μm, respectively (Dubus et al., 2005). Inefficient delivery and exhalation of inhaled aerosol therapy has been addressed by reducing aerosol MMAD to < 1.8 μm, as suggested by Longest et al. (2014b), and inducing a charge on the aerosol to increase deposition in the lung (Chapter 4).

Delivery of aerosol therapy to infants using a metered dose inhaler (MDI), jet nebulizer, or a vibrating mesh nebulizer result in low lung delivery efficiencies ranging

from <1-14%, with the greatest efficiency coming from the vibrating mesh nebulizer (Dubus et al., 2005; Fink 2004; Fok et al., 1996; Mazela and Polin 2011; Sidler-Moix et al., 2013). The research and development of aerosol therapies such as vaccines, gene therapy, cancer treatment, and diabetes management were recently reviewed in clinical and *in vitro* studies (Rubin and Williams 2014). The high variability and low delivery efficiency of aerosolized medications need to be improved for the development of next generation medications and more efficient implementation of current inhaled therapies (Brion et al., 2006; Cole et al., 1999; Fink 2004; Rubin and Williams 2014; Shah et al., 2007).

In this chapter, depositional losses and delivery efficiency were determined in the BIL model using the same techniques described in Chapter 4. A modified signal was supplied to a vibrating mesh nebulizer (Aeroneb Lab; Aerogen, Galway, Ireland) to reduce the output rate and initial momentum of the generated aerosol (described in Chapter 3). This modified output was sprayed into a streamlined induction charger that has been previously optimized (Chapter 4) to deliver aerosol efficiently under cyclic ventilation conditions in an infant ventilation circuit. The experiments of Chapter 4 demonstrated a dramatic 26-fold increase in delivery efficiency, but a reduction in the rate of delivered mass to the inhalation filter. However, these *in vitro* tests were conducted assuming zero exhalation of the aerosol from the lung. The systems designed and implemented in Chapters 3, 4, and 5 will be applied to a test case of aerosolized albuterol sulfate (Spectrum Chemicals, New Brunswick, NJ; a model drug commonly used as a bronchodilator) to determine the impact of charging on the exhalation of an aerosol < 1.8 μm (MMAD) and test the ability of the BIL model to simulate the exhalation of inhaled aerosol. The lung deposition in this study is expected to be lower than the filter data collected in Chapter 4

(34%), but the difference between the commercial system and the modified and charged delivery system is expected to be greater than the 26-fold increase demonstrated in Chapter 4.

The object of this study was to compare the performance of the previously implemented LF-IC with a commercially available nebulizer under realistic flow conditions in a BIL model (Chapter 5) designed to capture both deposited and exhaled dose. Conventional and modified aerosol delivery techniques with a vibrating mesh nebulizer were considered and suggestions are given for method of administration based on:

1. Cost;
2. Adverse side effects;
3. Dosage; and
4. Speed of delivery.

After creating an *in vitro* method of testing lung deposition of aerosol therapy without assuming perfect capture within the lungs, the LF-IC is suggested for use with drugs that have a high cost and significant side effects such as surfactants, antibiotics, and steroids because the emphasis of the LF-IC design was on maximizing delivery efficiency rather than maximizing the rate of mass delivery. Still, mass delivery rate appears acceptable for many high dose medications considering that continuous long-term delivery is possible during mechanical ventilation and may be preferred from a clinical standpoint in some cases.

6.2 Methods

The BIL model was composed of two regions: the upper airways through the third tracheobronchial bifurcation (B3), which were derived from CT scan data, and the lower airways, which were experimentally modeled using packed spheres within a pleural shell built from CT data. Functional residual capacity (FRC) is defined as the volume of air within the lung after passive exhalation and was used in the scaling of the pleural model. The scaled model was rapid prototyped and is shown in Figure 6.1. Full details on the construction and properties of the BIL model can be found in Chapter 5. The BIL model was tested under the same cyclic ventilation conditions as Chapter 5 and using the same aerosol generators developed in Chapter 4, with commercial (CM), modified - uncharged (M-UC) and modified - charged (M-C) systems defined in Table 6.1. CM, M-UC, and M-C components are summarized in the system schematics, Figure 6.2.

The systems were evaluated using three metrics: lung delivery efficiency (η), mass of drug delivered per 4 mL loading ($Mass_{4mL}$ [μg]), and the mass of drug delivered to the lung in one minute ($Mass_{1min}$ [μg]). The delivery efficiency, η, was defined as the lung dose (μg) divided by the recovered dose (μg) multiplied by 100. The drug formulation (0.25% albuterol sulfate, 0.25% sodium chloride) and the process of recovering the drug (washing and HPLC analysis) were unchanged from Chapter 4.

6.2.1 Model Design and Construction

Two thousand two hundred fifty spheres at a random packing density of 0.641 with a 6 mm diameter and a mass of 0.12 grams per sphere were used to model the alveolar

region in a 3.55 kg infant. The pleural space that housed the spheres was digitally constructed from an infant CT scan and combined with an adult mouth throat model, Model D, (Walenga et al., 2013) which was scaled to infant dimensions (using a length scale factor of 0.377). The spheres used (Crosman Corporation; Bloomfield, NY) were 6 mm, light weight (density is approximately equal to water), plastic and the characteristic dimension between the spheres was 1.36 mm (Figure 6.3), which is an approximation of the expected alveolar airway outer diameter of 0.54 mm (Khajeh-Hosseini-Dalasm and Longest 2014). The characteristic dimension between the spheres was calculated based on the area between three adjacent 6 mm (diameter) circles on a plane. Chapter 5 confirmed realistic response of the BIL model to instilled surfactants without visible pooling of the 12 mL of injected solution to represent airway surface liquid.

6.2.2 Implementation in Ventilation Circuit

After construction with a stereolithography rapid prototyper from 3D Systems, each pleural cavity was loaded with the appropriate number of spheres to achieve the desired FRC. The pleural cavity was not filled completely, this allowed for expansion between the spheres during inhalation. The number of spheres added was determined gravimetrically using a mass balance. A rapid prototyped mesh was fixed to the pleural outlets to prevent bulk motion of the packed spheres and a flexible membrane was attached after the mesh. The ventilator circuit was connected to a 3 mm infant ETT as outlined in Chapter 4. This ETT was inserted past the glottis and near the first bifurcation of the breathing lung model (Figure 6.1).

6.2.3 Experimental Parameters and Analysis

As described in chapters three and four, washing with deionized water and analysis using validated High Performance Liquid Chromatography (HPLC) method followed each experiment. Three replicate experiments were conducted using the CM system, three using M-UC, and three using M-C. The system was disassembled for washing, the spheres and the BIL shell were washed together as one part, and the 6 mm spheres were discarded after one use. The ETT was separated from the LF-IC and removed from the BIL model before washing. As in previous chapters, nominal dose was calculated by weighing the nebulizer before and after an experimental run on a mass balance and multiplying by the concentration of the solution. Total mass recovery of greater than 90% of the nominal dose indicated a high quality experiment. Additional information on the nebulizer synchronization, ventilation parameters, and analysis techniques were presented in Chapter 4 and are clarified for the CM, M-UC, and M-C systems in Table 6.1.

6.3 Results

CM, M-C, and M-UC delivery of aerosolized AS was evaluated in an infant lung model designed to simulate both realistic airway deposition and exhalation of inhaled drug using an *in vitro* approach. The results of CM, M-C, and M-UC delivery in the BIL model are shown in Figure 6.4. The modified delivery was accomplished using the LF-IC developed in Chapter 3 and Chapter 4, with and without an induction charging voltage. The lung efficiency, η, is defined as the mass of drug depositing in the lungs divided by the total deposited mass. The expected dose to the lung was also reported as the amount (μg) of drug deposited in the lung normalized by a typically administered volume of solution, 4 mL

($Mass_{4mL}$). Finally, the delivery rate over one minute of the CM and modified systems was calculated, $Mass_{1min}$. In addition to the lung delivery values, the depositional loss in the ventilation circuit was reported in this new *in vitro* BIL model.

6.3.1 CM System

Depositional loss and drug delivery to the lung was assessed in the BIL model using a commercially available vibrating mesh nebulizer for comparison with clinical studies of aerosol delivery to ventilated infant patients. Results are summarized in Figure 6.4 as mean (SD) % deposition, which is calculated based on the drug mass in each section divided by the total recovered dose and expressed as a percentage. The nebulizer and T-connector had a high depositional loss of 68.4 (2.8)% of the aerosol. The fraction of drug deposited in the exhalation filter was 18.7 (1.5)%. A large portion, 7.4 (0.6)% of the aerosol deposited in the Y-connector and 4.1 (2.0)% deposited in the flow meter. Only 1.0 (0.1)% of the aerosol deposited in the ETT, due to high upstream losses. The patient received 0.36 (0.1)% of the total recovered dose in the lungs. This low lung delivery efficiency ($\eta = 0.36\%$) was also demonstrated in the amount of drug delivered to the patient for a typical 4 mL loading, which was 36 μg (Table 6.2). However, the delivery rate of the commercial vibrating mesh nebulizer was 7.15 μg/min to the lungs under the specified parameters with the previously characterized system. The percentage of aerosolized AS recovered within the experimental system was $\geq$ 90% of the nominal dose in all CM experiments.

6.3.2 Modified aerosol delivery to the BIL model

6.3.2.1 M-UC System

To provide a reference value for the effect of inducing a charge on the aerosolized AS, the depositional loss and delivery efficiency was first examined without the high voltage power supply (M-UC), as summarized in Figure 6.4. The depositional loss on the nebulizer and the T-connector was 23.7 (6.5)% of the total recovered mass. In the modified delivery system, the nebulizer and T-connector were directly connected to the ETT. The depositional loss in the ETT was 24.2 (4.2)%, leaving 52.1% of the nebulized AS to potentially deposit in the BIL model. Of this, the majority was exhaled and only 20.6 (6.8)% deposited in the lung (but with 57-fold improvement in delivery efficiency over CM delivery). This exhaled dose deposited in the flow meter [4.8 (1.0)%], Y-connector [1.0 (0.5)%], and eventually in the exhalation filter [25.8 (8.7)%]. Excellent mass balance was achieved during uncharged delivery as 98.2 (5.3)% of the nominal mass was recovered in the three experiments. The increased lung delivery efficiency (η = 20.6%) was reflected in the mass of drug delivered to a patient in a typical 4 mL loading, which was 2,056.9 μg. The delivery rate of the uncharged and modified delivery system decreased to 2.87 μg/min in the BIL (2.5-fold decrease compared with the CM system). In the uncharged system, 60.5% of the aerosol that reached the lung was exhaled.

6.3.2.2 M-C System

The M-C delivery system was evaluated with an induction charging voltage of 500 volts and compared with the CM and M-UC system in terms of depositional loss and drug

delivery efficiency to the lungs (Figure 6.4). The charging field present in the nebulizer and T-connector caused the depositional losses to increase to 32.2 (6.2)%. The charged aerosol also experiences greater deposition in the 3 mm ETT, 26.5 (4.3)%. These losses left 41.4% of the nebulized aerosol to potentially deposit in the BIL model before exhalation. However, only 21.3 (2.4)% of the aerosol deposited in the lungs, with the remaining fraction exhaled from the lungs. This exhaled fraction deposited first in the flow meter [3.42 (0.4)%], then in the Y-connector [0.76 (0.1)%], and finally in the exhalation filter [15.9 (0.5)%]. Normalizing the exhalation by the amount of drug entering the BIL, 48.6% of the aerosol that reached the lung was exhaled. The depositional efficiency (η = 21.3%) found in the lung was reflected as the dose to the lung per 4 mL solution loading, which was 2,127 μg. The lung delivery rate decreased in the charged and modified delivery system from the CM rate of 7.15 μg/min to 2.65 μg/min [2.7-fold decrease], but the delivery efficiency, η, increased 59-fold compared to the CM system.

6.4 Discussion

This chapter evaluated the low flow induction charger (developed in Chapters 3 and 4) together with other techniques to optimize aerosol delivery η outlined in Table 6.1 using the BIL model of Chapter 5. Previous *in vitro* models cannot simulate drug loss due to exhalation (Fink and Ari 2013). The importance of accounting for exhalation when measuring lung dose was demonstrated and the impact of aerosol charge on the reduction of exhalation in a realistic model was quantified. The LF-IC implementation in the BIL model was evaluated in terms of lung delivery efficiency, lung delivery rate, and lung delivery per 4 mL solution loading of the nebulizer. Based on these criteria, the LF-IC is

recommended for further optimization and implementation in animal models for inhaled therapies that require efficient delivery over long treatment times.

Comparing performance of the CM case evaluated in Chapter 4 and now evaluated with the BIL model illustrated the impact of exhalation on deposition in two key areas, the nebulizer and T-connector as well as the inhalation filter or the BIL model. As expected, the exhaled fraction did not have considerable effect on the depositional losses in the nebulizer and T-connector. The results from Chapter 4 and the BIL model results showed very high deposition of approximately 68%. Unlike the depositional losses near the nebulizer, the already low lung delivery efficiency of 1.6% decreased 4-fold to 0.36% when exhalation was modeled *in vitro*. This efficiency was similar to many observed nebulization therapies *in vivo*, but much lower than the vibrating mesh nebulizer delivery in the animal model of Dubus et al. (2005), for reasons described in Chapter 4.

The drug delivery rate was also calculated and compared against the inhaled dose established in Chapter 4. The CM delivery rate to the inhalation filter was reported to be 25.6 μg/min using a 0.25% AS solution. Replacing the inhalation filter with a breathing model of an infant lung reduced the delivery rate 3.6-fold to 7.15 μg/min. Based on this finding, studies such as Finer et al. (2010), which used an *in vitro* system to determine the delivery rate of the aerosol and in turn the patient's treatment time, may need to increase delivery duration approximately 3.5-fold to account for the reduction in delivery due to exhaled dose. It is recommended that this *in vitro* determination of *in vivo* delivery duration be conducted with a more realistic breathing model. The modified system also

experienced a decreased delivery rate under exhalation conditions, but instead of a 3.6-fold decrease it was a 1.3-fold decrease of $Mass_{1min}$ from 3.5 to 2.7 μg/min.

The CM system delivered more drug to the lung in a fixed amount of time because of two factors: the reduced mass output resulting from the modified signal and the reduced nebulization time resulting from the synchronized delivery of aerosol. The CM system was continuously operated, whereas the modified system was running for 0.11 seconds of every 2 second breath (1/18th) and 1/10th of the drug was produced from the nebulizer when it was operated using the modified signal. Considering both of these aspects, there was 1/180 of the drug in the circuit. The charged system was about 60x more efficient (21.3% / 0.36%), which means that approximately 60/180 of the CM delivery (2.38 μg/min) was expected to reach the infant lung.

As mentioned in the Introduction, the improvement in lung deposition due to modified delivery and induction charging was expected to be even greater than the 26-fold improvement of inhaled dose from Chapter 4. The CM system provided an inefficient delivery of 0.36% to the BIL model. The modified system, used a 500 Volt induction charger improved the lung delivery efficiency to 21.3%. As expected, this 21.3% efficiency was less than the inhaled efficiency determined in Chapter 4, of 34% (Figure 6.5). However, the improvement over CM delivery was greater than the Chapter 4 26-fold improvement of inhaled dose, achieving a 59-fold improvement in delivery efficiency to the BIL model.

To consider the impact the induction charger had on the exhaled fraction, the modified system was run without and with the high voltage source in the induction

charger. The deposition in the LF-IC and the ETT was increased when the charger was operational; meaning that less drug reached the lung model to be deposited or exhaled. To examine the effect of charging on exhaled dose, the exhaled dose was normalized by the amount entering the BIL model. Using this normalization technique, the mean(SD) exhaled fraction of drug that entered the BIL model was 65.7 (12)% in the uncharged case. Applying an induction charging voltage of 500 Volts decreased the exhaled fraction to 48.5 (9)%, a 17.2% increase. However, conducting a two tailed Student's t-test resulted in a p value of 0.112 which means that the effect of induction charging on improving lung deposition is not significant at $p<0.05$ but does provide a weak correlation with the current sample size of 3 replicates per experiment. Increasing the number of replicate experiments in future revisions of the LF-IC and the BIL model is expected to provide a stronger correlation due to a lowered variability and a higher signal to noise ratio.

The commercial mesh nebulizer (Aeroneb Lab) that was used for all experiments had a capacity of 10 mL, but many nebulizer ampules are in 4 ml quantities. To demonstrate the increased efficiency of the modified system, the dose (in μg) delivered for a typical 4 mL solution loading was determined (Table 6.2). This produced an estimate of the total amount of drug that could be administered to a patient with a typical single nebulizer loading. In the case of the CM system, this would mean that a care provider would need to refill the nebulizer (10 mL) about every 15 minutes to deliver more than 90 μg (the amount delivered to the lung in 10 mL of solution) of drug at the concentration used (0.25%). This was in contrast to the modified system's ability to spray for approximately 30 hours without needing to be refilled by a care provider. In some instances, like delivery of

Illoprost for pulmonary hypertension, long delivery times are preferred. The total dose that could be delivered to a patient in the 10 ml loading was 5,142 μg.

The novel infant lung model developed in Chapter 5 was used with the low flow induction charger improved in Chapter 4 to simulate the exhalation of an inhaled aerosol in an *in vitro* model for the first time. Optimization in the LF-IC using the BIL model could increase the drug delivery rate by determining the best timing and duration of nebulization. In addition, the BIL model could be used to optimize the induction charging voltage to minimize depositional losses and the exhaled fraction. Furthermore, the LF-IC design could still be improved to reduce depositional loss in the device. The CM system is acceptable when quick delivery is needed with an inexpensive drug that has low side effects and does not require a high dose for a clinical response. A 59-fold improvement in lung delivery efficiency was seen in the LF-IC over the CM vibrating mesh nebulizer and a reduction in exhaled aerosol was the result of induction charging a 1.6 um aerosol under infant ventilation conditions in the novel BIL model.

Table 6.1 Naming convention and parameters for the commercial (CM), modified and uncharged (M-UC), and the modified and charged (M-C) systems.

	Mass output reduced	**Breath Synchronized**	**0.5 kV charging**	**Streamlined Components**	**Nebulizer located after Y-connector**
CM	No	No	No	No	No
M-UC	Yes	Yes	No	Yes	Yes
M-C	Yes	Yes	Yes	Yes	Yes

Table 6.2 Lung delivery efficiency (η), mass of AS (μg) delivered to BIL model per 4 mL loading ($Mass_{4mL}$), and mass of AS (μg) per minute ($Mass_{1min}$).

	Lung delivery efficiency (η)	**Mass of AS (μg) delivered to BIL model per 4 mL loading ($Mass_{4mL}$)**	**Mass of AS (μg) delivered to BIL model per minute ($Mass_{1min}$)**
CM	0.36 (0.1)%	36.09 (8.34)	7.15 (1.88)
M-UC	20.57 (6.8)%	2056.85 (684.5)	2.87 (1.01)
M-C	21.27 (2.4)%	2127.27 (239.3)	2.65 (0.72)

Mean (SD) BIL model results for 0.25% AS, 0.25% NaCl (N=3)

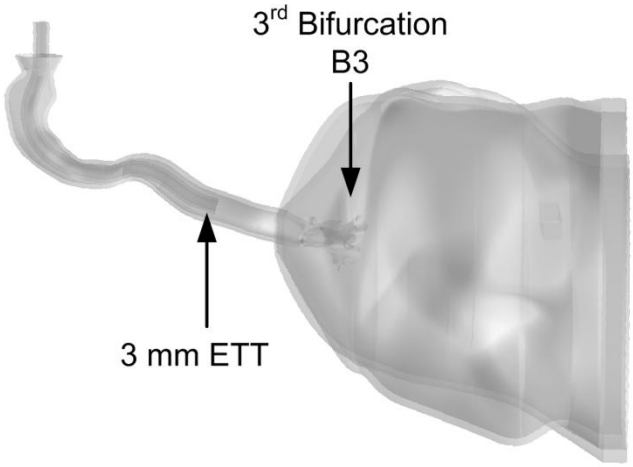

Figure 6.1 Breathing infant lung model digitally constructed from patient CT scans and rapid prototyped to estimate the exhaled fraction in an *in* vitro study of mechanical ventilation through a 3 mm endotracheal tube.

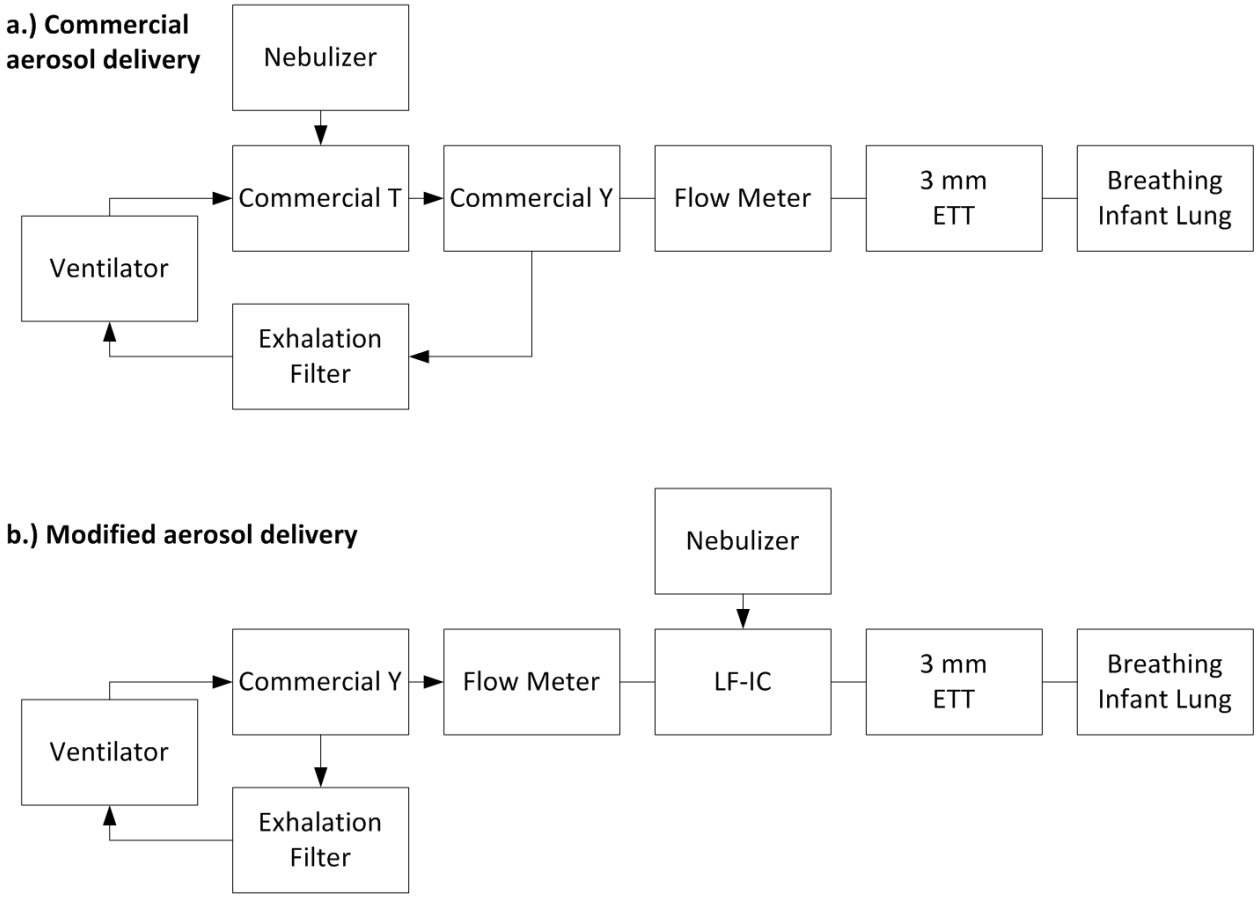

Figure 6.2 Connection configuration for (a) Commercial aerosol delivery (CM) and (b) Modified aerosol delivery (M-UC & M-C).

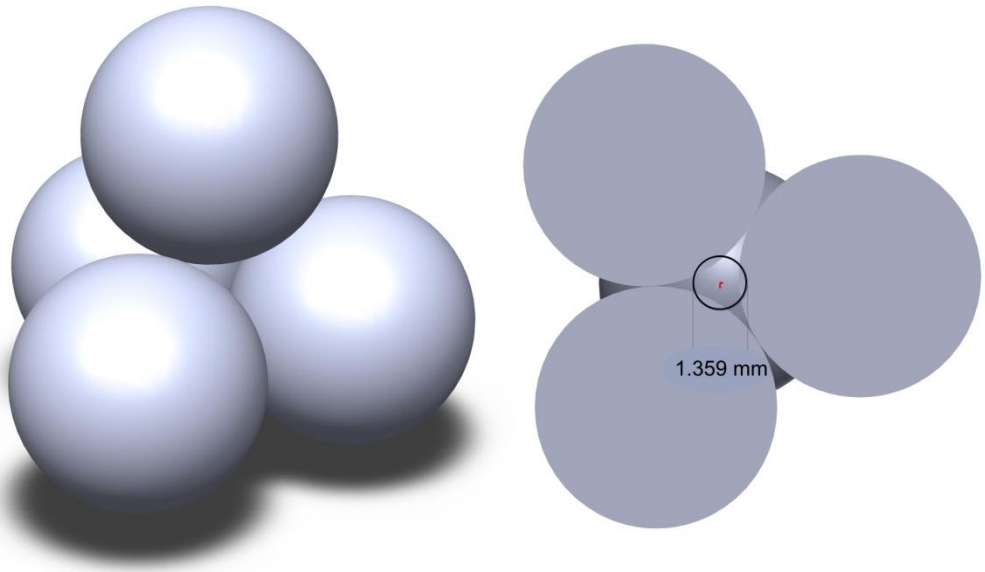

Figure 6.3 6 mm spheres arranged to show approximate average area between the spheres.

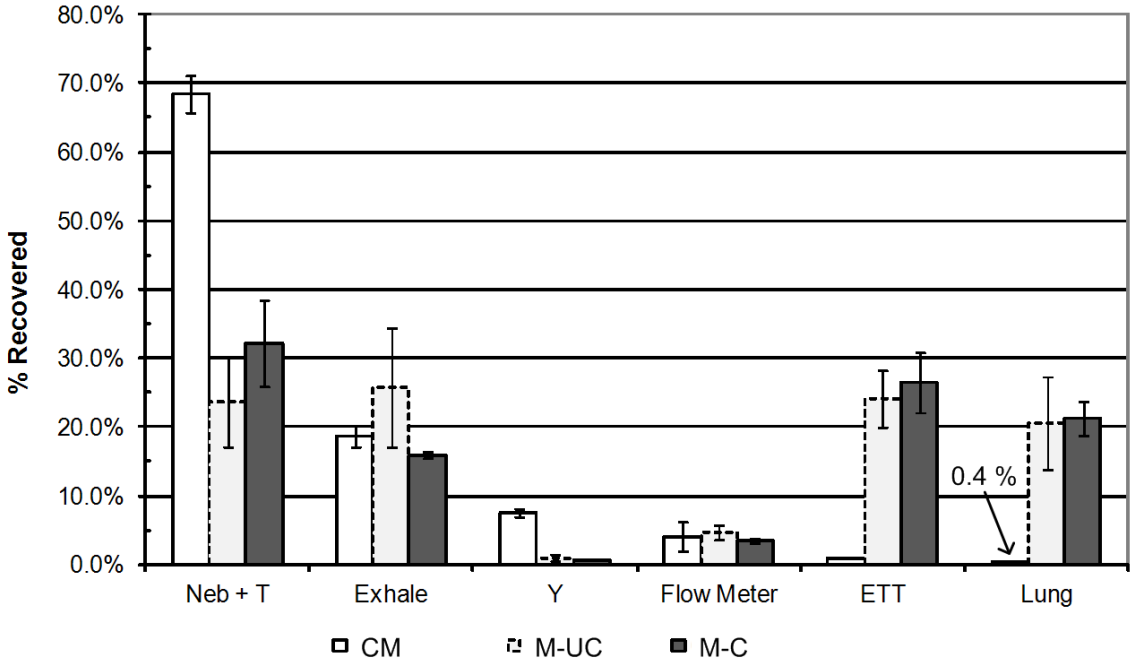

Figure 6.4 Comparison of drug (AS) delivery efficiency in a commercial vibrating mesh nebulizer (CM), the uncharged vibrating mesh nebulizer with a reduced mass output (M-UC), and the vibrating mesh nebulizer with an induced charge and a reduced mass output(M-C).

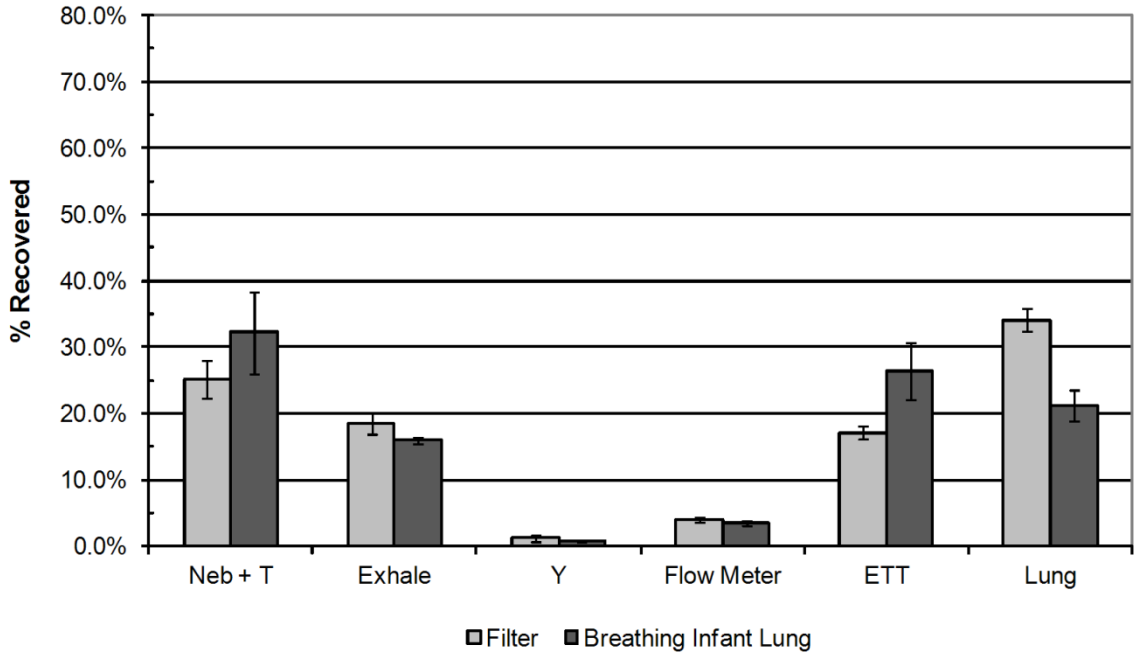

Figure 6.5 Modified and charged (M-C) albuterol sulfate deposition in the *in vitro* breathing infant lung model as compared to a mechanically ventilated filter model system capturing modified and charged (500 V) albuterol sulfate from Chapter 4.

Chapter 7 Conclusions and Future Work

As described in Chapter 1, the specific aims are divided into two objectives and seven tasks. Each of these objectives has been met and each task will be briefly summarized. In Task 1.1 an electrospray device was designed and prototyped for the generation of a highly charged submicrometer aerosol with no moving parts, but the mass output of the device was not high enough for delivery of pharmaceutically relevant concentrations of aerosol. Task 1.2 consisted of the development of a condensational vapor device designed to generate a submicrometer aerosol through heated phase change in a thin walled metal capillary followed by condensation after ejection from the heated region. The completion of Task 1.2 resulted in a very small aerosol that was not charged due to unsuccessful radial gradient charging, necessitating a third device. Task 1.3 utilized a commercial vibrating mesh nebulizer with a modified electrical input signal to produce less aerosol (by mass) and a smaller initial aerosol momentum coupled with induction charging that was measured for the polydisperse aerosol. Task 1.4 made use of the low flow induction charger (LF-IC) to evaluate the depositional loss in an infant ventilation circuit under steady state flow conditions. Having determined the appropriate runtime in Task 1.4, Task 1.5 considered implementation of the LF-IC in a ventilation circuit within realistic cyclic flow conditions, which made necessary a movement of the nebulizer location from before the Y-connector to after for the reduction of depositional losses in the flow-meter

and a redesign of the LF-IC to reduce the dead volume for patient safety in the new nebulizer location. In Task 2.1 a novel breathing infant lung (BIL) model was developed from a previously constructed mouth throat model and CT scan reconstruction of an infant pleural cavity. This model was filled with 6 mm spheres to represent the alveolar region and used to test lung response and surfactant administration techniques. The developed model from Task 2.1 was then used in Task 2.2 to quantify the exhaled fraction from a vibrating mesh nebulizer and the refined delivery system from Task 1.5 under realistic ventilation parameters. Conclusions are drawn from these tasks and summarized under each objective below with an identification of future study areas.

Objective 1: Development of an effective method for generating charged pharmaceutical aerosols with low depositional loss for use with invasive mechanical ventilation.

An electrospray device was developed and considered for infant delivery, but the chosen wick material was not substantial enough to spray the chosen drug formulation without degrading the wick material and causing the spray to end after approximately 20 minutes. The rate of delivery of the electrospray device would have required more than 8 hours of therapy to achieve a pharmaceutically meaningful dose, which is acceptable for some drugs. However, the electrospray device is not capable of spraying for long periods of time in the tested system configuration. For the purpose of this work, electrospray was not selected due to the sensitivity of the process to the drug solution and the low output rate of the tested system. Future work could be conducted to implement the electrospray using a metal capillary and a syringe pump to simplify the solution selection process and then implemented in a superior wicking material that will not degrade or dry out over an 8 hour

run. If an electrospray system is designed that can deliver a pharmaceutically relevant aerosol over the course of an 8 hour run, then the charge level will need to be assessed to determine if it is too high for delivery through the ventilator circuit.

A modified control signal was used to reduce the mass output of a commercially available vibrating mesh nebulizer and allow for effective size reduction of the generated aerosol with an infant flow rate. The droplet size distributions given by the impactors operating at 2 and 30 LPM (1.57 μm and 0.88 μm) demonstrate the importance of the volumetric flow rate of sampling air for the evaporation of an aerosol. It is important for ventilated patients to have a humidified supply line that is will not dry the lungs (Fink and Ari 2013). The difference between DSDs demonstrates the remaining water content of the aerosol at realistic infant flow rates that will enable delivery to the infant lungs without an additional humidity generator to prevent drying of the airways. Future characterization work should be done on multiple vibrating mesh nebulizers (VMN) of the same type as the work done here has been completed using a single unit. Consideration of the ventilation parameters and ETT on droplet MMAD and charge distribution would be beneficial for future CFD studies and comparison to clinical results (Dubus et al., 2005; Longest et al., 2013a). The impact of synchronized delivery on MMAD and charge distribution should also be determined after the 3mm ETT. Additional experiments determining the charge per particle with induction charging voltages varying from 0 to 2000 volts in 250 volt increments would better characterize the charging capabilities of the LF-IC.

The streamlined LF-IC was 5-fold more efficient at delivering aerosol to a filter than the commercial VMN in a commercial T under steady-state infant ventilator conditions.

This improvement resulted from the reduced momentum in the modified system causing less impaction in the LF-IC than in the commercial T as well as the reduced mass output system having a smaller MMAD and less deposition in components due to superior drying. The LF-IC was then modified for implementation in a different location of the ventilator circuit due to the presence of bias-flow and a built in flow meter (not previously considered) that is not removable from the Galileo ventilator [like many other ventilators (Schena et al., 2015)]. A reduction of LF-IC device volume was necessary to minimize the ventilator dead volume and potential re-breathing of exhaled gas. To reduce the exhaled drug, the nebulizer was breath synchronized to generate an aerosol that would be delivered to a lung filter instead of an exhalation filter. The redesigned LF-IC delivered 26-fold more aerosol to the inhalation filter as compared to the commercial VMN. Future studies are needed to optimize the timing and duration of synchronization. The current system generates aerosol during the last 0.11 seconds of exhalation, but it is suggested by the author that aerosol be generated during the last 0.1 seconds of exhalation and the first 0.1 seconds of inhalation as a starting point to determine the most efficient timing. Most importantly, optimization of the redesigned LF-IC is recommended to reduce the depositional loss in the device and increase the filter delivery to the potential fraction determined by CFD, approximately 60% (Longest et al., 2014a). In conclusion, an effective method was developed for generating a pharmaceutical aerosol for use with mechanical ventilation.

Objective 2: Use of charged aerosols for targeted deposition in infant airways.

A novel model of the infant lung was developed based on physiological data to allow testing of surfactant administration and the highly efficient LF-IC developed for the previous objective. This model provides a unique opportunity for realistic testing of inhaled aerosols and instilled therapies without the ethical considerations or high costs associated with clinical research in infants. The BIL simulates the deposition of an aerosol within the lung unlike any known model and allows for a more realistic measurement of delivered and exhaled dose. This is particularly helpful when developing a method to reduce the exhaled fraction of inhaled aerosol. Characteristic traits of the lung are exhibited in the pressure-volume curve, which was recorded during invasive mechanical ventilations using infant ventilations parameters. The specific compliance of the BIL was shown to fall within a range of values observed in a clinical study of surfactant deficient infants before treatment with surfactant (Kelly et al., 1993). The model also demonstrated an increase in inspiratory resistance immediately following instillation of surfactant. This is thought to reflect the airway obstruction that has been observed in multiple studies of instilled surfactants in infants, with harmful consequences (Tarawneh et al., 2012; Wheeler et al., 2009). The BIL model could be very useful to the American Academy of Pediatrics as a tool to assess methods of administration and evaluate the harm that can be inflicted by instillation and the benefit of aerosol administration. A small amount of aerosol (49.5 μg) delivered to the BIL was shown to improve physiological lung function in the BIL model as was also described in the study of Lewis et al. (1993) considering deposition of 0.5 mg/kg. The next study with the BIL should consider an increased dose of surfactant

(approximately 10 to 100 times more) by some combination of an increased solution concentration, improved delivery efficiency, and increased runtime. Additional experimentation needs to be conducted in parallel with Mr. Karl Bass' CFD work to determine the sphere size that should be used in future versions of the BIL model, the initial recommendation of this researcher is a 2-2.5mm sphere instead of the 6mm sphere to more closely mimic the alveolar diameter of 0.54mm (Khajeh-Hosseini-Dalasm and Longest 2014). The BIL model can also be digitally reconstructed with a functional residual capacity of 110mL, which is more representative of newborn infants (Lumb 2012). With this rescaled model that utilizes smaller spheres, the appropriate volume of fluid will need to be reconsidered using the same method described in Chapter 5. Finally, even without modifying the BIL it could prove informative to consider the physiological response of the model to a bovine derived surfactant such as Survanta (Abbvie; North Chicago, IL), which is approved for clinical use by the United States FDA.

Another application of the BIL which was evaluated is the use of the developed LF-IC to target delivery in the lung. As determined in the previous objective, the output aerosol size of the LF-IC was less than 1.8μm, which should greatly reduce the losses in the ventilator circuit, but is also expected to reach the alveolar region and have reduced deposition in the upper airways. The delivery efficiency of the LF-IC is compared with the commercial vibrating mesh nebulizer and is found to increase from 0.36% to 21.3%. This 59-fold improvement over commercial delivery demonstrates the importance of minimizing depositional losses in the device due to impaction, losses due to bias-flow, losses due to the built in flow meter, and depositional losses in the ETT due to an initially large MMAD. The primary purpose of this device was to increase the delivery efficiency,

but the trade-off for 59-fold increased efficiency was a 2.6-fold decreased delivery rate from 7.15μg/min to 2.7μg/min. Induction charging of the aerosol increased the depositional loss on the LF-IC, but considering the fraction of drug entering the BIL, charging the aerosol decreased the exhaled fraction by 17% (not statistically significant). The BIL enables additional considerations to be evaluated in future studies. In cases when increased delivery rate is more desirable than efficiency, it will be important to increase the duration of nebulization from the current 0.11 seconds to 0.33 seconds. This is expected to directly increase the delivery rate, but may decrease the delivery efficiency. It is recommended that the beginning of nebulization remain 0.11 seconds before inhalation, but the nebulization period extend 0.22 seconds into inspiration. This is still less than the first half of inspiration used in the study of Longest et al. (2014a). The LF-IC can also be used to deliver medicines that are expensive or have adverse secondary effects in an *in vivo* rat study comparing invasive and non-invasive delivery of aerosol generated by the LF-IC and by the commercial VMN as well as an additional conventional method, such as instilled. This *in vivo* study can be used as another benchmark for the BIL model by aerosolizing a radio labeled dose and comparing the regional deposition in the animal model and the BIL model using gamma scintigraphy (Biddiscombe et al., 2011).

The BIL model also provides a way of evaluating additional administration techniques such as dry powder inhalers, metered dose inhalers, and jet nebulizers. The same study of albuterol sulfate should be considered again after the BIL model has been modified with refined sphere size (2.5 mm), additional morphology in the upper airways (to generation 7), and potentially altered ventilation parameters such as inspiratory time and positive end expiratory pressure. Finally, the development of a breathing adult lung

(BAL) model to accompany the BIL model could be useful for testing adult therapies which have a larger amount of clinical data for validation

List of References

Abbasi, S., Sivieri, E., Roberts, R., and Kirpalani, H. (2012) Accuracy of tidal volume, compliance, and resistance measurements on neonatal ventilator displays: An in vitro assessment. *Pediatric Critical Care Medicine*, *13*(4), e262-e268.

Ari, A., and Fink, J. B. (2015) Aerosol Drug Delivery During Mechanical Ventilation: Devices, Selection, Delivery Technique, and Evaluation of Clinical Response to Therapy. *Clinical Pulmonary Medicine*, *22*(2), 79-86.

Armangil, D., Yurdakok, M., Korkmaz, A., Yigit, S., and Tekinalp, G. (2011) Inhaled Beta-2 agonist salbutamol for the treatment of transient tachypnea of the newborn. *The Journal of Pediatrics*, *159*, 398-403.

Arnal, J.-M., Bancalari, E., Clement, K. C., Courtney, S. E., Danan, C., Donn, S. M., Durrmeyer, X., Emeriaud, G., Essouri, S., and Grasso, F. (2015) Mechanical Ventilation. Pediatric and Neonatal Mechanical Ventilation, Springer, 149-274.

Azhdarzadeh, M., Olfert, J. S., Vehring, R., and Finlay, W. H. (2014a) Effect of electrostatic charge on oral-extrathoracic deposition for uniformly charged monodisperse aerosols. *Journal of Aerosol Science*, *68*, 38-45.

Azhdarzadeh, M., Olfert, J. S., Vehring, R., and Finlay, W. H. (2014b) Effect of induced charge on deposition of uniformly charged particles in a pediatric oral-extrathoracic airway. *Aerosol Science and Technology*, *48*(5), 508-514.

Bacon, R. E., Pitcairn, G. R., Schmidt, O., Church, A., Limb, M., Davidson, B., McVeety, B., Matis, R. J., Cline, D., and Triplett, M. D. (2009) The Battelle Mystic inhaler delivers fluticasone propionate to the lungs more efficintly than an HFA pMDI with spacer as determined by scintigraphy. *Respiratory Drug Delivery Europe*, 345-350.

Bailey, A. G. (1997) The inhalation and deposition of charged particles within the human lung. *Journal of Electrostatics*, *42*, 25-32.

Bailey, A. G., Hashish, A. H., and Williams, T. J. (1998) Drug delivery by inhalation of charged particles. *Journal of Electrostatics*, *44*, 3-10.

Balachandran, W., Machowski, W., Gaura, E., and Hudon, C. (1997) Control of drug aerosol in human airways using electrostatic forces. *Journal of Electrostatics*, *40&41*, 579-584.

Berggren, E., Liljedahl, M., Winbladh, B., Andreasson, B., Cursted, T., and Robertson, B. (2000) Pilot study of nebulized surfactant therapy for neonatal respiratory distress syndrome. *Acta Paediatr.*, *89*(4), 460-464.

Bhat, R., Dziedzic, K., Bhutani, V. K., and Vidyasagar, D. (1990) Effect of single dose surfactant on pulmonary function. *Critical care medicine*, *18*(6), 590-595.

Biddiscombe, M. F., Meah, S. N., Underwood, S. R., and Usmani, O. S. (2011) Comparing Lung Regions of Interest in Gamma Scintigraphy for Assessing Inhaled Therapeutic Aerosol Deposition. *Journal Of Aerosol Medicine And Pulmonary Drug Delivery*, *24*(3), 165-173.

Brion, L. P., Primhak, R. A., and Yong, W. (2006) Aerosolized diuretics for preterm infants with (or developing) chronic lung disease. *Cochrane Database Of Systematic Reviews*, (3).

Brochard, L. (2006) What is a pressure-volume curve? *Critical Care*, *10*(4), 156.

Byron, P. R., Hindle, M., Lange, C. F., Longest, P. W., McRobbie, D., Oldham, M. J., Olsson, B., Thiel, C. G., Wachtel, H., and Finlay, W. H. (2010) In Vivo-In Vitro Correlations: Predicting Pulmonary Drug Deposition from Pharmaceutical Aerosols. *Journal Of Aerosol Medicine And Pulmonary Drug Delivery*, *23*, S59-S69.

Carrigy, N. B., Ruzycki, C. A., Golshahi, L., and Finlay, W. H. (2014) Pediatric in vitro and in silico models of deposition via oral and nasal inhalation. *Journal of aerosol medicine and pulmonary drug delivery*, *27*(3), 149-169.

Chan, T. L., Lippmann, M., Cohen, V., and Schlesinger, R. B. (1978) Effect of electrostatic charges on particle deposition in a hollow cast of the human larynx-tracheobronchial tree. *Journal of Aerosol Science*, *9*, 463-468.

Chen, D.-R., Pui, D. Y. H., and Kaufman, S. L. (1995) Electrospraying of conducting liquids for monodisperse aerosol generation in the 4 nm to 1.8 Î¼m diameter range. *Journal of Aerosol Science*, *26*(6), 963-977.

Chiarot, P. R., Sullivan, P., and Ben Mrad, R. (2012) Electrospray from a droplet. *Experimental Thermal and Fluid Science*, *37*, 184-188.

Cloupeau, M., and Prunet-Foch, B. (1994) Electrohydrodynamic spraying functioning modes: a critical review. *Journal of Aerosol Science*, *25*(6), 1021-1036.

Cole, C. H. (2000) Special problems in aerosol delivery: neonatal and pediatric considerations. *Respiratory care*, *45*(6), 646-651.

Cole, C. H., Colton, T., Shah, B. L., Abbasi, S., MacKinnon, B. L., Demissie, S., and Frantz, I. D. (1999) Early inhaled glucocorticoid therapy to prevent bronchopulmonary dysplasia. *New England Journal Of Medicine*, *340*(13), 1005-1010.

Collaborative European Multicenter Study, G. (1988) Surfactant replacement therapy for severe neonatal respiratory distress syndrome: an international randomized clinical trial. *Pediatrics*, *82*(5), 683-691.

Cornelius, G. J., Noakes, T. J., Jefferies, A., Green, M. L., and Prendergast, M. J. (1998). "Electrostatic spraying device." US5810265.

Darquenne, C. (2012) Aerosol deposition in health and disease. *Journal of aerosol medicine and pulmonary drug delivery*, *25*(3), 140-147.

de Juan, L., and De la Mora, J. F. (1997) Charge and size distribution of electrospray drops. *Jounral of colloid and interface science*, *186*, 280-293.

de la Mora, J. F. (2007) The fluid dynamics of Taylor cones. *Annual Review Of Fluid Mechanics*, *39*, 217-243.

Delvadia, R., Hindle, M., Longest, P. W., and Byron, P. R. (2013) In vitro tests for aerosol deposition II: IVIVCs for different dry powder inhalers in normal adults. *Journal of Aerosol Medicine and Pulmonary Drug Delivery*, *26*(3), 138-144.

Delvadia, R., Longest, P. W., and Byron, P. R. (2012) In vitro tests for aerosol deposition. I. Scaling a physical model of the upper airways to predict drug deposition variation in normal humans. *Journal of Aerosol Medicine*, *25*(1), 32-40.

Dhand, R. (2002) Nebulizers that use a vibrating mesh or plate with multiple apertures to generate aerosol. *Respiratory Care*, *47*(12), 1406-1416.

Dhand, R. (2008) Aerosol delivery during mechanical ventilation: From basic techniques to new devices. *Journal of Aerosol Medicine and Pulmonary Drug Delivery*, *21*(1), 45-60.

Drake, R., Vogl, A. W., and Mitchell, A. W. M. *Gray's anatomy for students*. Elsevier Health Sciences; (2005)

Dubus, J. C., Vecellio, L., De Monte, M., Fink, J. B., Grimbert, D., Montharu, J., Valat, C., Behan, N., and Diot, P. (2005) Aerosol deposition in neonatal ventilation. *Pediatric Research*, *58*(1), 10-14.

Dutkiewicz, E., and Jakubowska, A. (2002) Effect of electrolytes on the physicochemical behaviour of sodium dodecyl sulphate micelles. *Colloid and Polymer Science*, *280*(11), 1009-1014.

Finer, N. N., Merritt, T. A., Bernstein, G., Job, L., Mazela, J., and Segal, R. (2010) An open label, pilot study of Aerosurf combined with nCPAP to prevent RDS in preterm neonates. *Journal of Aerosol Medicine and Pulmonary Drug Delivery*, *23*(5), 303-309.

Fink, J., and Ari, A. (2013) Aerosol delivery to intubated patients. *Expert opinion on drug delivery*, *10*(8), 1077-1093.

Fink, J. B. (2004) Aerosol delivery to ventilated infant and pediatric patients. *Respiratory Care*, *49*(6), 653-665.

Finlay, W. H. *The Mechanics of Inhaled Pharmaceutical Aerosols*. Academic Press: San Diego; (2001)

Fisher, J. B., Mammel, M. C., Coleman, J. M., Bing, D. R., and Boros, S. J. (1988) Identifying lung overdistention during mechanical ventilation by using volume-pressure loops. *Pediatric pulmonology*, *5*, 10-14.

Fok, T. F., Monkman, S., Dolovich, M., Gray, S., Coates, G., Paes, B., Rashid, F., Newhouse, M., and Kirpalani, H. (1996) Efficiency of aerosol medication delivery from a metered dose inhaler versus jet nebulizer in infants with bronchopulmonary dysplasia. *Pediatric Pulmonology*, *21*(5), 301-309.

Fu, H. J., Patel, A. C., Holtzman, M. J., and Chen, D. R. (2011) A new electrospray aerosol generator with high particle transmission efficiency. *Aerosol Science And Technology*, *45*(10), 1176-1183.

Ganan-Calvo, A. M., Davila, J., and Barrero, A. (1997) Current and droplet size in the electrospraying of liquids. Scaling laws. *J. Aerosol Sci.*, *28*(2), 249-275.

Golshahi, L., Longest, P. W., Holbrook, L., Snead, J., and Hindle, M. (2015) Produciton of highly charged pharmaceutical aerosols using a new aerosol induction charger. *Pharmaceutical Research*, *in review*.

Grigg, J., Arnon, S., Jones, T., Clarke, A., and Silverman, M. (1992) Delivery of therapeutic aerosols to intubated babies. *Archives of disease in childhood*, *67*(1 Spec No), 25-30.

Guerin, C., Fassier, T., Bayle, F. d. r., Lemasson, S. p., and Richard, J.-C. (2008) Inhaled bronchodilator administration during mechanical ventilation: how to optimize it, and for which clinical benefit? *Journal of aerosol medicine and pulmonary drug delivery*, *21*(1), 85-96.

Hindle, M. (2004) Soft mist inhalers: A review of current technology. *The Drug Delivery Companies Report Autumn/Winter*, 31-34.

Hindle, M., Byron, P. R., Jashnani, R. N., Howell, T. M., and Cox, K. A. (1998) High efficiency fine particle generation using novel condensation technology. Proceedings of Respiratory Drug Delivery VI, R. N. Dalby, P. R. Byron, and S. J. Farr, eds., Interpharm Press, Inc., Buffalo Grove, IL, 97-102.

Hindle, M., Gupta, R., and Cox, K. A. (2004) Adding pharmaceutical flexibility to the capillary aerosol generator. Respiratory Drug Delivery IX, R. N. Dalby, P. R. Byron, J. Peart, J. D. Suman, and S. J. Farr, eds., DHI Publishing, River Grove, IL, 247-254.

Hindle, M., and Longest, P. W. (2013) Quantitative analysis and design of a spray aerosol inhaler. Part 2: Improvements in mouthpiece performance. *Journal of Aerosol Medicine and Pulmonary Drug Delivery 26*(5), 237-247.

Hinds, W. C. *Aerosol Technology: Properties, Behavior, and Measurement of Airborne Particles*. John Wiley and Sons: New York; (1999)

Holbrook, L., Hindle, M., and Longest, P. W. (2015) Generating charged pharmaceutical aerosols intended to improve targeted drug delivery in ventilated infants. *Journal of Aerosol Science*, *88*, 35-47.

Hong, J. N., Hindle, M., and Byron, P. R. (2002) Control of particle size by coagulation of novel condensation aerosols in reservoir chambers. *Journal of Aerosol Medicine*, *15*(4), 359-368.

Howell, T. M., and Sweeney, W. R. (1998) Aerosol and a method and apparatus for generating an aerosol. *United States Patent 5/743,251*.

Hu, B., So, P.-K., Chen, H., and Yao, Z.-P. (2011) Electrospray ionization using wooden tips. *Analytical chemistry*, *83*(21), 8201-8207.

ICRP. *Human Respiratory Tract Model for Radiological Protection*. Elsevier Science Ltd.: New York; (1994)

Ijsebaert, J. C., Geerse, K. B., Marijnissen, J. C. M., Lammers, J.-W. J., and Zanen, P. (2001) Electro-hydrodynamic atomization of drug solutions for inhalation purposes. *Journal of Applied Physiology*, *91*, 2735-2741.

Kacmarek, R. M. (2011) The mechanical ventilator: past, present, and future. *Respiratory care*, *56*(8), 1170-1180.

Kelly, E., Bryan, H., Possmayer, F., Frndova, H., and Bryan, C. (1993) Compliance of the respiratory system in newborn infants pre- and postsurfactant replacement therapy. *Pediatric pulmonology*, *15*(4), 225-230.

Khajeh-Hosseini-Dalasm, N., and Longest, P. W. (2014) Deposition of Particles in the Alveolar Airways: Inhalation and Breath-Hold with Pharmaceutical Aerosols. *Journal of aerosol science*.

Koolpiruck, D., Prakoonwit, S., and Balachandran, W. (2004) Numerical modeling of inhaled charged aerosol deposition in human airways. *Industry Applications, IEEE Transactions on*, *40*(5), 1239-1248.

Koren, H. S., Devlin, R. B., Graham, D. E., Mann, R., McGee, M. P., Horstman, D. H., Kozumbo, W. J., Becker, S., House, D. E., McDonnell, W. F., and Bromberg, P. A. (1989) Ozone-Induced Inflammation In The Lower Airways Of Human-Subjects. *American Review Of Respiratory Disease*, *139*(2), 407-415.

Kotian, R., Peart, J., Bryner, J., and Byron, P. R. (2009) Calibration of the modified electrical low-pressure impactor (ELPI) for use with pressurized pharmaceutical aerosols. *Journal of Aerosol Medicine and Pulmonary Drug Delivery*, *22*(1), 55-65.

Kwok, P. C. L., and Chan, H. K. (2009) Electrostatics of pharmaceutical inhalation aerosols. *Journal Of Pharmacy And Pharmacology*, *61*(12), 1587-1599.

Lee, Y. H., Zhang, J. J., and Chen, D. R. (2011) Note: Electrohydrodynamic atomization of liquid sheet. *Review Of Scientific Instruments*, *82*(2).

Lehne, R. A., and Rosenthal, L. *Pharmacology for nursing care*. Elsevier Health Sciences: Philadelphia, PA; (2014)

Lesniewski, T. K., and Friedlander, S. K. (1995) The effect of turbulence on rates of particle formation by homogeneous nucleation. *Aerosol Science and Technology*, *23*, 174-182.

Lesniewski, T. K., and Friedlander, S. K. (1998) Particle nucleation and growth in a free turbulent jet. *Proceedings of the Royal Society of London A*, *454*, 2477-2504.

Lewis, J. F., Tabor, B., Ikegami, M., Jobe, A. H., Joseph, M., and Absolom, D. (1993) Lung function and surfactant distribution in saline-lavaged sheep given instilled vs. nebulized surfactant. *Journal of Applied Physiology*, *74*(3), 1256-1264.

Liu, J., Wang, H., Manicke, N. E., Lin, J.-M., Cooks, R. G., and Ouyang, Z. (2010) Development, characterization, and application of paper spray ionization. *Analytical chemistry*, *82*(6), 2463-2471.

Longest, P. W., Azimi, M., Golshahi, L., and Hindle, M. (2013a) Improving aerosol drug delivery during invasive mechanical ventilation with redesigned components. *Respiratory Care*, respcare. 02782.

Longest, P. W., Azimi, M., Golshahi, L., and Hindle, M. (2014a) Improving aerosol drug delivery during invasive mechanical ventilation with redesigned components. *Respiratory Care*, *59*(5), 686-698.

Longest, P. W., Azimi, M., and Hindle, M. (2014b) Optimal delivery of aerosols to infants during mechanical ventilation. *Journal of Aerosol Medicine and Pulmonary Drug Delivery*, *27*(5), 371-385.

Longest, P. W., Golshahi, L., and Hindle, M. (2013b) Improving pharmaceutical aerosol delivery during noninvasive ventilation: Effects of streamlined components. *Annals of Biomedical Engineering*, *41*(6), 1217-1232.

Longest, P. W., and Hindle, M. (2009) Quantitative analysis and design of a spray aerosol inhaler. Part 1: Effects of dilution air inlets and flow paths. *Journal of Aerosol Medicine and Pulmonary Drug Delivery*, *22*(3), 271-283.

Longest, P. W., Hindle, M., Das Choudhuri, S., and Byron, P. R. (2007) Numerical simulations of capillary aerosol generation: CFD model development and comparisons with experimental data. *Aerosol Science and Technology*, *41*(10), 952-973.

Longest, P. W., Hindle, M., Das Choudhuri, S., and Xi, J. (2008) Comparison of ambient and spray aerosol deposition in a standard induction port and more realistic mouth-throat geometry. *Journal of Aerosol Science*, *39*(7), 572-591.

Longest, P. W., Spence, B. M., Holbrook, L. T., Mossi, K. M., Son, Y.-J., and Hindle, M. (2012) Production of inhalable submicrometer aerosols from conventional mesh nebulizers for improved respiratory drug delivery. *Journal of Aerosol Science*, *51*, 66-80.

Longest, P. W., and Tian, G. (2014) Development of a New Technique for the Efficient Delivery of Aerosolized Medications to Infants on Mechanical Ventilation. *Pharmaceutical research*, 1-16.

Longest, P. W., and Tian, G. (2015) Development of a new technique for the efficient delivery of aerosolized medications to infants on mechanical ventilation. *Pharmaceutical Research*, *32*, 321-336.

Longest, P. W., Walenga, R. L., Son, Y.-J., and Hindle, M. (2013c) High efficiency generation and delivery of aerosols through nasal cannula during noninvasive ventilation. *Journal of Aerosol Medicine and Pulmonary Drug Delivery*, *26*(5), 266-279.

Lumb, A. B. *Nunn's Applied Respiratory Physiology*. Churchill Livingstone: Oxford; (2012)

Macintyre, N. R., Silver, R. M., Miller, C. W., Schuler, F., and Coleman, R. E. (1985) Aerosol Delivery In Intubated, Mechanically Ventilated Patients. *Critical Care Medicine*, *13*(2), 81-84.

Mainelis, G., Willeke, K., Baron, P., Grinshpun, S. A., and Reponen, T. (2002) Induction charging and electrostatic classification of micrometer-size particles for investigating the electrobiological properties of airborne microorganisms. *Aerosol Science & Technology*, *36*(4), 479-491.

Martin, A. R., and Finlay, W. H. (2014) Nebulizers for drug delivery to the lungs. *Expert opinion on drug delivery*, *12*(6), 889-900.

Mazela, J., Chmura, K., Kulza, M., Henderson, C., Gregory, T. J., Moskal, A., Sosnowski, T. R., Florek, E., Kramer, L., and Keszler, M. (2014) Aerosolized albuterol sulfate delivery under neonatal ventilatory conditions: In vitro evaluation of a novel ventilator circuit patient interface connector. *Journal of Aerosol Medicine and Pulmonary Drug Delivery*, *27*(1), 58-65.

Mazela, J., and Polin, R. A. (2011) Aerosol delivery to ventilated newborn infants: historical challenges and new directions. *Eur. J. Pediatr.*, *170*, 433-444.

Melandri, C., Tarroni, G., Prodi, V., Zaiacomo, T., De Formignan, M., and Lombardi, C. C. (1983) Deposition of charged particles in the human airways. *J. Aerosol Science*, *14*, 657-669.

Miedema, M., de Jongh, F. H., Frerichs, I., van Veenendaal, M. t. B., and van Kaam, A. H. (2011) Changes in lung volume and ventilation during surfactant treatment in ventilated preterm infants. *American journal of respiratory and critical care medicine*, *184*(1), 100-105.

Ouyang, J. T., Hui, H. X., Zhang, Y., and Cui, M. (1995) Generation of charged aerosol from superheated steam in laval nozzle. *J. Aerosol Sci.*, *26*(4), 559-562.

Park, I., Kim, W., and Kim, S. S. (2011) Multi-jet model electrospray for non-conducting fluids using two fluids and a coxail grooved nozzle. *Aerosol Science and Technology*, *45*, 629-634.

Phalen, R. F., Oldham, M. J., Beaucage, C. B., Crocker, T. T., and Mortensen, J. D. (1985) Postnatal enlargement of human tracheobronchial airways and implications for particle deposition. *Anat. Rec.*, *212*, 368-380.

Pillow, J., and Minocchieri, S. (2012) Innovation in surfactant therapy II: surfactant administration by aerosolization. *Neonatology*, *101*(4), 337-344.

Polin, R. A., Carlo, W. A., Papile, L.-A., Carlo, W., Tan, R., Kumar, P., Benitz, W., Eichenwald, E., Cummings, J., and Baley, J. (2014) Surfactant replacement therapy for preterm and term neonates with respiratory distress. *Pediatrics*, *133*(1), 156-163.

Rebello, C. M., Jobe, A. H., Eisele, J. W., and Ikegami, M. (1996) Alveolar and tissue surfactant pool sizes in humans. *American journal of respiratory and critical care medicine*, *154*(3), 625-628.

Reischl, G., John, W., and Devor, W. (1977) Uniform electrical charging of monodisperse aerosols. *Journal of Aerosol Science*, *8*(1), 55-65.

Rubin, B. K., and Fink, J. B. (2001) Aerosol therapy for children. *Respir Care Clin N Am*, *7*(2), 175-213.

Rubin, B. K., and Williams, R. W. (2014) Emerging aerosol drug delivery strategies: From bench to clinic. *Advanced drug delivery reviews*, *75*, 141-148.

Schena, E., Massaroni, C., Saccomandi, P., and Cecchini, S. (2015) Flow measurement in mechanical ventilation: a review. *Medical engineering & physics*, *37*(3), 257-264.

Shah, V., Ohlsson, A., Halliday, H. L., and Dunn, M. S. (2007) Early administration of inhaled corticosteroids for preventing chronic lung disease in ventilated very low birth weight preterm neonates. *Cochrane Database Of Systematic Reviews*, (4).

Shen, X., Hindle, M., and Byron, P. R. (2004) Effect of energy on propylene glycol aerosols using the capillary aerosol generator. *International Journal of Pharmaceutics*, *275*(1-2), 249-258.

Sidler-Moix, A. L., Dolci, U., Berger-Gryllaki, M., Pannatier, A., Cotting, J., and Di Paolo, E. R. (2013) Albuterol Delivery in an In Vitro Pediatric Ventilator Lung Model: Comparison of Jet, Ultrasonic, and Mesh Nebulizers. *Pediatric Critical Care Medicine*, *14*(2), E98-E102.

Slutsky, A. S. (2015) History of Mechanical Ventilation. From Vesalius to Ventilator-induced Lung Injury. *American journal of respiratory and critical care medicine*, *191*(10), 1106-1115.

Sood, B. G., Delaney-Black, V., Aranda, J. V., and Shankaran, S. (2004) Aerosolized PGE(1): A selective pulmonary vasodilator in neonatal hypoxemic respiratory failure results of a phase I/II open label clinical. *Pediatric Research*, *56*(4), 579-585.

Stenfors, N., Pourazar, J., Blomberg, A., Krishna, M. T., Mudway, I., Helleday, R., Kelly, F. J., Frew, A. J., and Sandstrom, T. (2002) Effect of ozone on bronchial mucosal inflammation in asthmatic and healthy subjects. *Respiratory Medicine*, *96*(5), 352-358.

Sun, Y., Yang, R., Zhong, J.-g., Fang, F., Jiang, J.-j., Liu, M.-y., and Lu, J. (2009) Aerosolised surfactant generated by a novel noninvasive apparatus reduced acute lung injury in rats. *Critical Care*, *13*(2), R31-R31.

Tang, K., and Gomez, A. (1994) Generation by electrospray of monodisperse water droplets for targeted drug delivery by inhalation. *Journal of aerosol science*, *25*(6), 1237-1249.

Tarawneh, A., Kaczmarek, J., Bottino, M. N., and Sant'Anna, G. M. (2012) Severe airway obstruction during surfactant administration using a standardized protocol: a prospective, observational study. *Journal of Perinatology*, *32*(4), 270-275.

Taylor, G. (1964) Disintegration of Water Drops in an Electric Field. *Proceedings of the Royal Society of London. Series A, Mathematical and Physical Sciences*, *280*(1382), 383-397.

Tepper, G., and Kessick, R. (2008) A study of ionization and collection efficiencies in electrospray-based electrostatic precipitators. *Aerosol Science*, *39*, 609-617.

Tepper, G., and Kessick, R. (2009) Nanoelectrospray aerosols from microporous polymer wick sources. *Applied Physics Letters*, *94*, 084106.

Tepper, G., Kessick, R., and Pestov, D. (2007) An electrospray-based, ozone-free air purification technology. *Journal Of Applied Physics*, *102*(11).

Tu, K.-W. (1982) A condensation aerosol generator system for monodisperse aerosols of different physicochemical properties. *Journal of Aerosol Science*, *13*(5), 363-371.

Usmani, O. S., Biddiscombe, M. F., Nightingale, J. A., Underwood, S. R., and Barnes, P. J. (2003) Effects of bronchodilator particle size in asthmatic patients using monodisperse aerosols. *Journal Of Applied Physiology*, *95*(5), 2106-2112.

Vehring, R., Aardahl, C. L., Davis, E. J., Schweiger, G., and Covert, D. S. (1997) Electrodynamic trapping and manipulation of particle clouds. *Review of scientific instruments*, *68*(1), 70-78.

Walenga, R. L., Tian, G., and Longest, P. W. (2013) Development of characteristic upper tracheobronchial airway models for testing pharmaceutical aerosol delivery. *ASME Journal of Biomechanical Engineering*, *135(9)*, 091010.

Walsh, B. K., and DiBlasi, R. M. (2010) Mechanical ventilation of the neonate and pediatric patient. Perinatal and Pediatric Respiratory Care, B. K. Walsh, M. P. Czervinske, and R. M. DiBlasi, eds., Saunders Elsevier, St. Louis, 325-347.

Walther, F. J., Hernandez-Juviel, J. M., and Waring, A. J. (2014) Aerosol delivery of synthetic lung surfactant. *PeerJ*, *2*, e403.

Watterberg, K. L., Clark, A. R., Kelly, H. W., and Murphy, S. (1991) Delivery of aerosolized medication to intubated babies. *Pediatric pulmonology*, *10*(2), 136-141.

West, J. B. *Respiratory Physiology: The Essentials*. Lippincott Williams and Wilkins: Baltimore, MD; (2012)

Wheeler, K. I., Davis, P. G., Kamlin, C. O. F., and Morley, C. J. (2009) Assist control volume guarantee ventilation during surfactant administration. *Archives of Disease in Childhood-Fetal and Neonatal Edition*, *94*(5), F336-F338.

Willson, D. F. (2015) Aerosolized Surfactants, Anti-Inflammatory Drugs, and Analgesics. *Respiratory care*, *60*(6), 774-793.

Wong, J., Chan, H.-K., and Kwok, P. C. L. (2013) Electrostatics in pharmaceutical aerosols for inhalation. *Therapeutic delivery*, *4*(8), 981-1002.

Xi, J., and Longest, P. W. (2008) Effects of oral airway geometry characteristics on the diffusional deposition of inhaled nanoparticles. *ASME Journal of Biomechanical Engineering*, *130*, 011008.

Yang, Q., Wang, H., Maas, J. D., Chappell, W. J., Manicke, N. E., Cooks, R. G., and Ouyang, Z. (2012) Paper spray ionization devices for direct, biomedical analysis using mass spectrometry. *International journal of mass spectrometry*, *312*, 201-207.

Yurteri, C. U., Hartman, R. P. A., and Marijnissen, J. C. M. (2010) Producing pharmaceutical particles via electrospraying with an emphasis on nano and nano structured particles - A review. *KONA Powder and Particle Journal*, *28*, 91-115.

Zeleny, J. (1914) The electrical discharge from liquid points, and a hydrostatic method of measuring the electric intensity at their surfaces. *Physical Review*, *3*(2), 69.

Zeleny, J. (On the conditions of instability of electrified drops, with applications to the electrical discharge from liquid points) Proc. Camb. Phil. Soc, *18*, 71-83, (1915).

Zeleny, J. (1917) Instability of electrified liquid surfaces. *Physical Review*, *10*(1), 1-6.

Zhao, S., Castle, G. S. P., and Adamiak, K. (2005) Comparison of conducting and induction charging in liquid spraying. *Journal of Electrostatics*, *63*, 871-876.

Vita

Department of Mechanical and Nuclear Engineering
Virginia Commonwealth University
401 West Main Street, Room E3235
P.O. Box 843015, Richmond, VA 23284-3015

Landon Tucker Holbrook
Cell phone: (804) 543-9995
E-mail: holbrooklt@gmail.com

EDUCATION

- **Virginia Commonwealth University**, Richmond, VA
  Ph.D. in Engineering; GPA 3.9; August 2015
  Dissertation: *Generation and Delivery of Charged Aerosols to Infant Airways*
- **Virginia Commonwealth University**, Richmond, VA
  B.S. in Mechanical Engineering; Magna Cum Laude GPA 3.84; 2009

RESEARCH EXPERIENCE

- **Research Assistant**, Spring 2010 – Present
  Virginia Commonwealth University, Aerosol Dynamics & Respiratory Transport Research Lab, Richmond, VA
  - Computational Fluid Dynamics and Solid Modeling of human lung
  - *In vitro* testing of lung compliance and inspiratory resistance
  - Rapid Prototyping and laboratory management
  - Generation of Albuterol Sulfate aerosol using commercial and novel devices
  - Aerosol characterization using impaction (ELPI, Anderson, Mini-MOUDI, NGI), particle counting (CPC), classifier (SMPS), and microscopy (optical, fluorescent and SEM)

RESEARCH INTERESTS

- **3D Printing and Rapid Prototyping (3D)**
  - Surface effects and coatings of prototyped materials
  - Inhaler design and development
- **Respiratory drug delivery (RDD)**
  - *In vivo* delivery of aerosolized treatment using high efficiency devices to reduce variability and enhance particle deposition

- Medical aerosol generation and transport for traditional and next generation systems
- Increasing delivery efficiency to enable pediatric drug delivery

- **Humanitarian Engineering (HE)**
  - Replacing wood with rice husks as a source of heating and cooking
  - Respiratory and environmental effects of open flame cook-stoves

JOURNAL PUBLICATIONS

In print –(Current 5-Year ISI Impact factors next to journal titles where available)

2015

Holbrook, L. T., Hindle, M., Longest, P.W. 2015. Generating charged pharmaceutical aerosols intended to improve targeted delivery in ventilated infants. *Journal of Aerosol Science*. [3.0]

Golshahi, L., Longest P. W., Holbrook, L. T., Snead, J. and Hindle, M. 2015. Production of Highly Charged Pharmaceutical Aerosols Using a New Aerosol Induction Charger. *Pharmaceutical Research*. [4.7]

2013

Holbrook, L. T. and Longest, P. W. 2013. Validating CFD predictions of highly localized aerosol deposition in airway models: In vitro data and effects of surface properties. *Journal of Aerosol Science*, 59: 6-21. [3.0]

Longest, P. W., Son, Y.-J., Holbrook, L., and Hindle, M. 2013. Aerodynamic factors responsible for the deaggregation of carrier-free drug powders to form micrometer and submicrometer aerosols. *Pharmaceutical Research*, 30.6: 1608 -1627. [4.7]

2012

Longest, P. W., Spence, B. M., Holbrook, L. T., Mossi, K. M., Son, Y.-J., Hindle, M. 2012. Production of inhalable submicrometer and nanoparticle aerosols from conventional mesh nebulizers for improved respiratory drug delivery. *Journal of Aerosol Science*, 51:66-80. [3.0]

Longest, P. W. and Holbrook, L. T. 2012. In silico models of aerosol delivery to the respiratory tract – Development and applications. *Advanced Drug Delivery Reviews*, 64: 296-311. [12.1]

Conference posters and presentations (Presenting authors are noted with an asterisk.)

Holbrook, L. T.* and Longest, P. W. 2014. Generating a Pharmaceutical Aerosol with High Charge and Low Device Losses. *2014 AAAR Annual Conference* (October 20 – 24), Orlando, FL. (Poster Presentation and peer-reviewed abstract).

Longest, P. W., Son, Y.-J., Holbrook, L.*, and Hindle, M. 2013. Deaggregation of Carrier-Free Powders by DPIs to form Submicrometer Aerosols. *2013 ISAM Annual*

Conference (April 6-10), Chapel Hill, NC (Poster Presentation and peer-reviewed abstract).

Holbrook, L. T.*, Behara, R. B., Hindle, M., and Longest, P. W. 2012. Development of a wick electrospray pharmaceutical aerosol generator. *2012 AAAR Annual Conference* (October 8 – 12), Minneapolis, MN. (Poster Presentation and peer-reviewed abstract).

Holbrook, L.*, Longest, P. W., Oldham, M. J. 2011. Validating highly localized deposition in a bifurcating airway model: Effects of surface properties. *2011 AAAR Annual Conference* (October 3 – 7), Orlando, FL. (Presentation and peer-reviewed abstract).

TEACHING and MENTORING EXPERIENCE

Graduate Assistance in Areas of National Need (GAANN) Fellow, 2010-2013

1 lecture on "Reaction Forces and Equilibrium" for ENGR 102 Engineering Statics (Fall 2012)
1 lecture and 1 review session for ENGR 301 Fluid Mechanics (Fall 2012)
2 lectures on "Similarity" for ENGR 301 Fluid Mechanics (Fall 2014)

Graduate Student Mentorship Program, Fall 2012- Spring 2013
Worked closely with a sophomore undergraduate engineering student to assist in the work – school balance, gave guidance about applying for a job, and introduced her to academic research

Teaching Assistant, Fall 2009
EGRM – 321 Numerical Methods

Academic Tutor, Spring 2007- Spring 2009
Led individual and group teaching sessions for Engineering Statics
Held weekly appointments tutoring Math and Physics at the Campus Learning Center
Math – Algebra, Pre-Calculus, Calculus, Differential Equations
Physics –University Physics I and II, Modern Physics

SERVICE

Engineering Ministries International Internship, 2008. –Danja, Niger
Assisted with survey and design of surgical clinic in Niger
Drafted design report in Calgary, Canada

Makunda Christian Hospital Mission Trip, 2013. –Assam, India
Assessed design of structural components of operating theater
Surveyed and mapped the boundaries of the land.

Engineers Without Borders Assessment Trip, 2011. –Virginia, USA

Provided consult to director of Allegheny Mountain School

Designed composting latrine

Investigated water quality at source and possible contamination site

Participation in Hiring committee for new faculty, 2013 – Virginia, USA

VCU Mechanical and Nuclear Engineering - Supathorn Phongikaroon

Peer reviewer for "Respiratory Care", 2015. –Virginia, USA

Science journal with impact factor 1.84

PROFESSIONAL SOCIETIES

American Society of Engineering Education (ASEE)
American Association for the Advancement of Science (AAAS)
American Society of Mechanical Engineers (ASME)
Engineers without Borders (EWB)
Phi Kappa Phi Honor Society

HONORS AND AWARDS

- School of Engineering Phi Kappa Phi Scholarship 2014- 2015
- Graduate Assistance in Areas of National Need (**GAANN**) Fellowship, 2010 – 2013
- "Important Contributions to the **Internationalization** of the University Community", VCU Global Education Office 2011
- Scholarship for **Graduate** and Professional Students, VCU Business Services 2010
- VCU School of Engineering, **Excellence in Design** Senior Design Expo, 2009
- VCU **University Honors** Summers Undergraduate Research Program, Holbrook, L. "Development of a respiratory tract model from the female visible human data set," Summer 2007.
- Rocheleau Scholarship 2008-2009
- Sandgren Scholarship 2008-2009
- Carl Burlock Scholarship 2005-2008
- Electro Technologies Scholarship 2005-2008